Supporting information
for the article:

Systematic study of FFF materials for digitalizing chemical reactors with 3D printing: superior performance of carbon-filled polyamide

Victoria A. Korabelnikova, Evgeniy G. Gordeev, Valentine P. Ananikov*

Content

1. Material selection

Table S1. Characteristics of plastics and basic printing parameters.

Material	PLA+	TPU	PC+	PA6-CF	PA	PP-GF	PP
Manufacturer	ESUN	ESUN	Raise3D	ESUN	ESUN	FILAMENTARNO	FL33
Color	White	Transparent	Transparent	Black	Transparent	Black	Transparent
Bar diameter, mm	1.75	1.75	1.75	1.75	1.75	1.75	1.75
Brim presence	no	no	no	no	yes	no	yes
Fixation to the platform	adhesive	adhesive	paper tape	adhesive	adhesive	PP tape	PP tape
Nozzle temperature, °C	230	230	260	275	245	245	240
Table temperature, °C	70	100	100	105	100	60	110
Radiator temperature, °C	52	80	90	80	80	80	80
Extrusion multiplier *	1.00	1.00	0.98	1.01	1.00	1.00	0.85
First layer nozzle temperature, °C	220	250	260	280	250	250	240
First layer table temperature, °C	70	100	100	110	100	95	110
First layer thickness, %	100	100	100	100	100	100	100
Part cooling, %	10	0	0	0	0	0	40

* for the manufacturing of samples for determining chemical resistance in various solvents, determining heat resistance, mechanical strength and shrinkage.

2. Chemical resistance of 3D printed test samples in various solvents

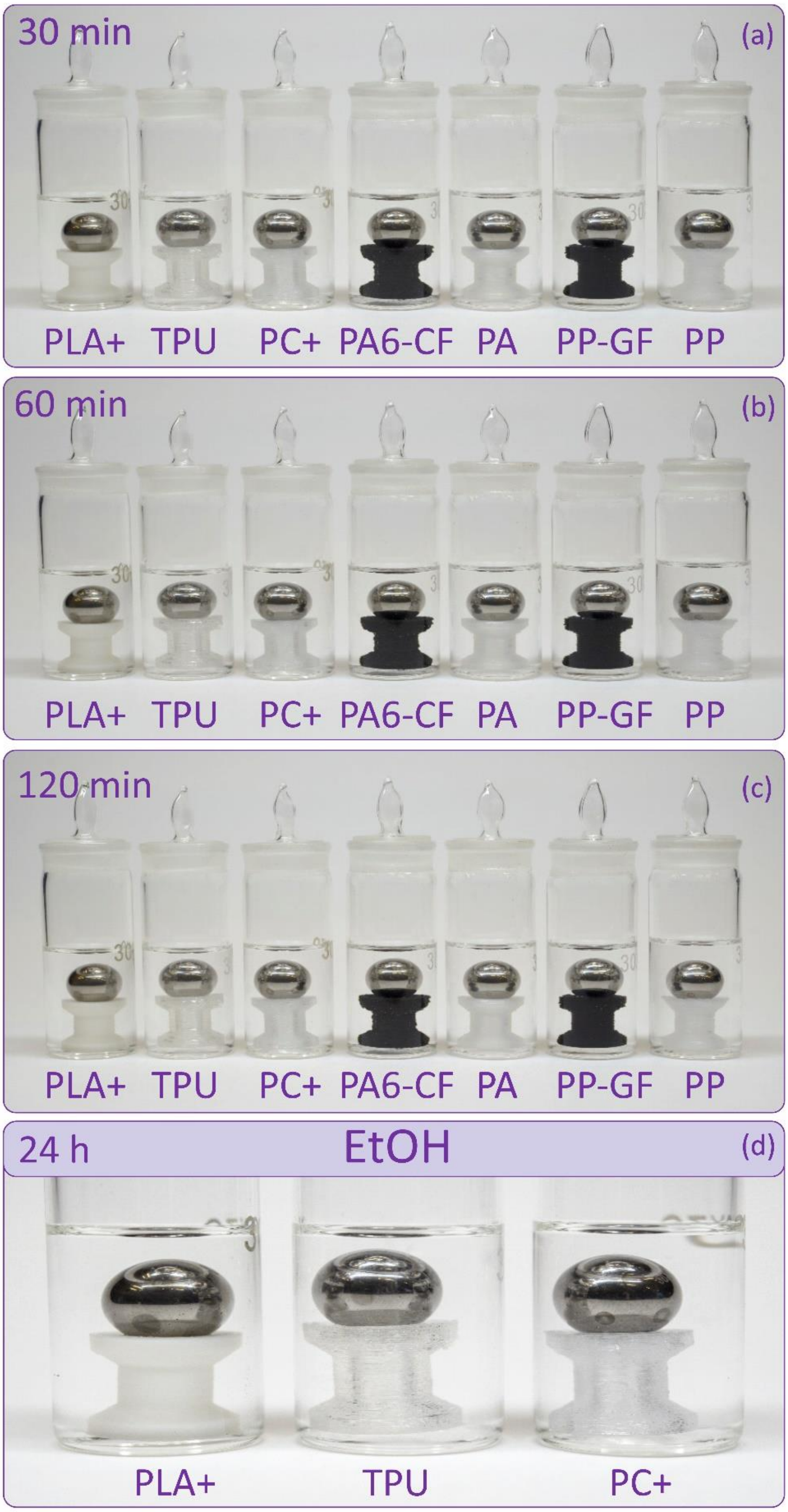

Figure S1. Stability test of parts manufactured by the FFF method in ethanol medium for 24 hours: (a) – result after 30 min in a solvent environment; (b) – after 60 min; (c) – after 120 min; (d) – after 2 hours.

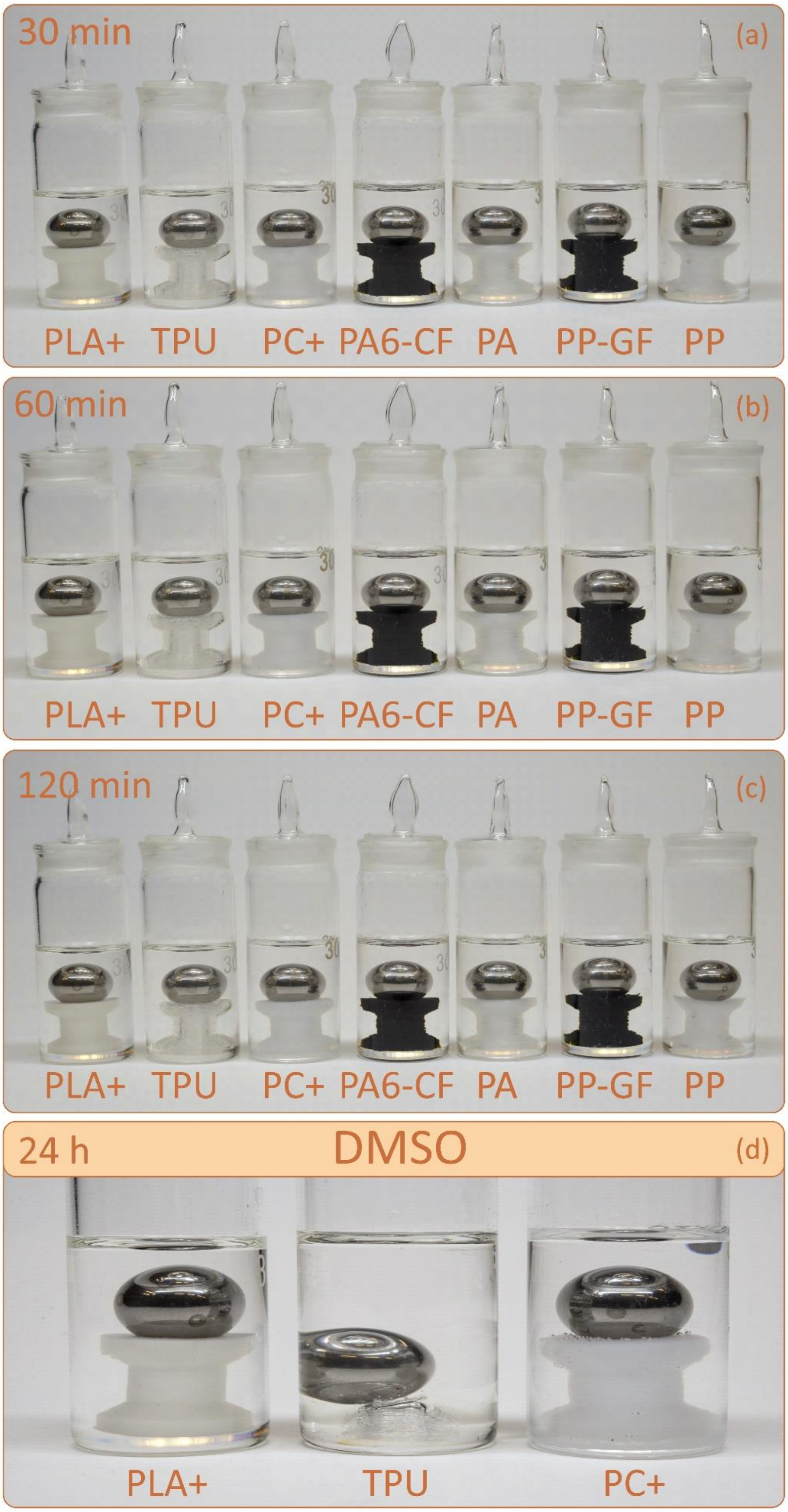

Figure S2. Stability test of parts manufactured by the FFF method in dimethyl sulfoxide for 24 hours: (a) – result after 30 minutes in a solvent medium; (b) – after 60 min; (c) – after 120 min; (d) – after 2 hours.

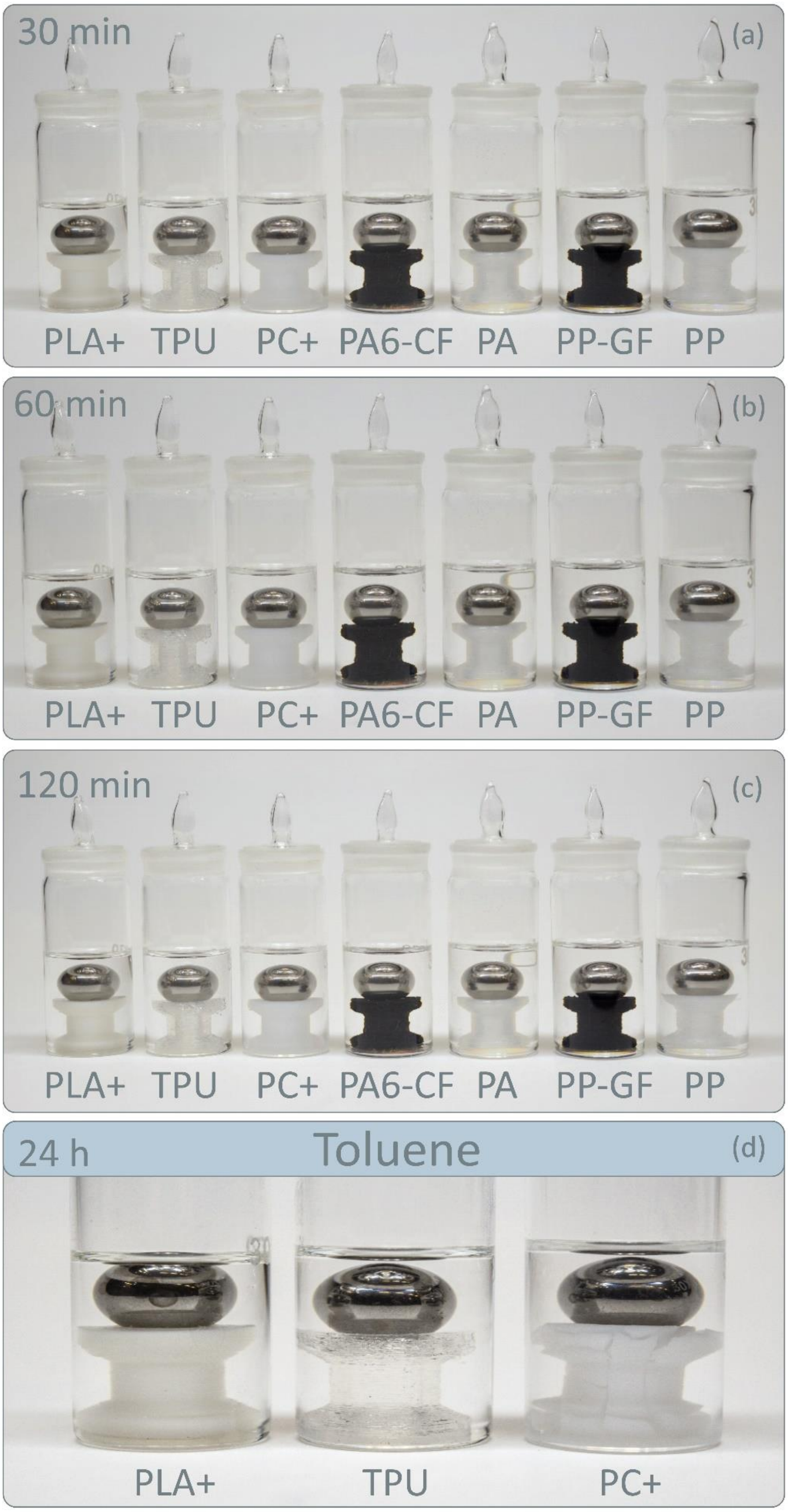

Figure S3. Stability test of parts manufactured by the FFF method in toluene for 24 hours: (a) – result after 30 minutes in a solvent medium; (b) – after 60 min; (c) – after 120 min; (d) – after 2 hours.

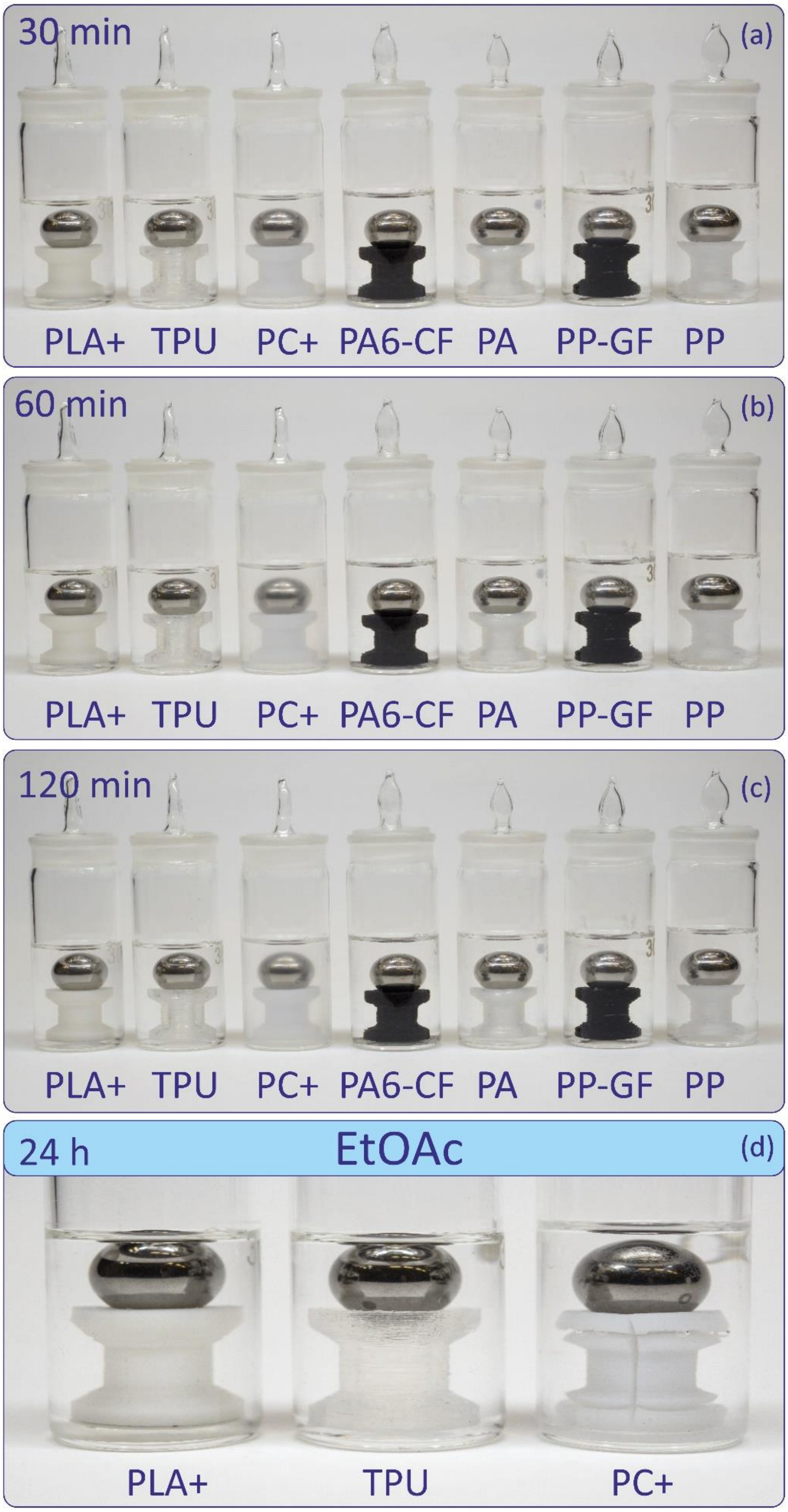

Figure S4. Stability test of parts manufactured by the FFF method in ethyl acetate medium for 24 hours: (a) – result after 30 minutes in a solvent medium; (b) – after 60 min; (c) – after 120 min; (d) – after 2 hours.

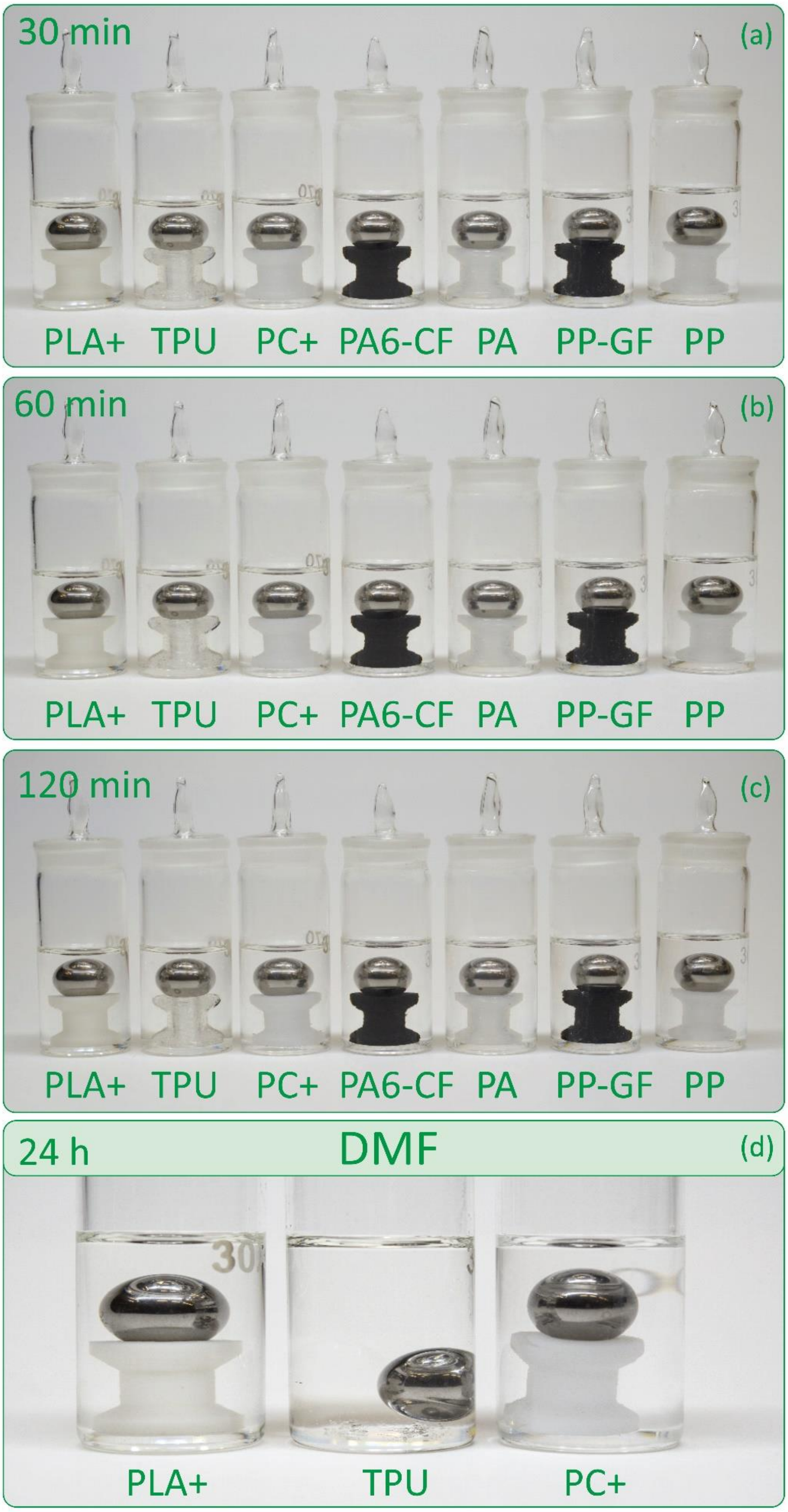

Figure S5. Stability test of parts manufactured by the FFF method in a dimethylformamide medium for 24 hours: (a) after 30 minutes in a solvent medium; (b) after 60 min; (c) after 120 min; (d) after 2 hours.

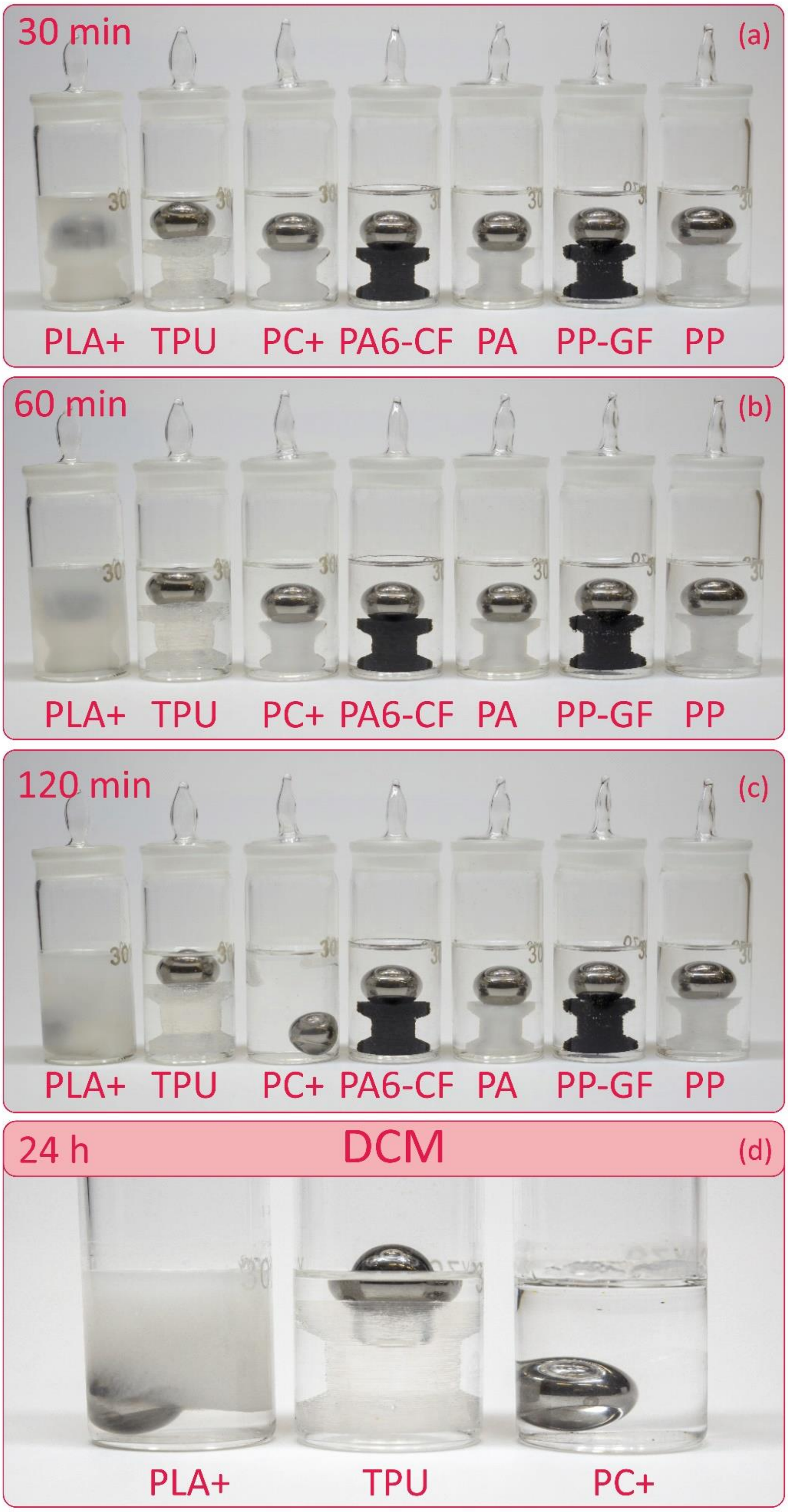

Figure S6. Stability test of parts manufactured by the FFF method in methylene chloride for 24 hours: (a) – result after 30 minutes in a solvent medium; (b) – after 60 min; (c) – after 120 min; (d) – after 2 hours.

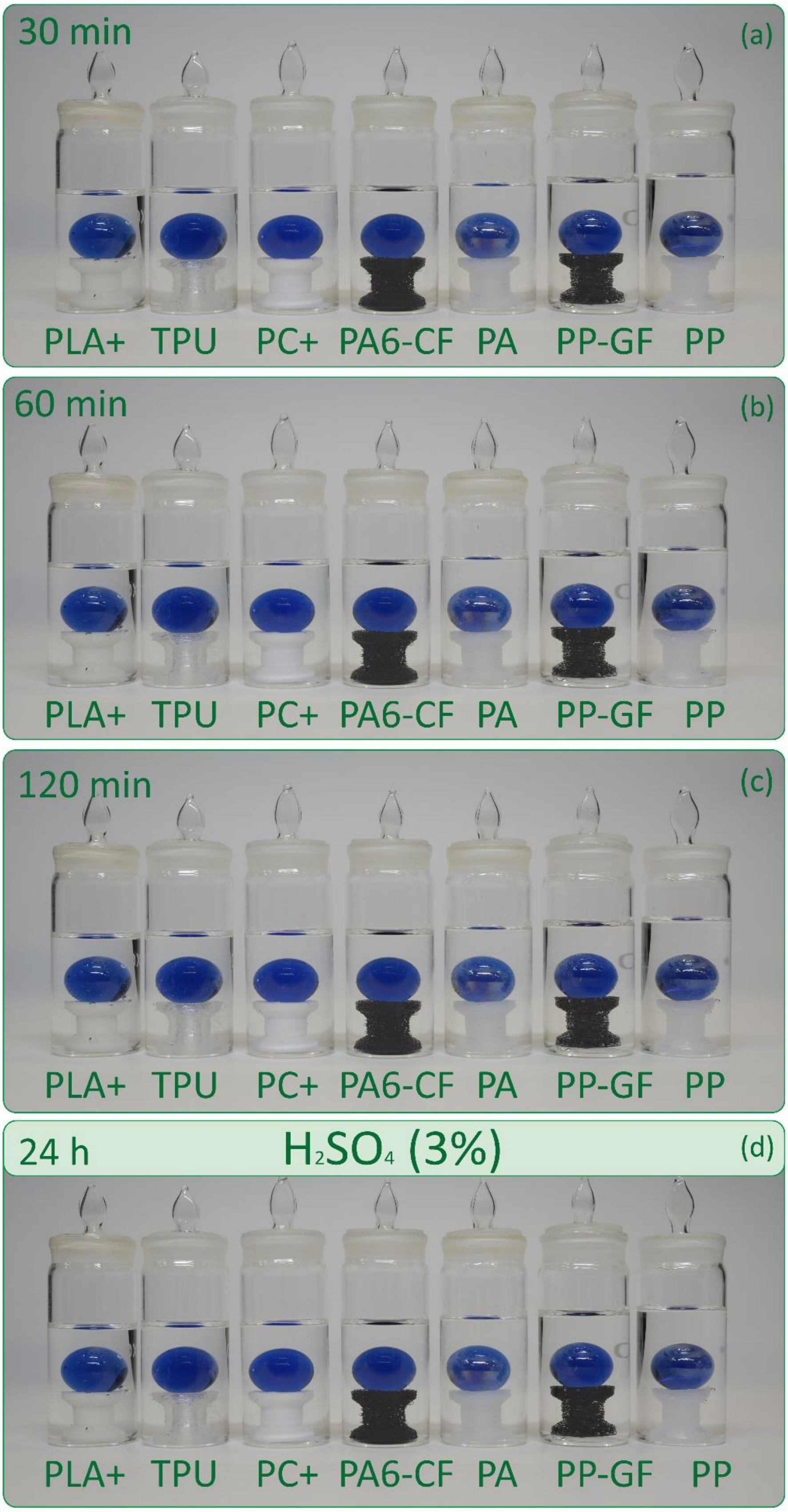

Figure S7. Stability test of parts manufactured by the FFF method in sulfuric acid with a concentration of 3% for 24 hours: (a) – result after 30 minutes in a solvent medium; (b) – after 60 min; (c) – after 120 min; (d) – after 2 hours.

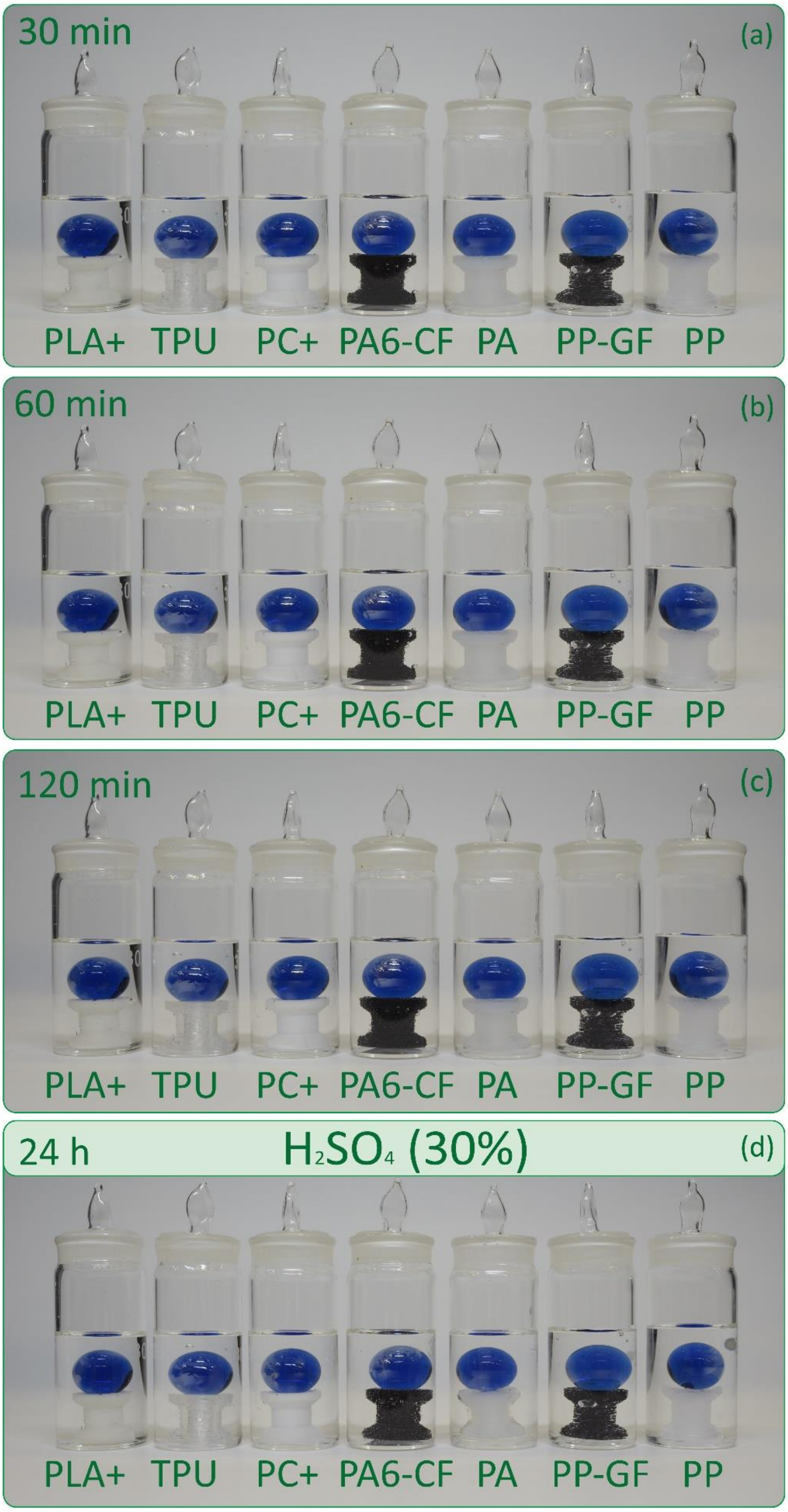

Figure S8. Stability test of parts manufactured by the FFF method in sulfuric acid with a concentration of 30% for 24 hours: (a) – result after 30 minutes in a solvent medium; (b) – after 60 min; (c) – after 120 min; (d) – after 2 hours.

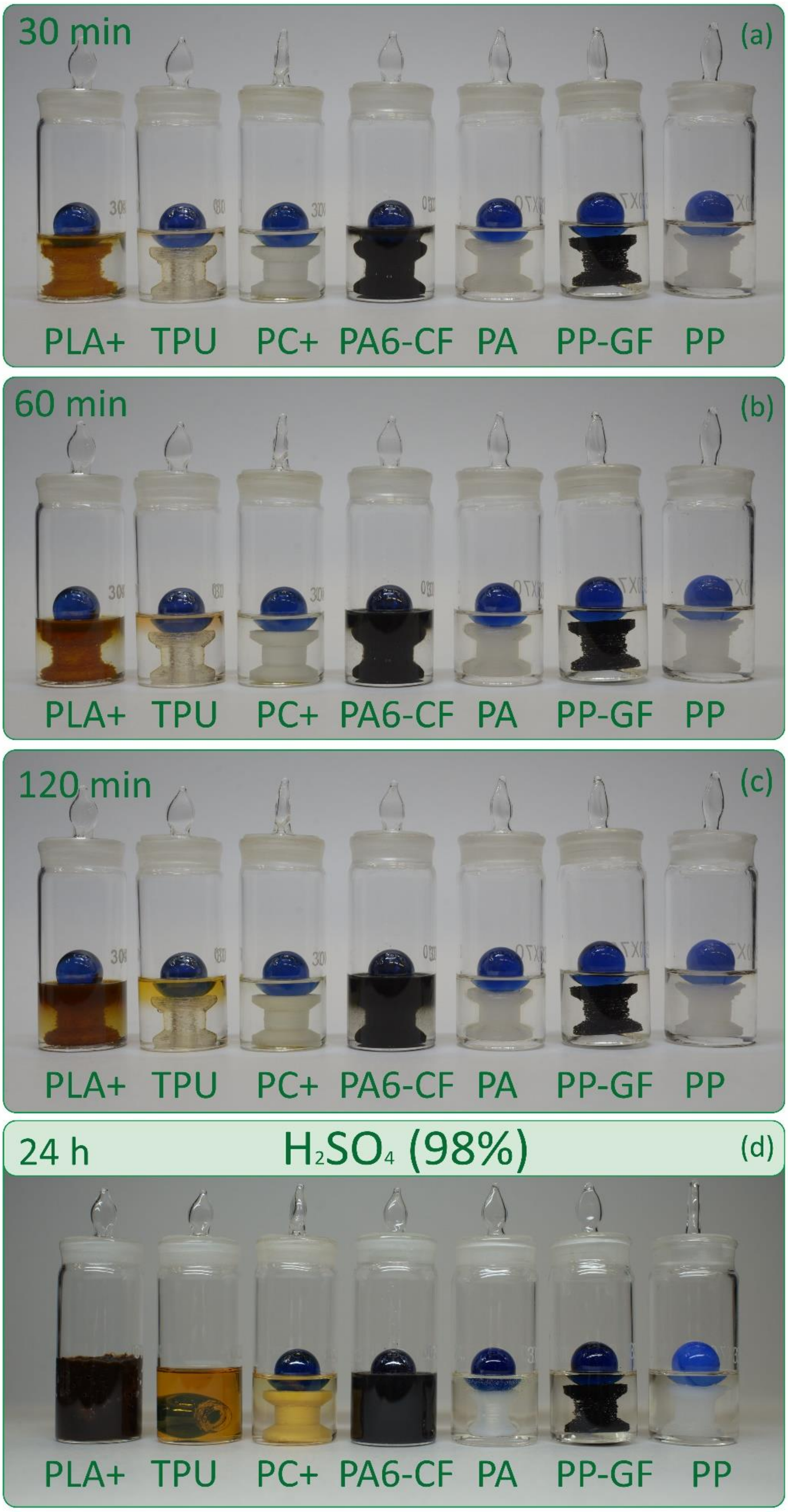

Figure S9. Stability test of parts manufactured by the FFF method in sulfuric acid with a concentration of 98% for 24 hours: (a) – result after 30 minutes in a solvent medium; (b) – after 60 min; (c) – after 120 min; (d) – after 2 hours.

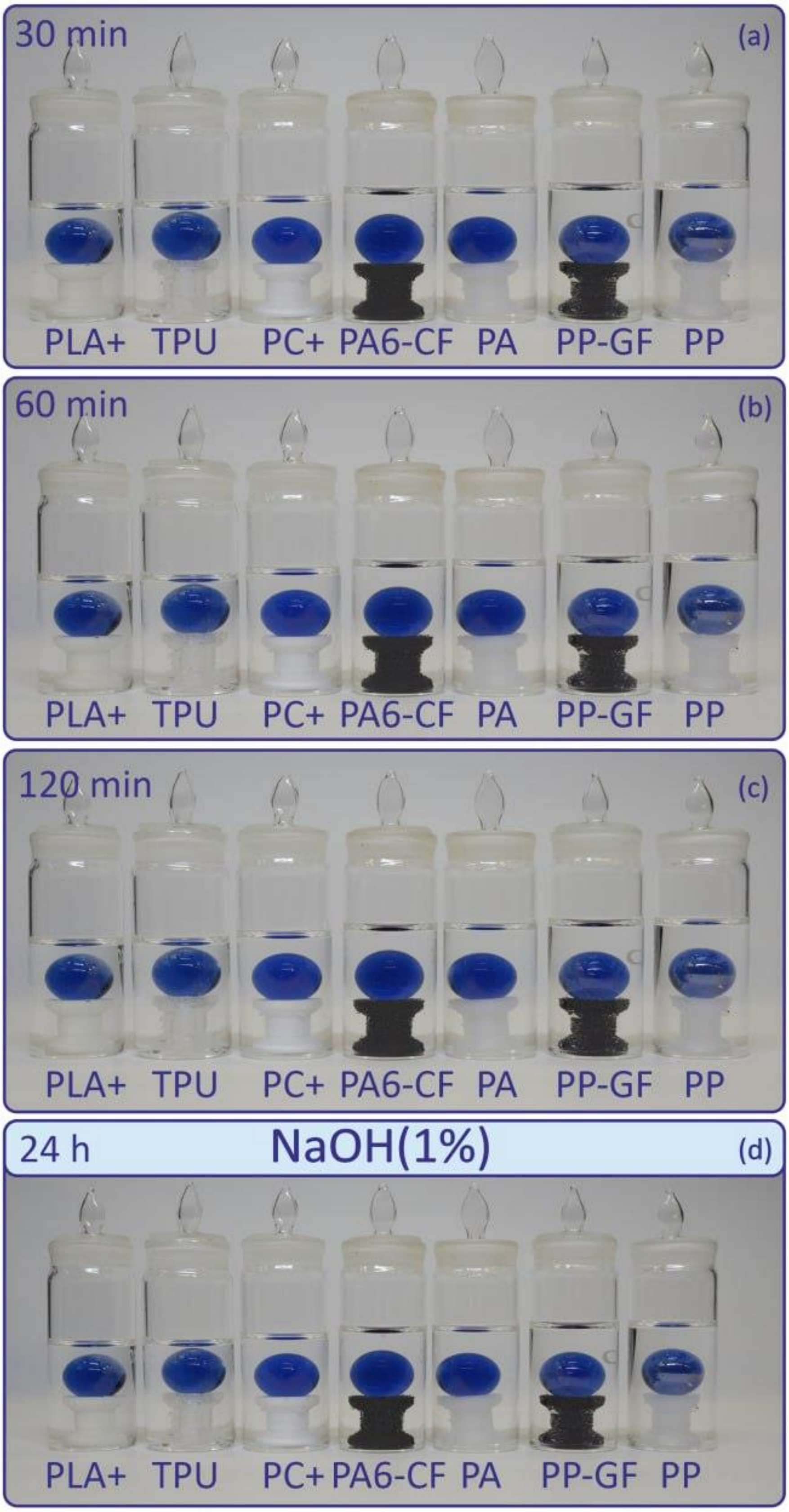

Figure S10. Stability test of parts manufactured by the FFF method in sodium hydroxide with a concentration of 1% for 24 hours: (a) – result after 30 minutes in a solvent medium; (b) – after 60 min; (c) – after 120 min; (d) – after 2 hours.

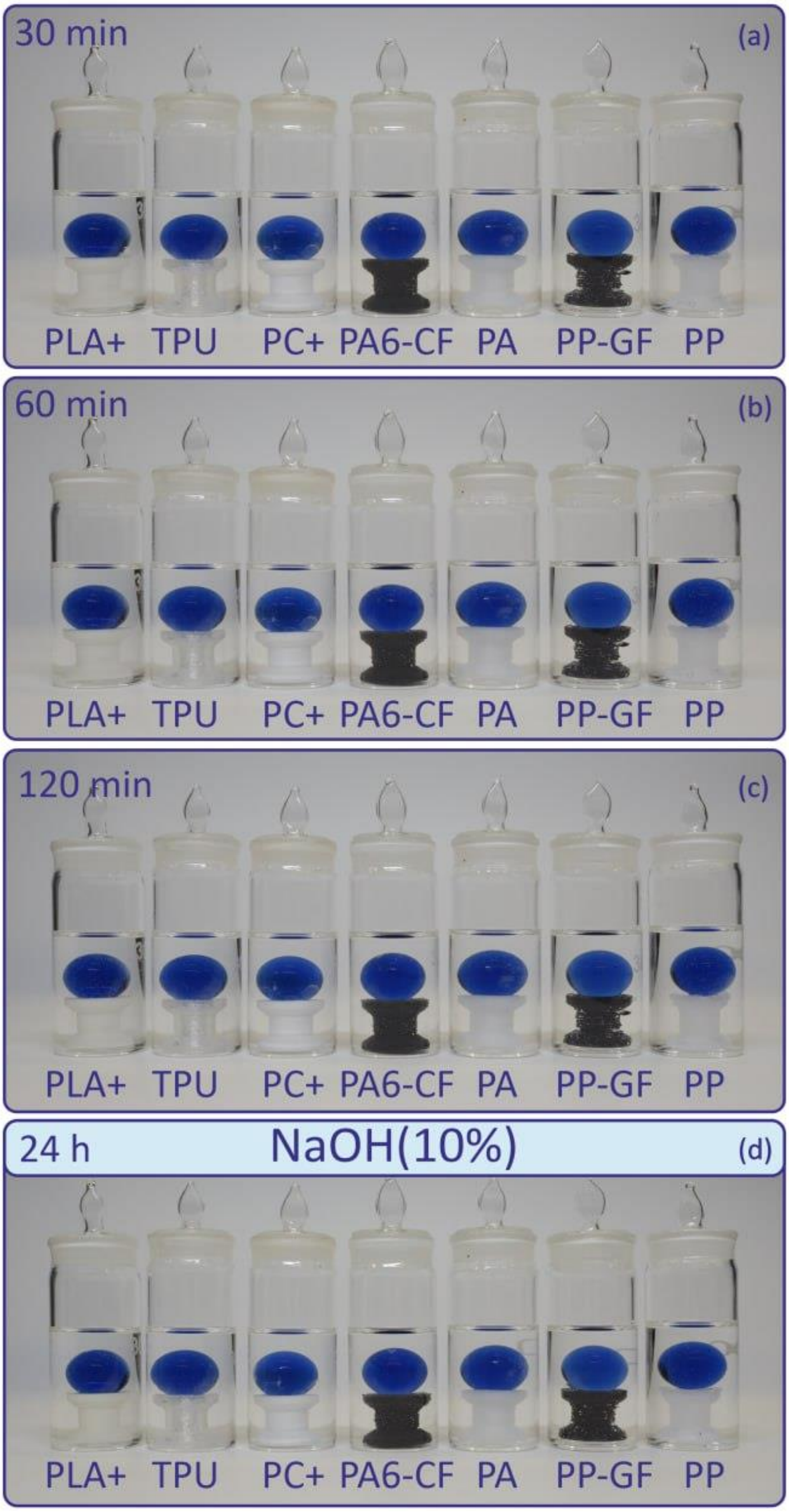

Figure S11. Stability test of parts manufactured by the FFF method in sodium hydroxide with a concentration of 10% for 24 hours: (a) – result after 30 minutes in a solvent medium; (b) – after 60 min; (c) – after 120 min; (d) – after 2 hours.

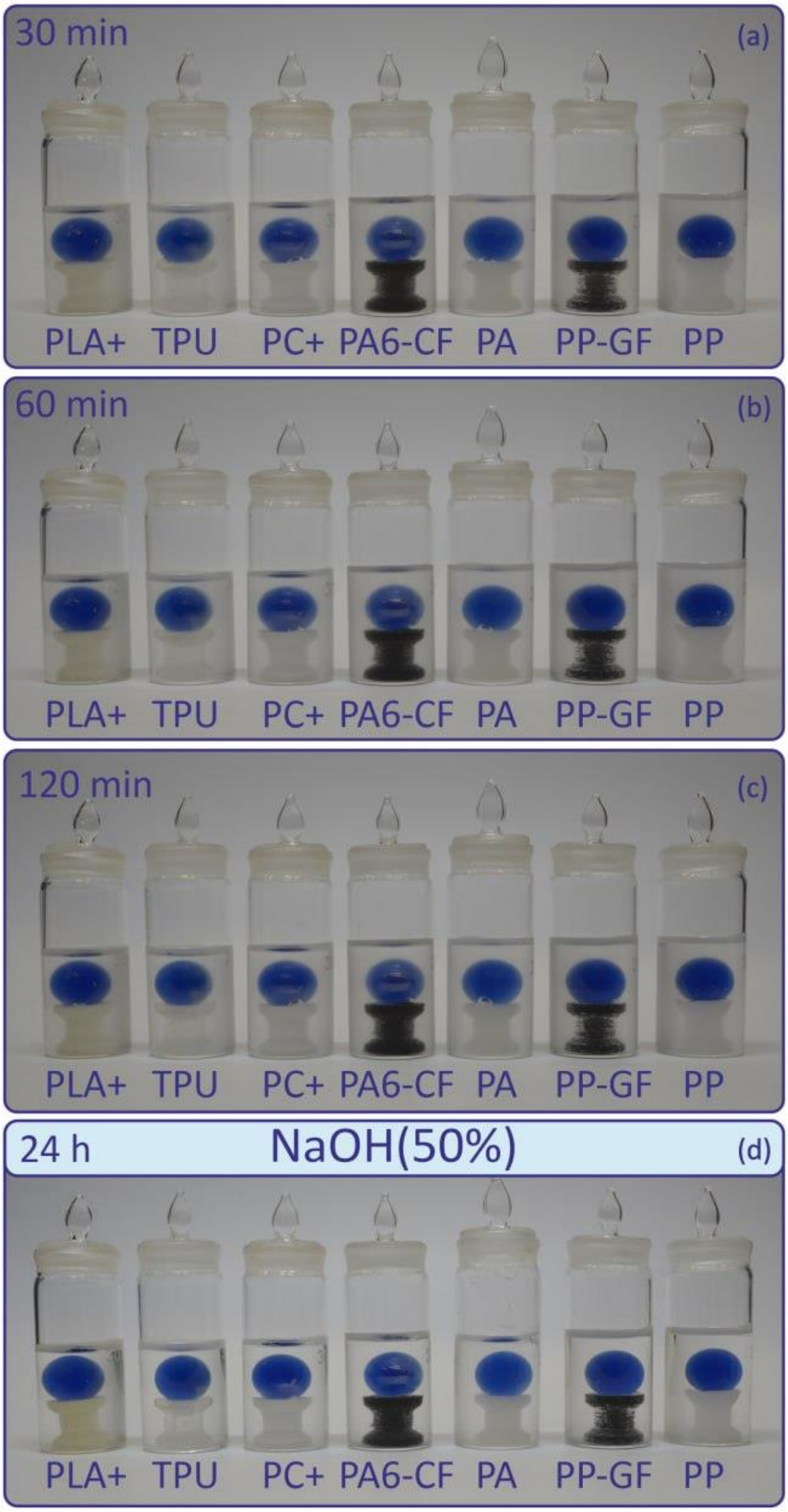

Figure S12. Stability test of parts manufactured by the FFF method in sodium hydroxide with a concentration of 50% for 24 hours: (a) – result after 30 minutes in a solvent medium; (b) – after 60 min; (c) – after 120 min; (d) – after 2 hours.

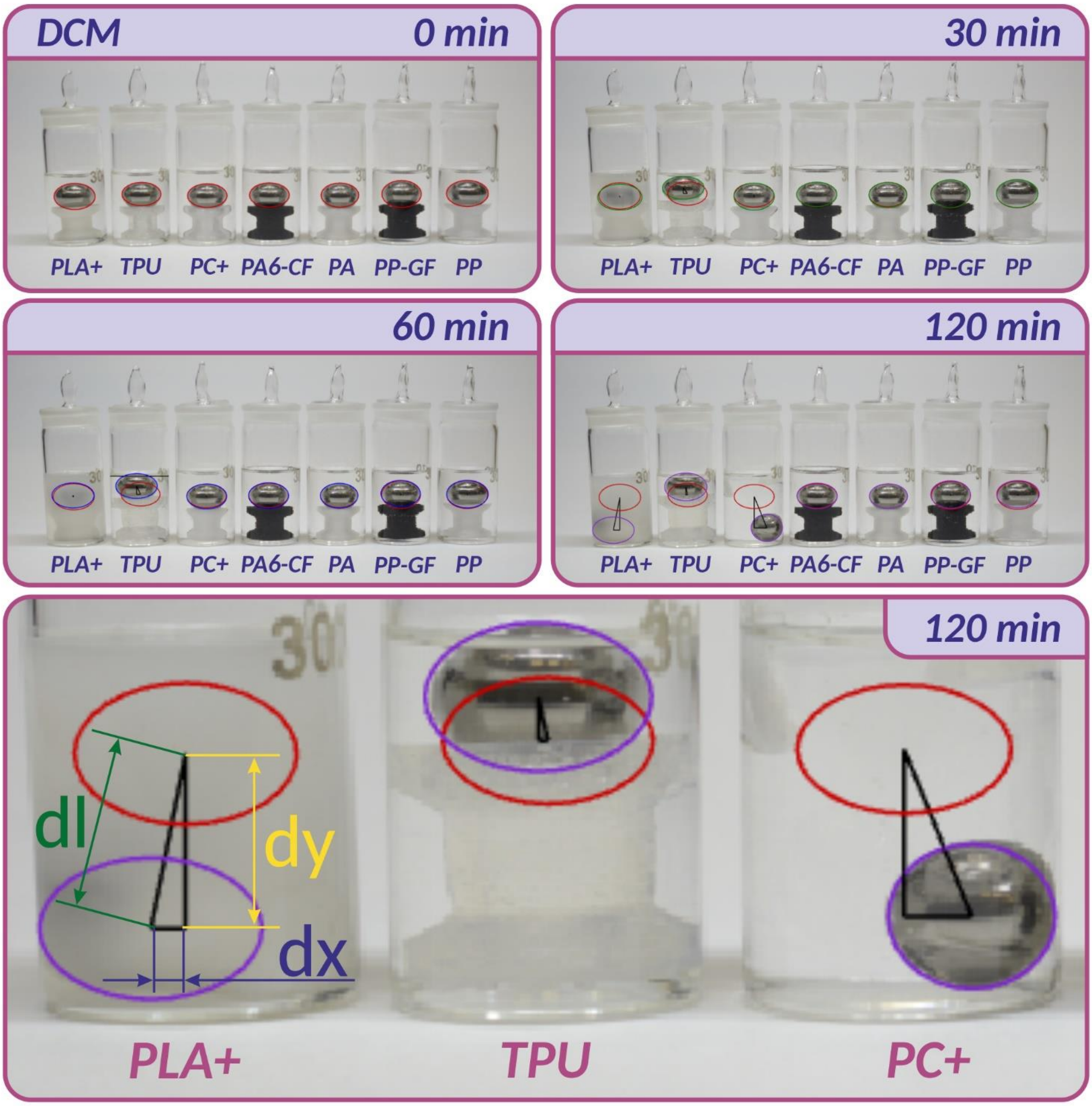

Figure S13. Quantitative determination of the chemical resistance of 3D printed samples in methylene chloride.

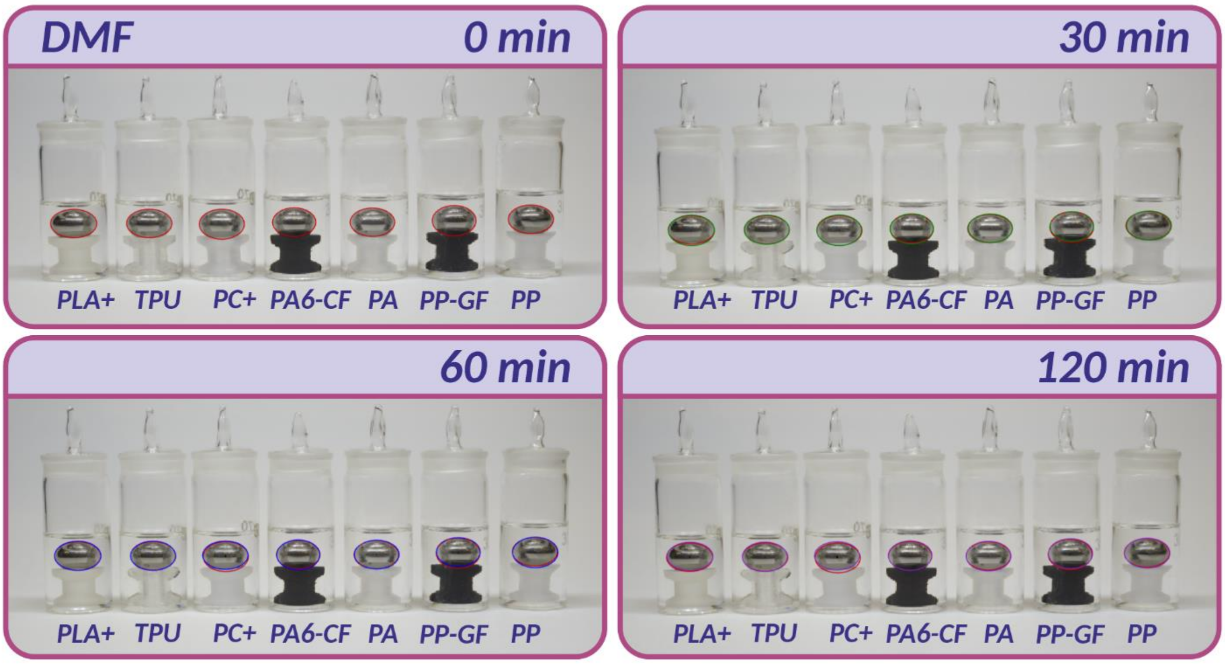

Figure S14. Quantitative determination of the chemical resistance of 3D printed samples in dimethylformamide.

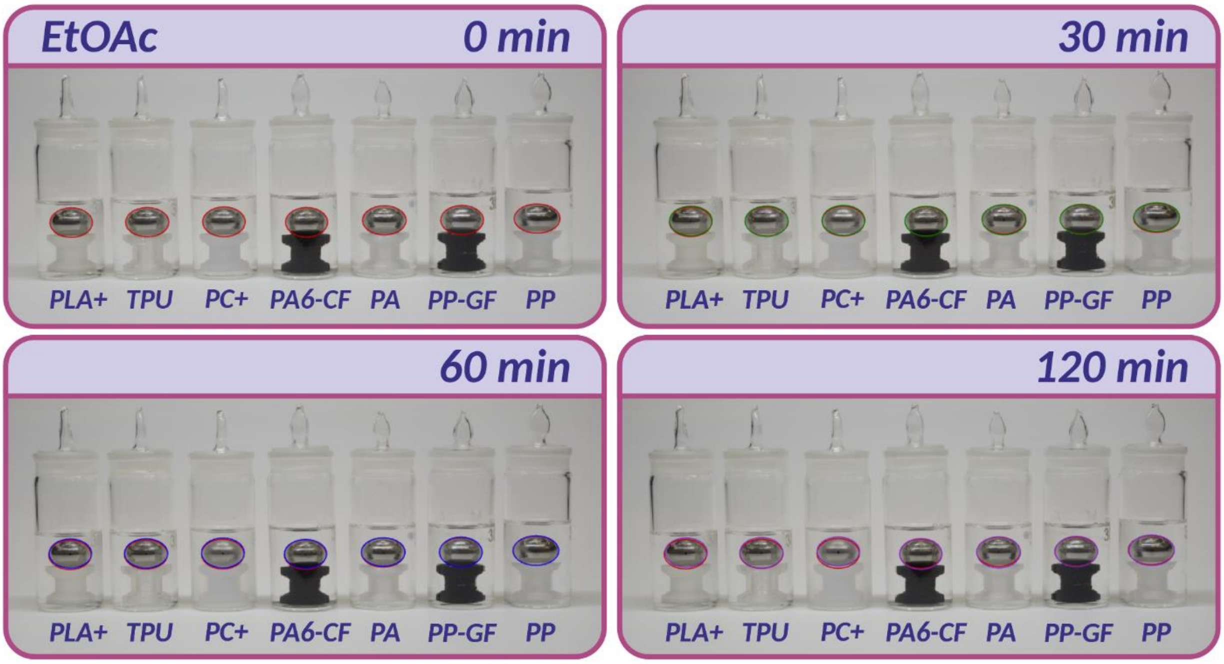

Figure S15. Quantitative determination of the chemical resistance of 3D printed samples in ethyl acetate.

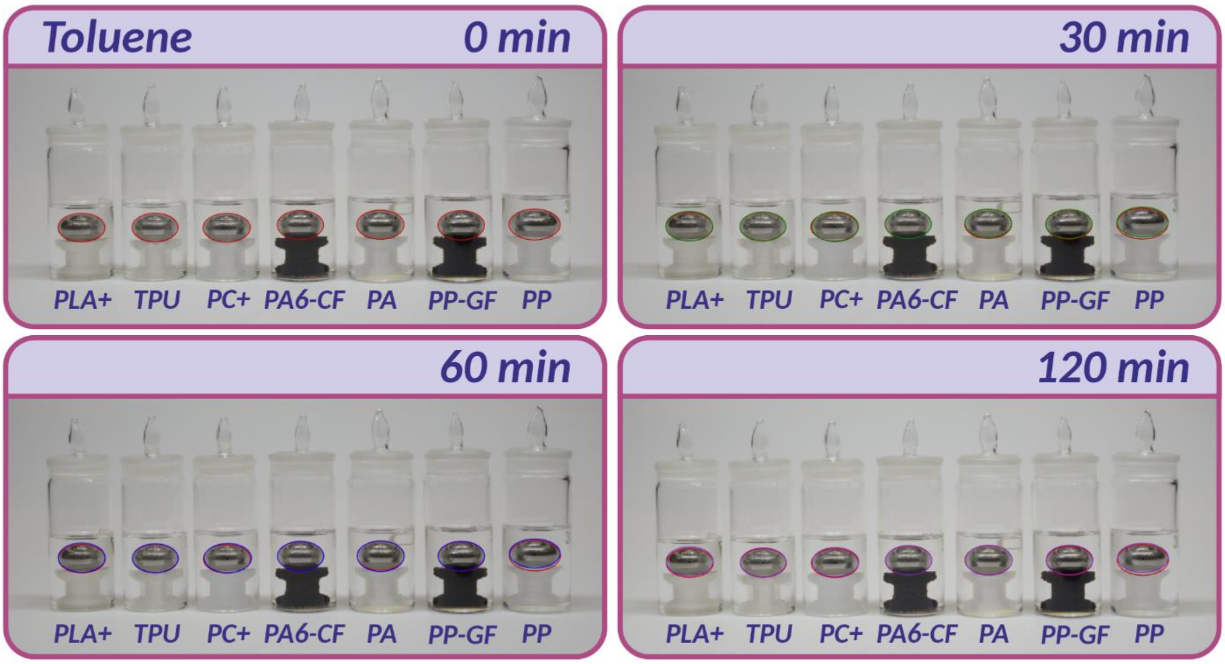

Figure S16. Quantitative determination of the chemical resistance of 3D printed samples in toluene.

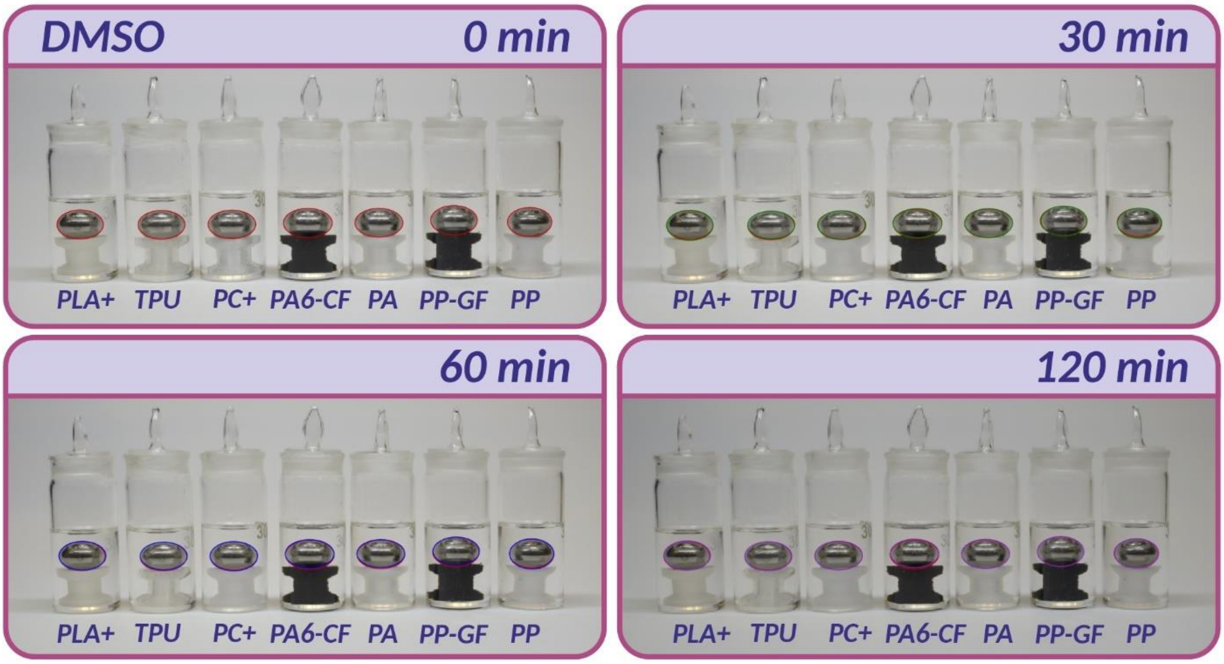

Figure S17. Quantitative determination of the chemical resistance of 3D printed samples in dimethyl sulfoxide.

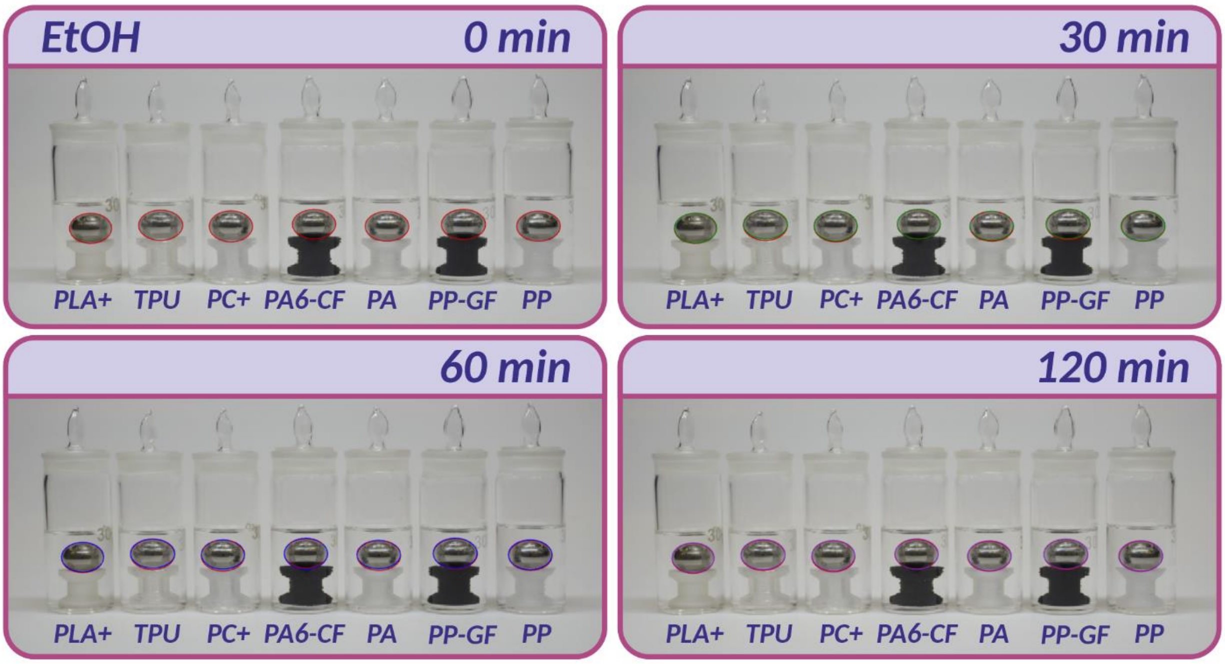

Figure S18. Quantitative determination of the chemical resistance of 3D printed samples in ethanol.

Table S2. Quantitative values of deformation of 3D printed samples. dx, dy, dl - measurement in mm.

PLA+	EtOH			DMSO			Toluene			EtOAc			DMF			DCM		
min	dx	dy	dl	dx	dy	dl	dx	dy	dl	dx	dy	dl	dx	dy	dl	dx	dy	dl
30.00	0.11	0.12	0.16	0.03	0.13	0.13	0.06	0.27	0.28	0.12	0.42	0.44	0.08	0.20	0.21	0.07	0.62	0.62
60.00	0.05	0.21	0.21	0.14	0.12	0.19	0.07	0.48	0.48	0.20	0.61	0.64	0.07	0.08	0.11	0.31	0.69	0.76
120.00	0.05	0.23	0.23	0.14	0.13	0.19	0.08	0.79	0.79	0.34	0.78	0.85	0.18	0.40	0.44	3.30	16.60	16.92
TPU	EtOH			DMSO			Toluene			EtOAc			DMF			DCM		
min	dx	dy	dl	dx	dy	dl	dx	dy	dl	dx	dy	dl	dx	dy	dl	dx	dy	dl
30.00	0.01	0.41	0.41	0.10	0.20	0.22	0.01	0.14	0.14	0.04	0.09	0.10	0.00	0.06	0.06	2.10	2.88	3.56
60.00	0.02	0.44	0.44	0.09	0.16	0.18	0.05	0.19	0.19	0.06	0.53	0.53	0.05	0.07	0.09	2.07	4.29	4.76
120.00	0.01	0.29	0.29	0.05	0.05	0.07	0.05	0.26	0.26	0.02	0.45	0.45	0.15	0.14	0.21	0.91	4.14	4.24
PC+	EtOH			DMSO			Toluene			EtOAc			DMF			DCM		
min	dx	dy	dl	dx	dy	dl	dx	dy	dl	dx	dy	dl	dx	dy	dl	dx	dy	dl
30.00	0.00	0.26	0.26	0.16	0.10	0.19	0.31	0.07	0.32	0.05	0.32	0.33	0.13	0.13	0.18	0.11	0.80	0.80
60.00	0.07	0.48	0.49	0.02	0.13	0.13	0.37	0.32	0.49	0.10	0.57	0.58	0.18	0.64	0.67	0.15	0.24	0.28
120.00	0.01	0.33	0.33	0.06	0.04	0.07	0.25	0.50	0.56	0.07	0.91	0.91	0.34	0.92	0.98	15.88	6.42	17.12
PA6-CF	EtOH			DMSO			Toluene			EtOAc			DMF			DCM		
min	dx	dy	dl	dx	dy	dl	dx	dy	dl	dx	dy	dl	dx	dy	dl	dx	dy	dl
30.00	0.00	0.09	0.09	0.05	0.21	0.22	0.06	0.05	0.08	0.08	0.14	0.16	0.01	0.13	0.13	0.01	0.04	0.05
60.00	0.02	0.09	0.10	0.06	0.37	0.37	0.00	0.07	0.07	0.11	0.29	0.31	0.08	0.09	0.12	0.02	0.15	0.16
120.00	0.09	0.08	0.12	0.03	0.43	0.43	0.05	0.12	0.13	0.03	0.07	0.08	0.02	0.12	0.12	0.04	0.01	0.04
PA	EtOH			DMSO			Toluene			EtOAc			DMF			DCM		
min	dx	dy	dl	dx	dy	dl	dx	dy	dl	dx	dy	dl	dx	dy	dl	dx	dy	dl
30.00	0.04	0.25	0.25	0.05	0.16	0.16	0.07	0.30	0.31	0.13	0.12	0.17	0.15	0.13	0.20	0.03	0.18	0.18
60.00	0.08	0.48	0.49	0.02	0.35	0.35	0.01	0.16	0.16	0.06	0.23	0.24	0.18	0.06	0.19	0.01	0.14	0.14
120.00	0.05	0.25	0.25	0.01	0.11	0.11	0.07	0.03	0.07	0.04	0.25	0.26	0.08	0.07	0.11	0.04	0.01	0.04
PP-GF	EtOH			DMSO			Toluene			EtOAc			DMF			DCM		
min	dx	dy	dl	dx	dy	dl	dx	dy	dl	dx	dy	dl	dx	dy	dl	dx	dy	dl
30.00	0.06	0.27	0.28	0.20	0.05	0.20	0.05	0.23	0.24	0.00	0.05	0.05	0.05	0.33	0.33	0.05	0.04	0.07
60.00	0.12	0.22	0.25	0.12	0.30	0.33	0.07	0.20	0.21	0.00	0.10	0.10	0.10	0.48	0.49	0.24	0.57	0.62
120.00	0.03	0.17	0.18	0.02	0.02	0.03	0.04	0.37	0.37	0.05	0.02	0.05	0.19	0.33	0.38	0.21	0.36	0.41
PP	EtOH			DMSO			Toluene			EtOAc			DMF			DCM		
min	dx	dy	dl	dx	dy	dl	dx	dy	dl	dx	dy	dl	dx	dy	dl	dx	dy	dl
30.00	0.09	0.12	0.15	0.15	0.31	0.35	0.11	0.75	0.76	0.07	0.27	0.28	0.23	0.05	0.23	0.01	0.07	0.07
60.00	0.10	0.30	0.31	0.07	0.15	0.17	0.06	0.99	0.99	0.06	0.09	0.11	0.18	0.32	0.36	0.15	0.25	0.29
120.00	0.01	0.10	0.10	0.01	0.11	0.11	0.01	1.00	1.00	0.15	0.07	0.17	0.19	0.07	0.20	0.09	0.54	0.55

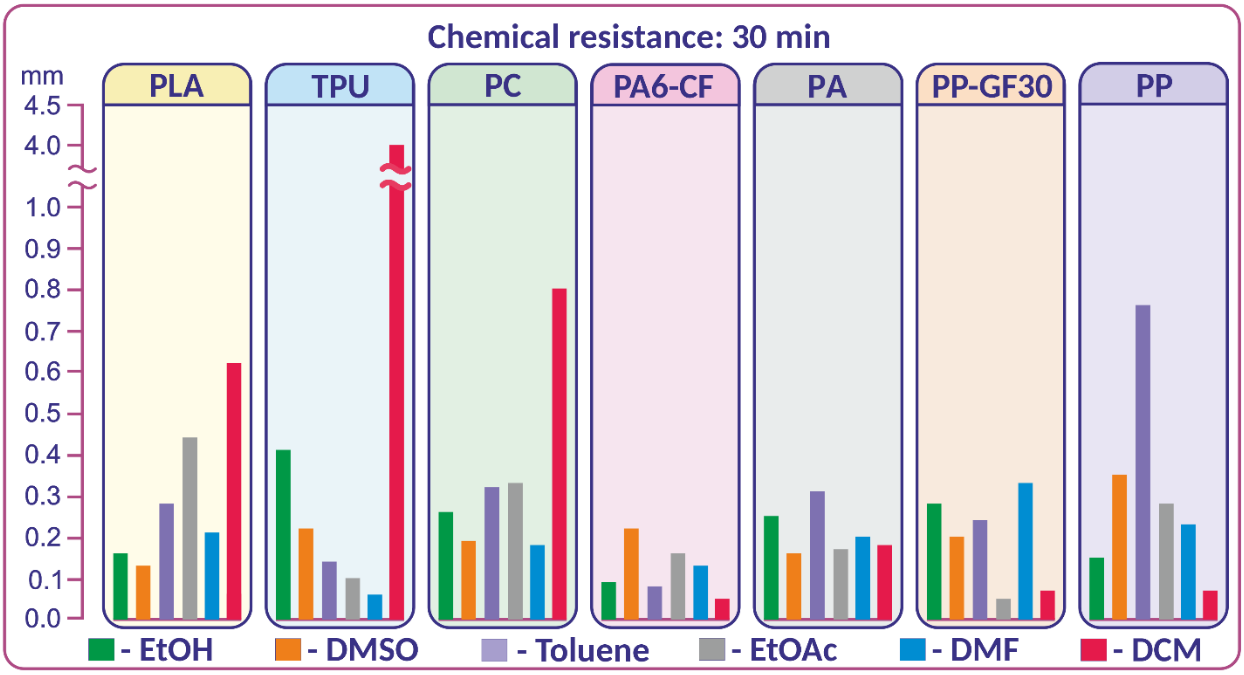

Figure S19. Diagram with quantitative calculations of the chemical resistance of 3D printed samples when exposed to various solvents for 30 minutes.

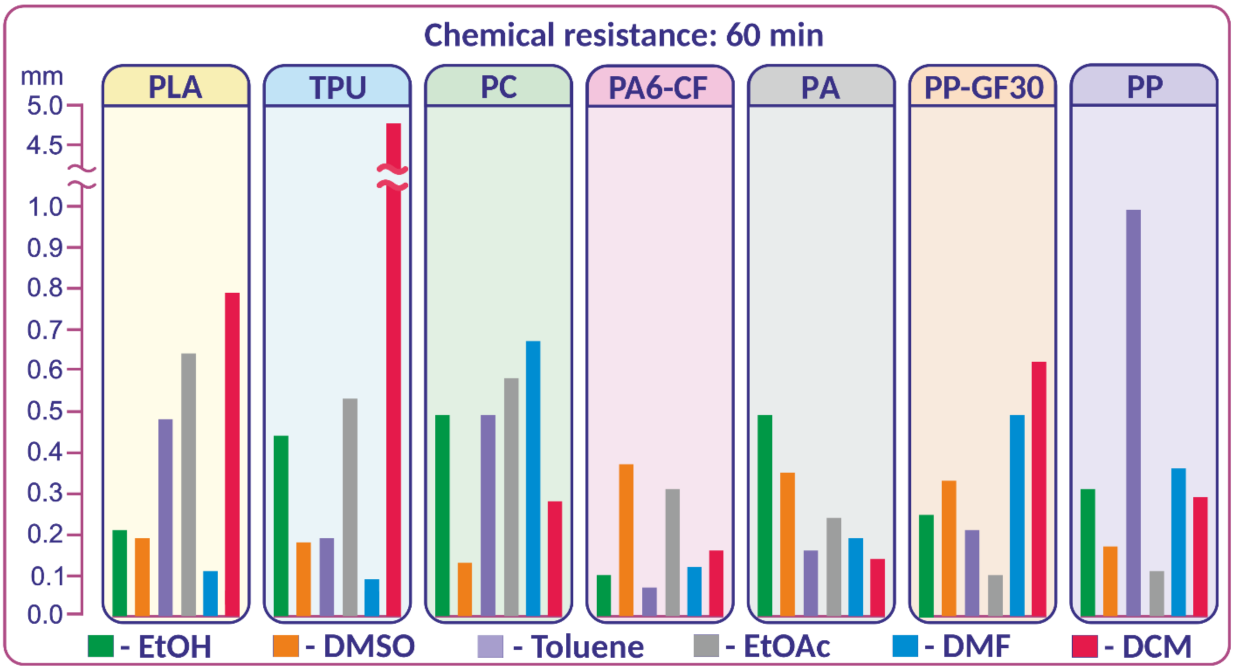

Figure S20. Diagram with quantitative calculations of the chemical resistance of 3D printed samples when exposed to various solvents for 60 minutes.

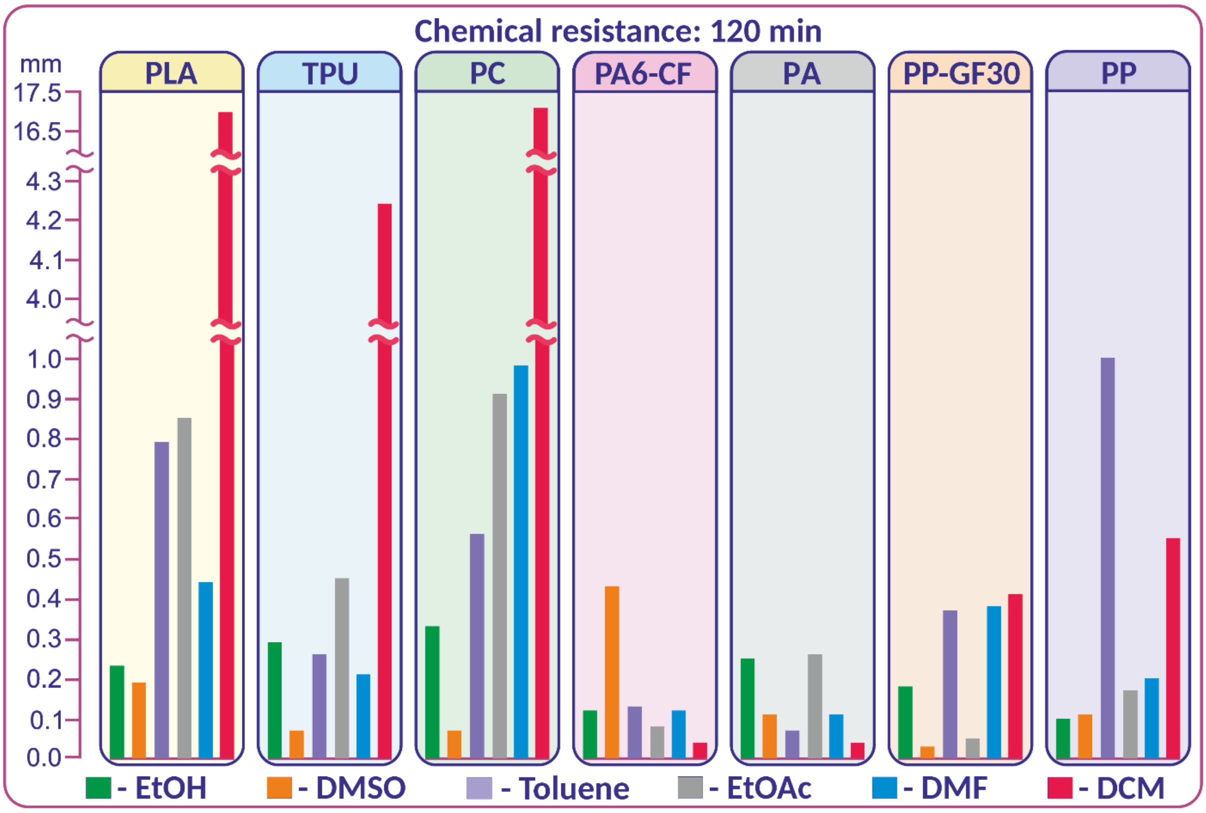

Figure S21. Diagram with quantitative calculations of the chemical resistance of 3D printed samples when exposed to various solvents for 120 minutes.

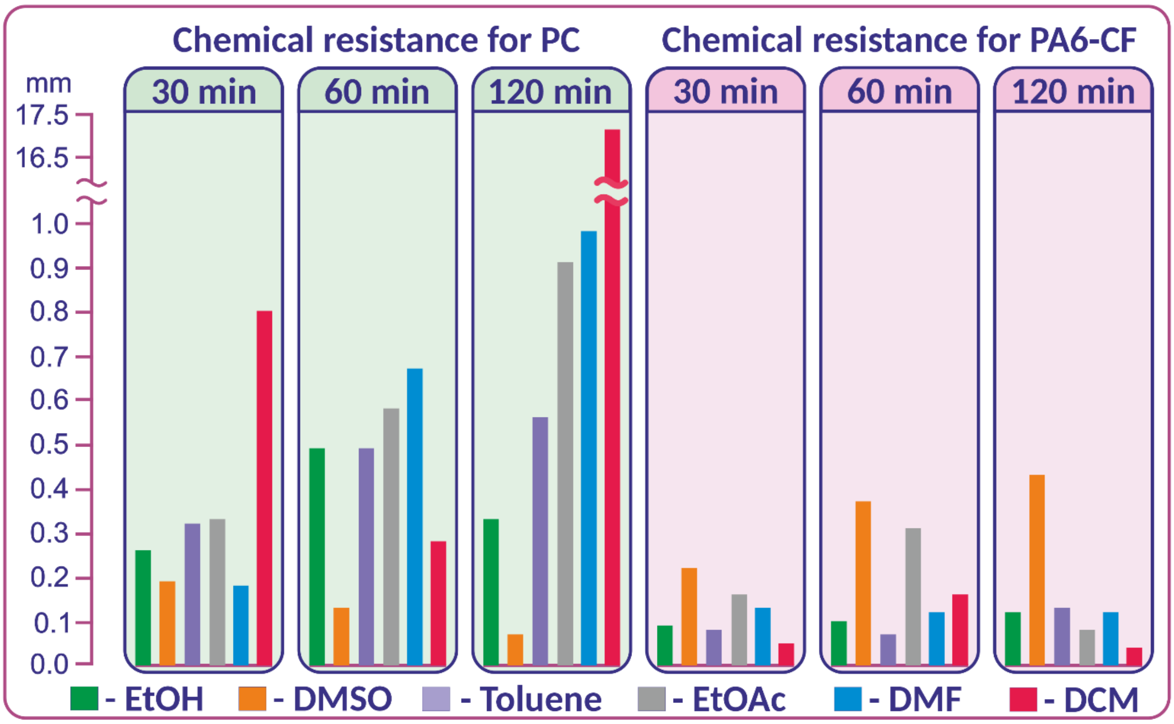

Figure S22. Comparative diagram with quantitative calculations of the chemical resistance of 3D printed samples from PC and PA6-CF when exposed to various solvents during different exposure times.

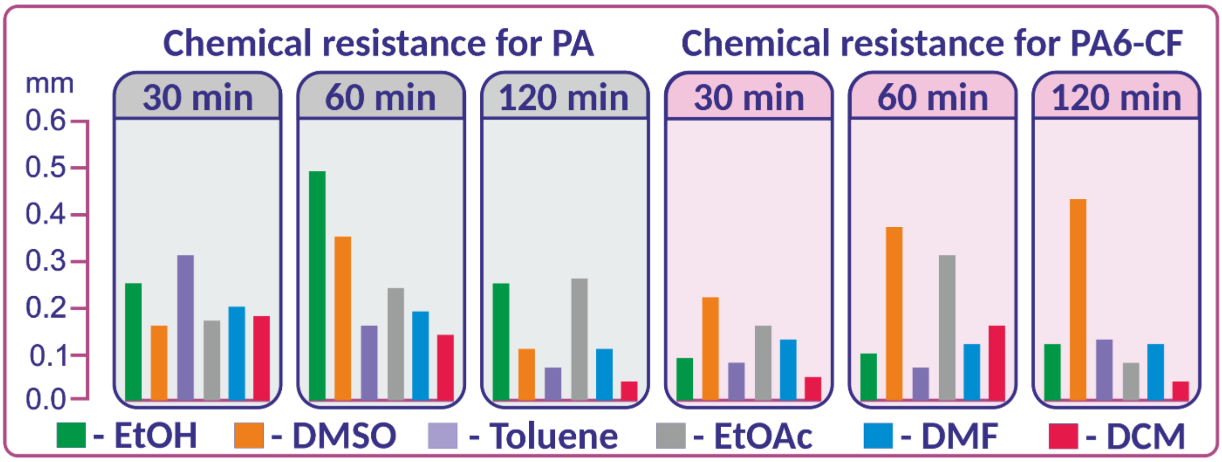

Figure S23. Comparative diagram with quantitative calculations of the chemical resistance of 3D printed samples from PA and PA6-CF when exposed to various solvents during different exposure times.

3. Thermal resistance of FFF parts

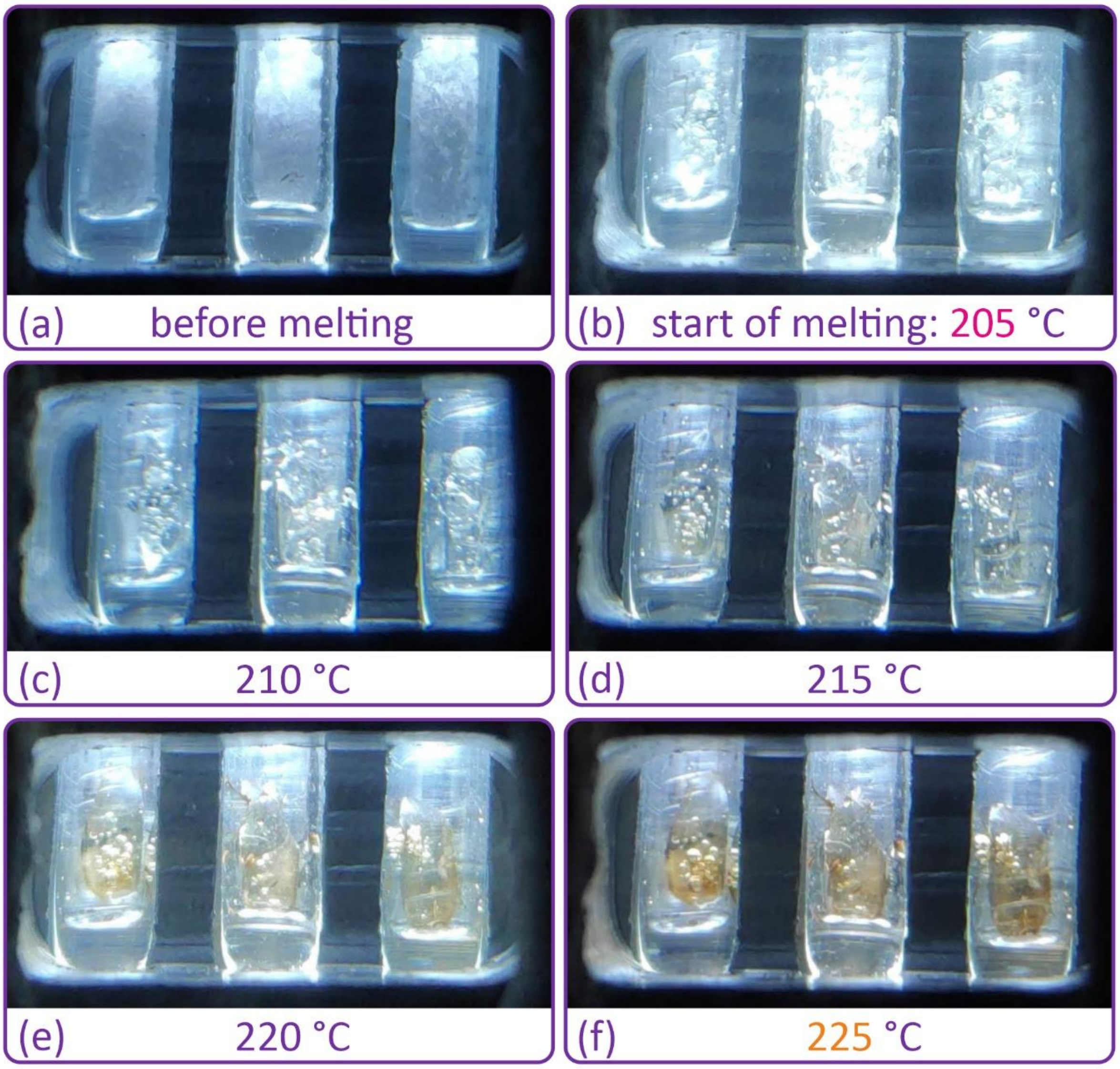

Figure S24. Melting point of PA measured using a melting-point apparatus: (a) – samples before melting; (b) – samples at the moment of the beginning of melting with the corresponding temperature; (c-e) – samples during further melting with the corresponding temperatures; (f) – samples at the time of melting at the temperature established during the test on the tile.

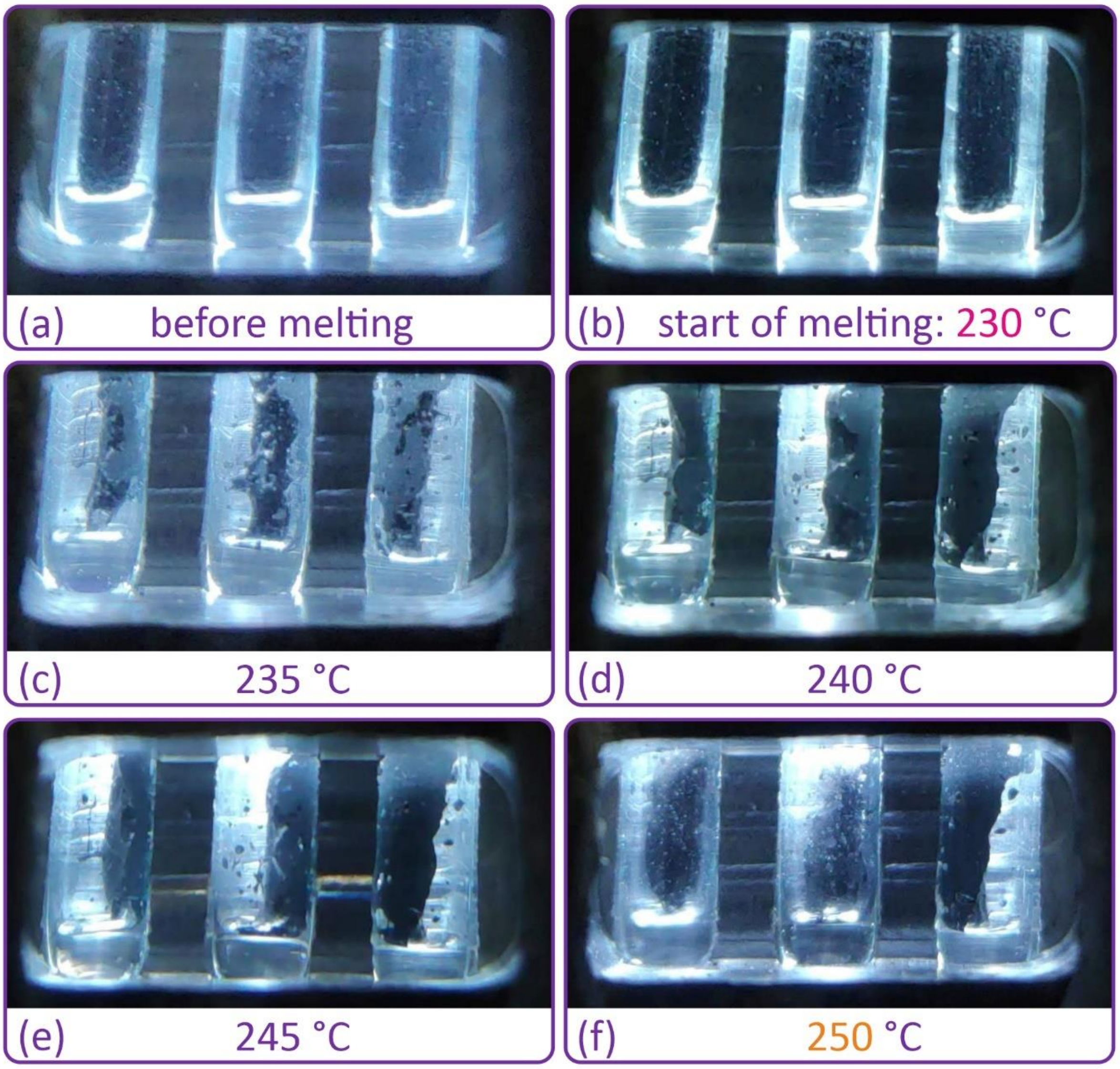

Figure S25. Melting point of PA6-CF measured using a melting-point apparatus: (a) – samples before melting; (b) – samples at the moment of the beginning of melting with the corresponding temperature; (c-e) – samples during further melting with the corresponding temperatures; (f) – samples at the moment of melting at the temperature established during the test on the tile.

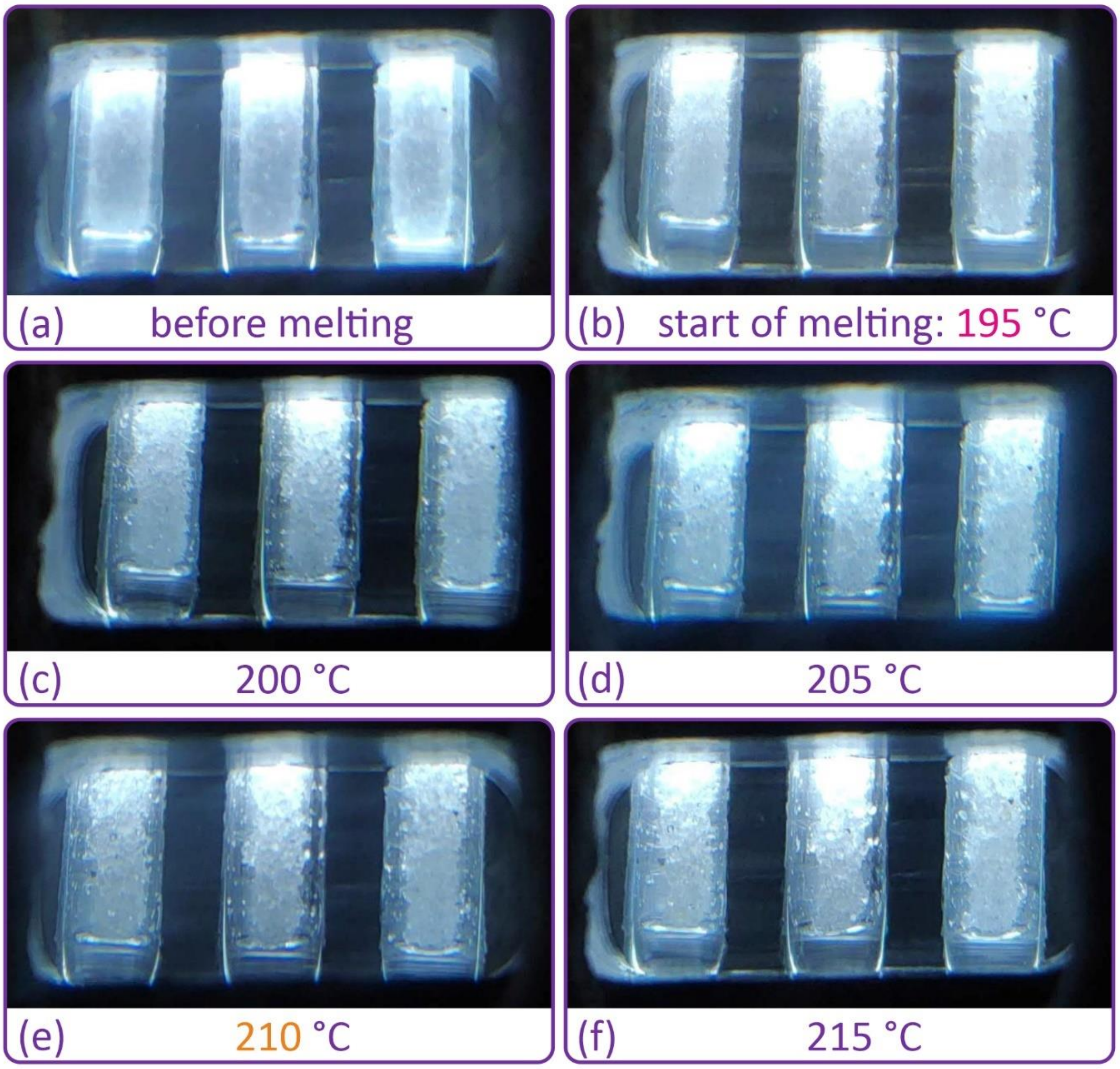

Figure S26. Melting point of PC+ measured using a melting-point apparatus: (a) – samples before melting; (b) – samples at the moment of the beginning of melting with the corresponding temperature; (c), (d) – samples during further melting with the corresponding temperatures; (e) – samples at the time of melting at the temperature established during the test on the tile; (f) – samples during further melting with the corresponding temperature.

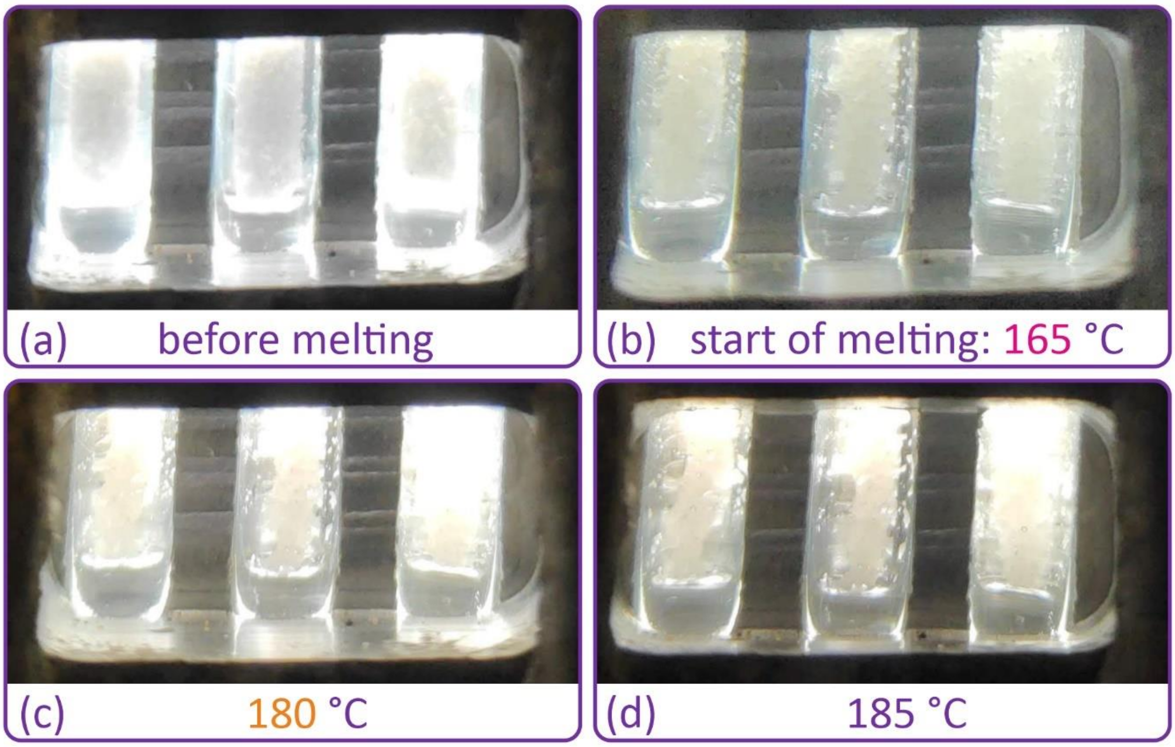

Figure S27. Melting temperature of PLA+ measured using a melting-point apparatus: (a) – samples before melting; (b) – samples at the moment of the beginning of melting with the corresponding temperature; (c) – samples at the moment of melting at the temperature established during the test on the tile; (d) – samples during further melting with the corresponding temperature.

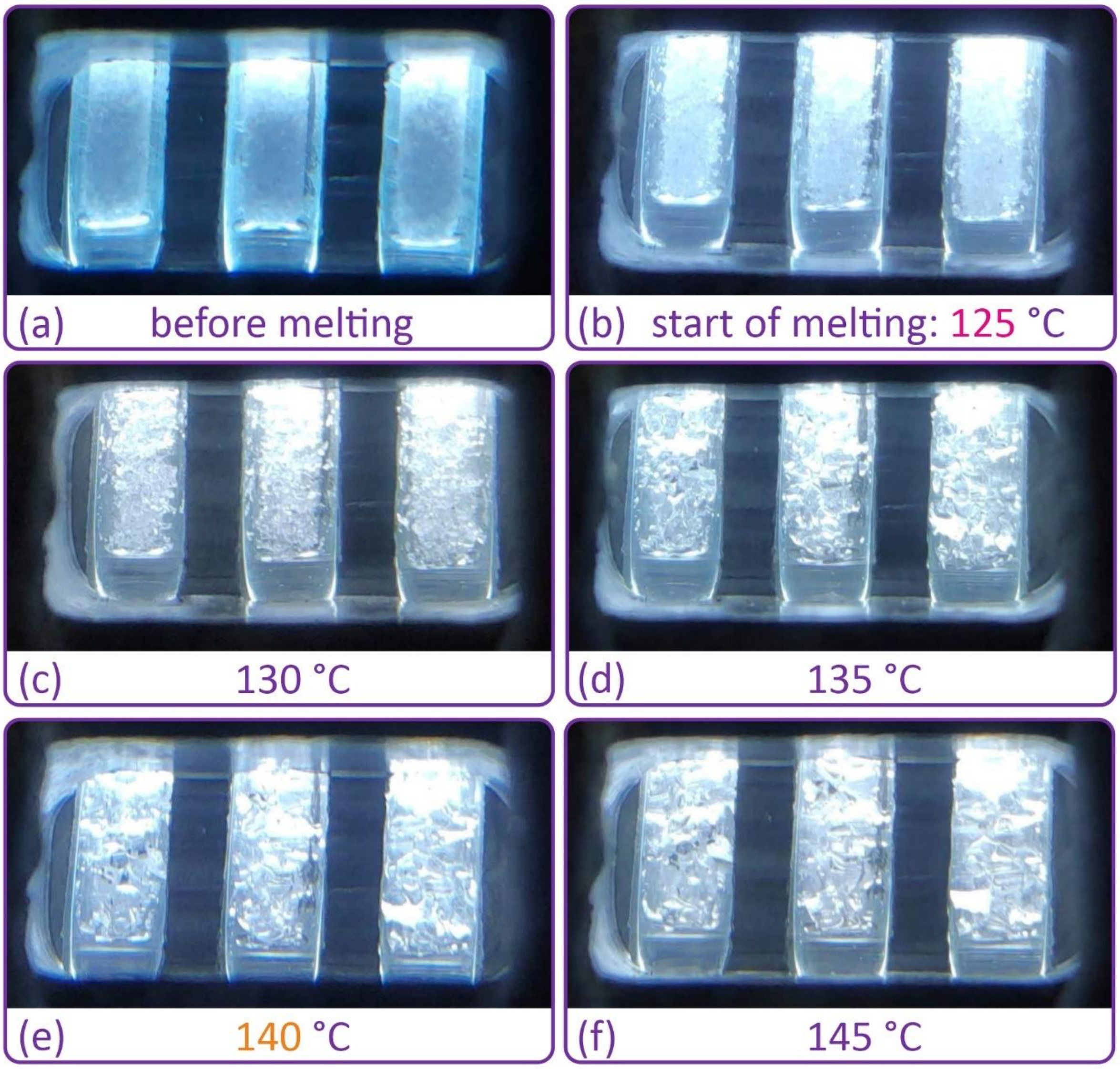

Figure S28. Melting temperature of PP measured using a melting-point apparatus: (a) – samples before melting; (b) – samples at the moment of the beginning of melting with the corresponding temperature; (c), (d) – samples during further melting with the corresponding temperatures; (e) – samples at the time of melting at the temperature established during the test on the tile; (f) – samples during further melting with the corresponding temperature.

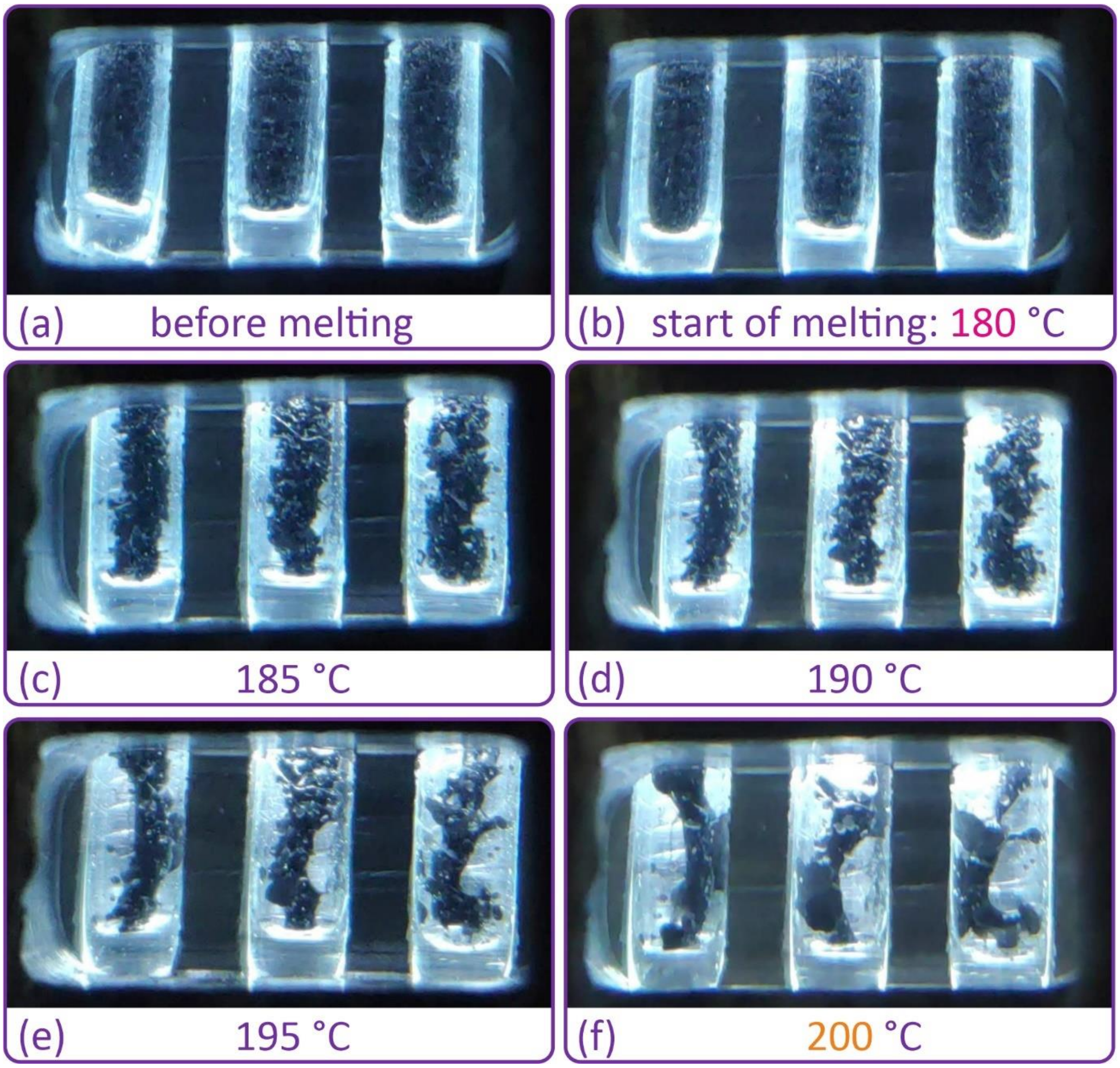

Figure S29. Melting point of PP-GF measured using a melting-point apparatus: (a) – samples before melting; (b) – samples at the moment of the beginning of melting with the corresponding temperature; (c-e) – samples during further melting with the corresponding temperatures; (f) – samples at the time of melting at the temperature established during the test on the tile.

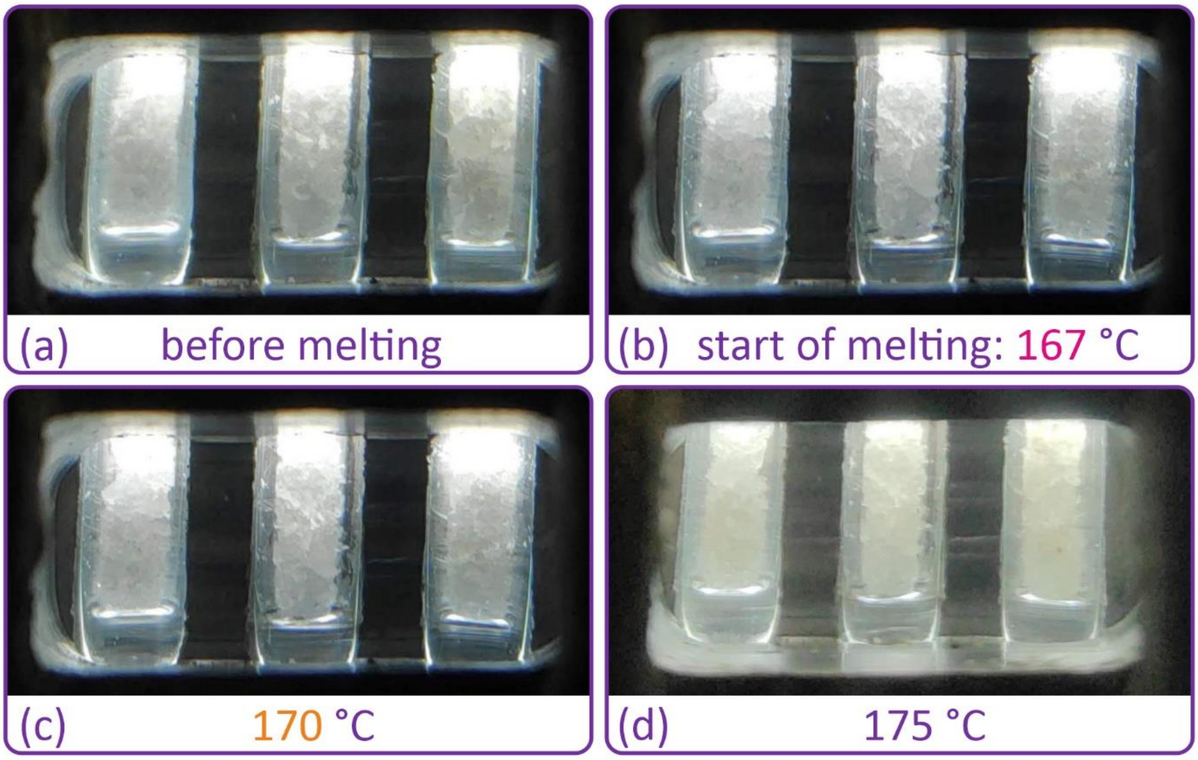

Figure S30. Melting point of TPU measured using a melting-point apparatus: (a) – samples before melting; (b) – samples at the moment of the beginning of melting with the corresponding temperature; (c) – samples at the moment of melting at the temperature established during the test on the tile; (d) – samples during further melting with the corresponding temperature.

4. Tensile testing

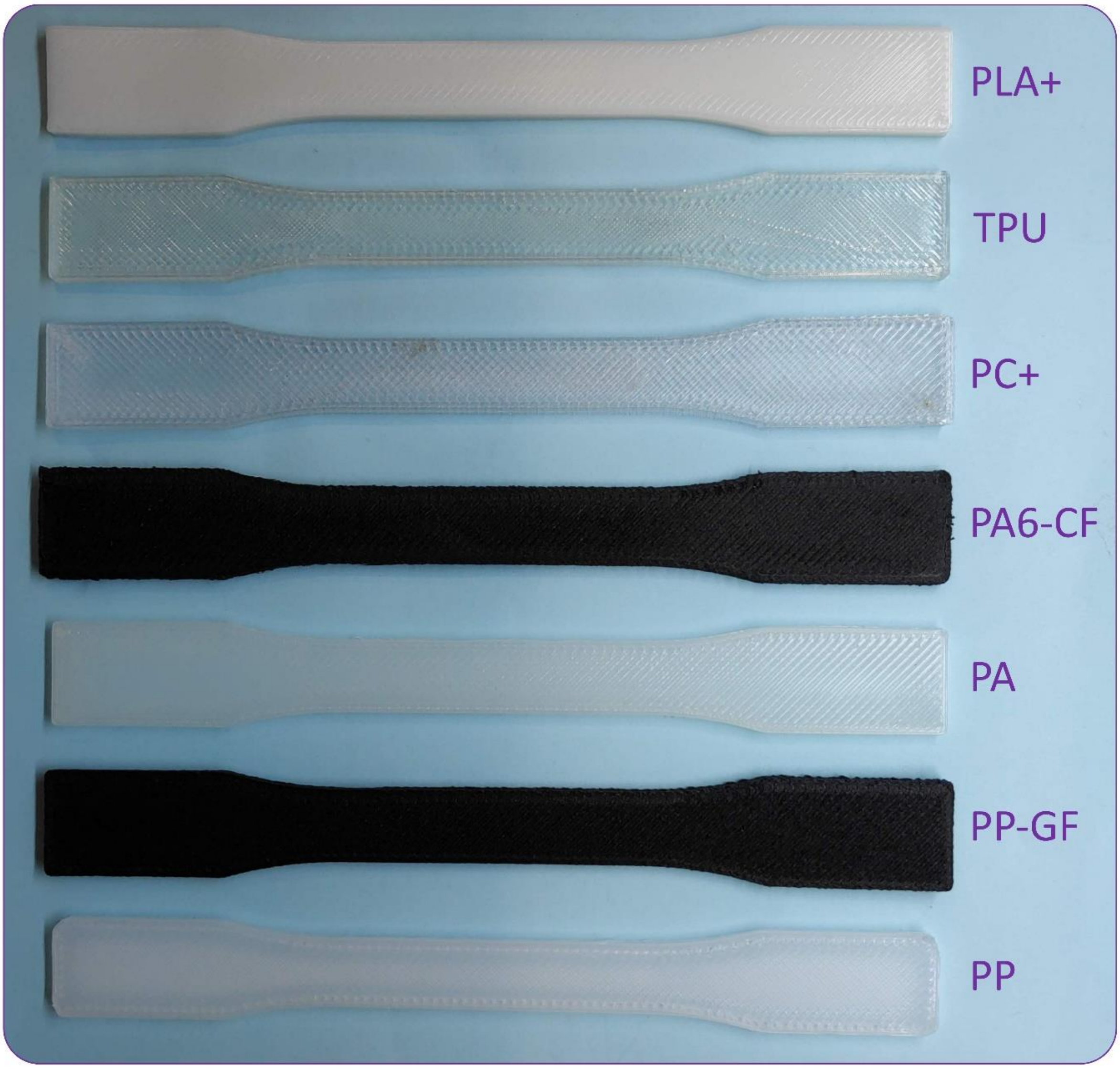

Figure S31. FFF samples for tensile testing with infill angle relative to the direction of load application equal to 45°.

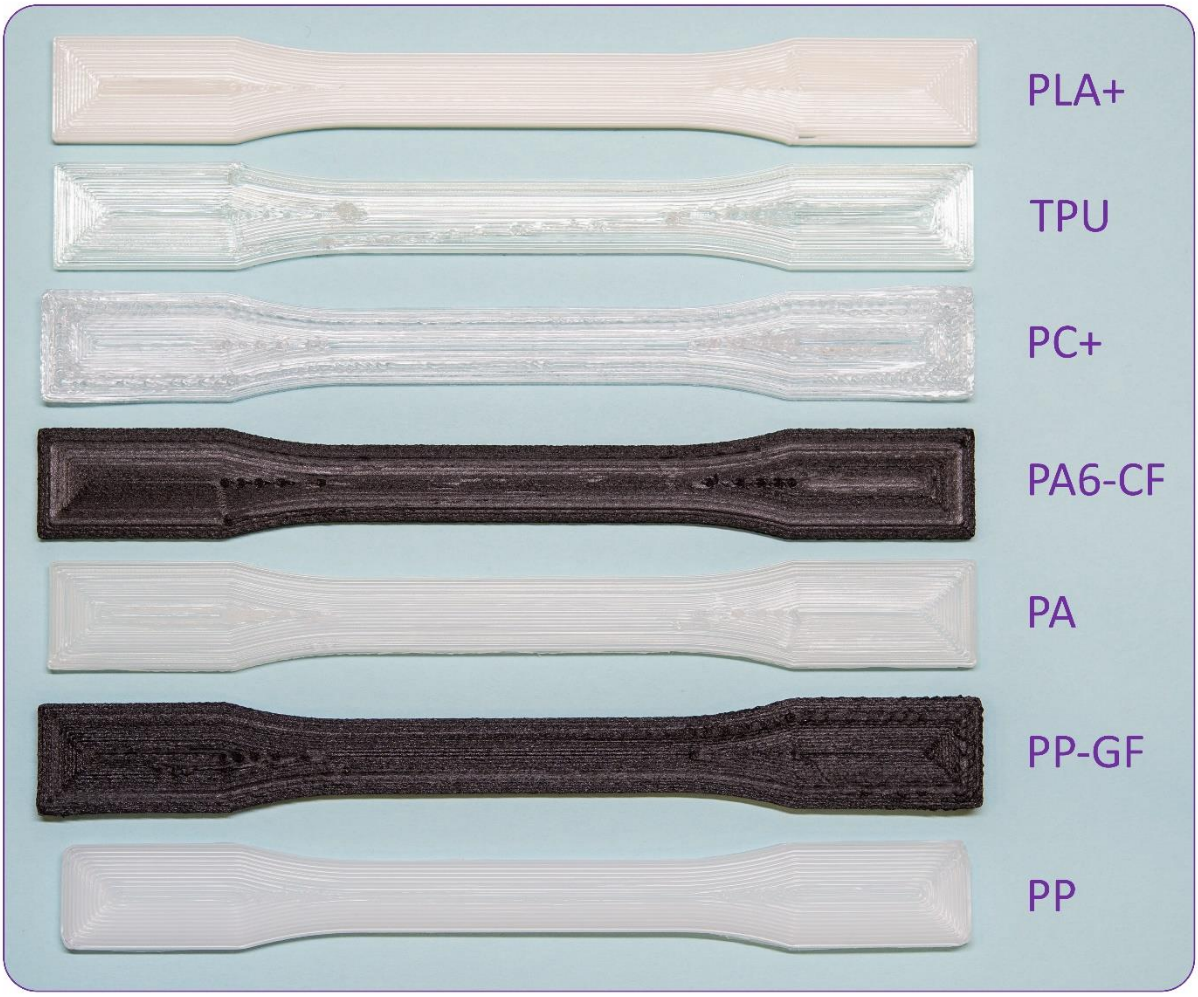

Figure S32. FFF samples for tensile testing with infill angle relative to the direction of load application equal to 0°.

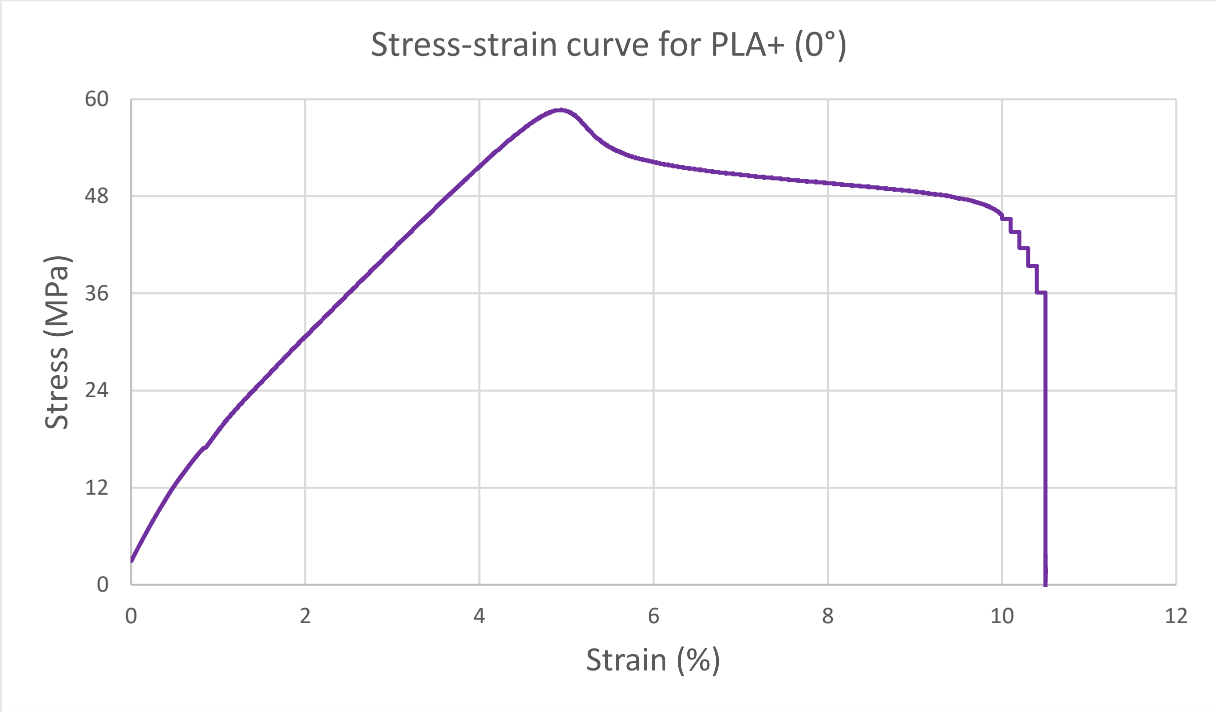

Figure S33. Stress-strain graph for a PLA+ FFF single sample with a print orientation angle equal to 0°.

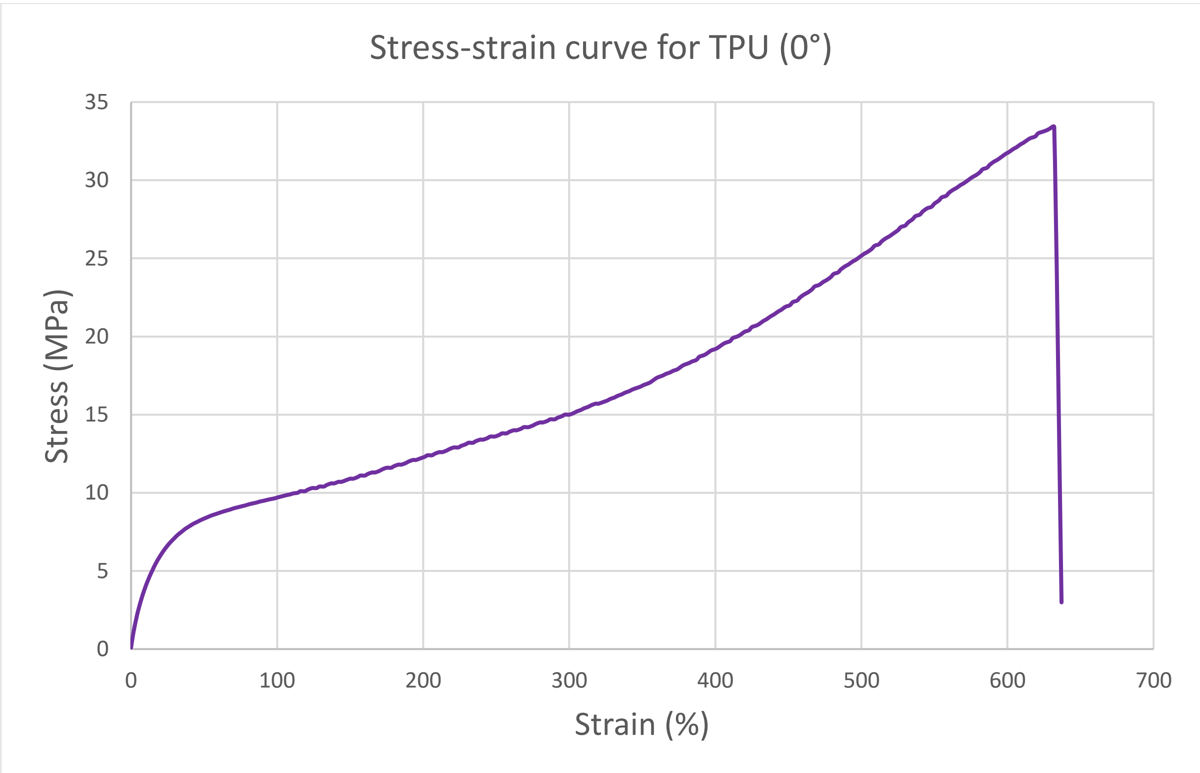

Figure S34. Stress-strain graph for a TPU FFF single sample with a print orientation angle equal to 0°.

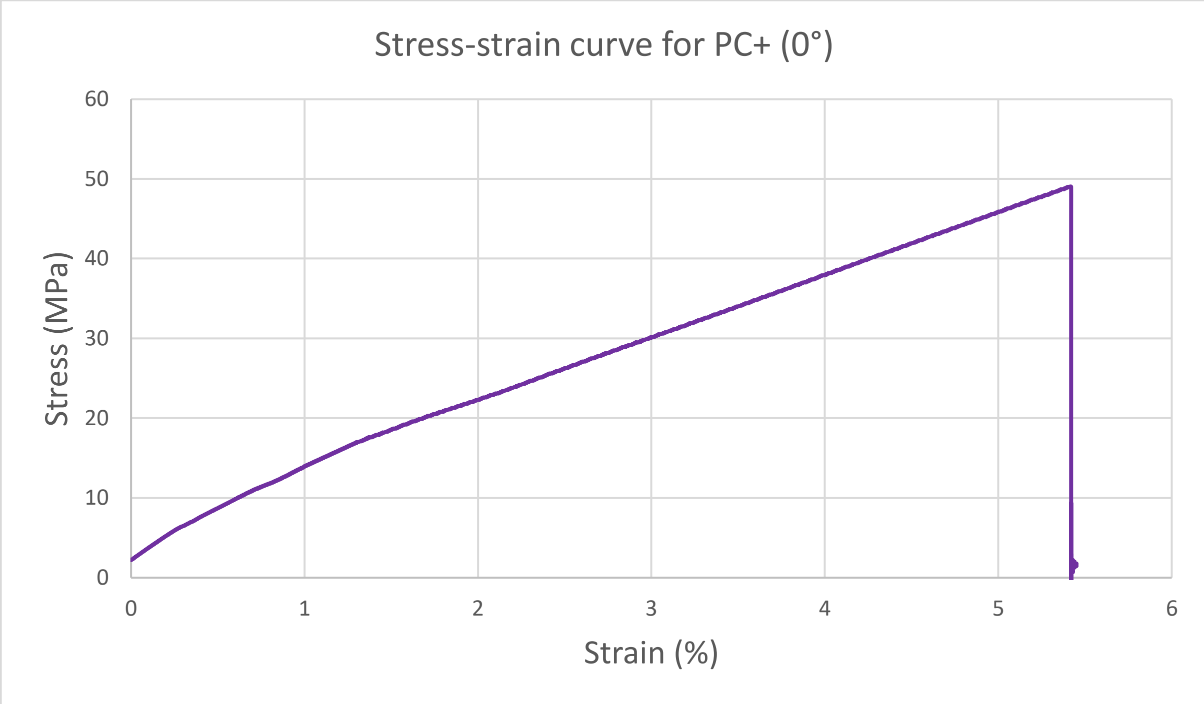

Figure S35. Stress-strain graph for a PC+ FFF single sample with a print orientation angle equal to 0°.

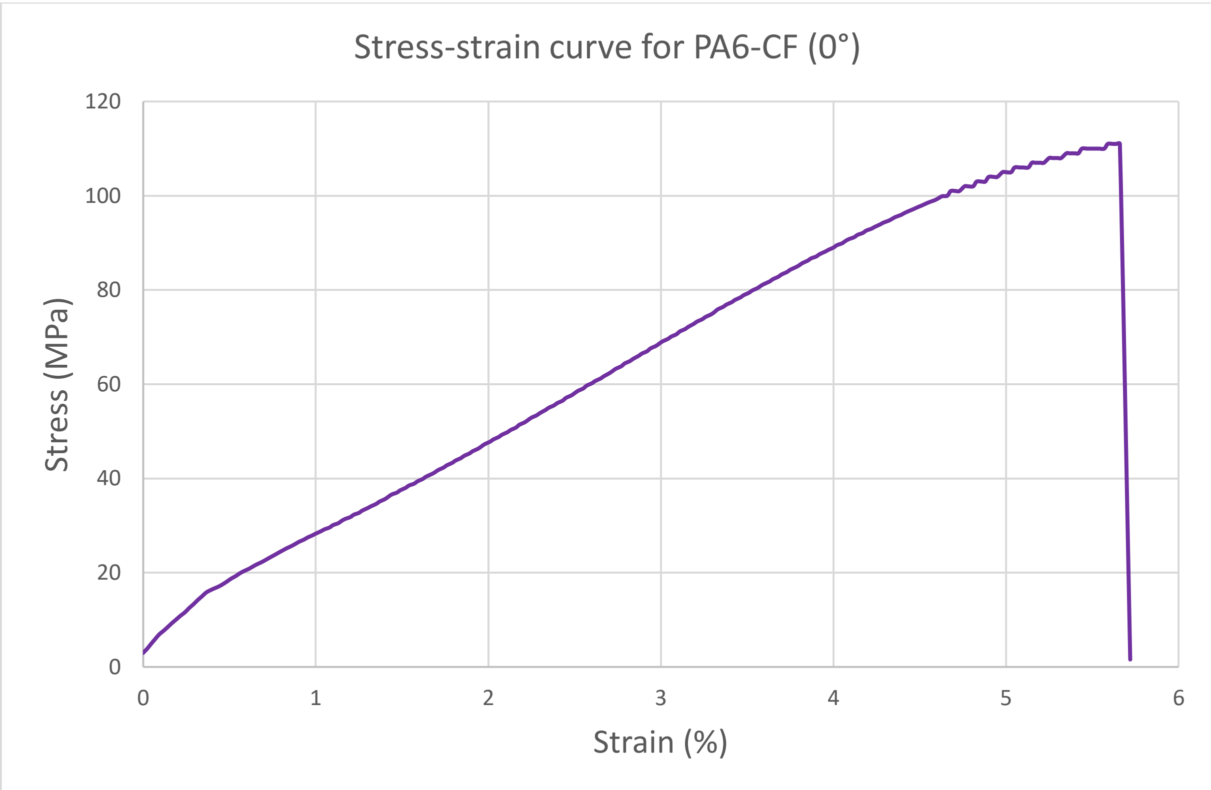

Figure S36. Stress-strain graph for a PA6-CF FFF single sample with a print orientation angle equal to 0°.

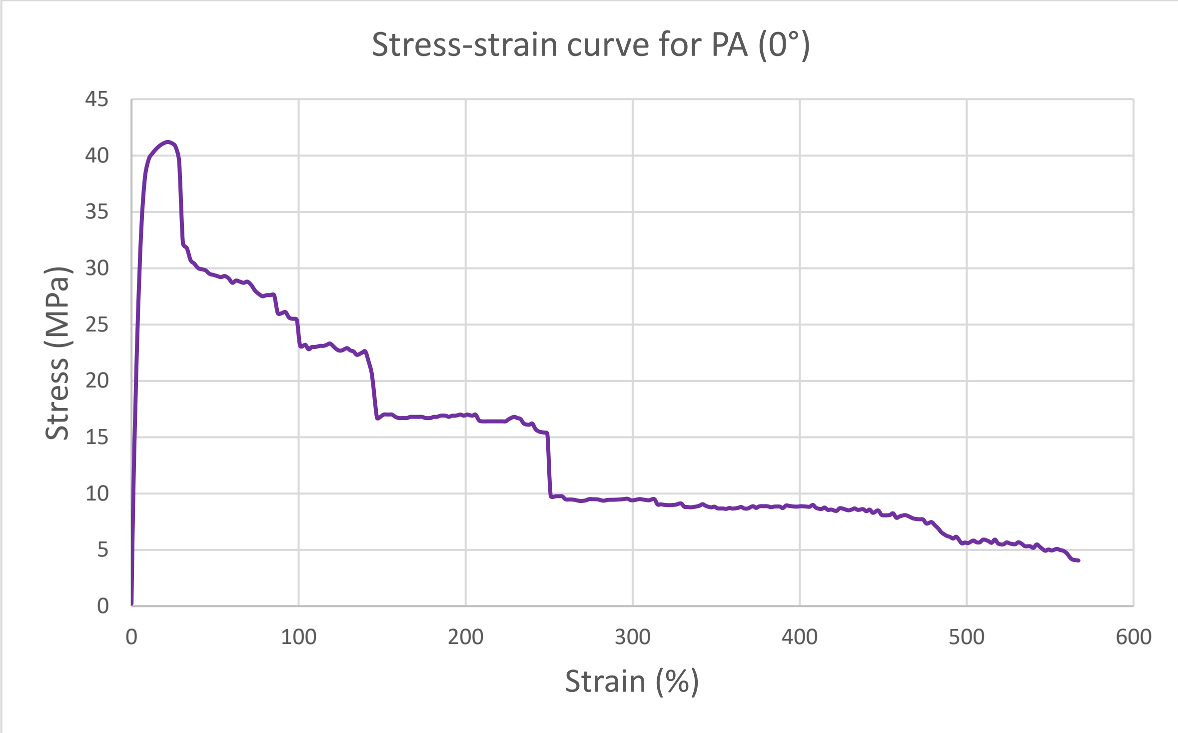

Figure S37. Stress-strain graph for a PA FFF single sample with a print orientation angle equal to 0°.

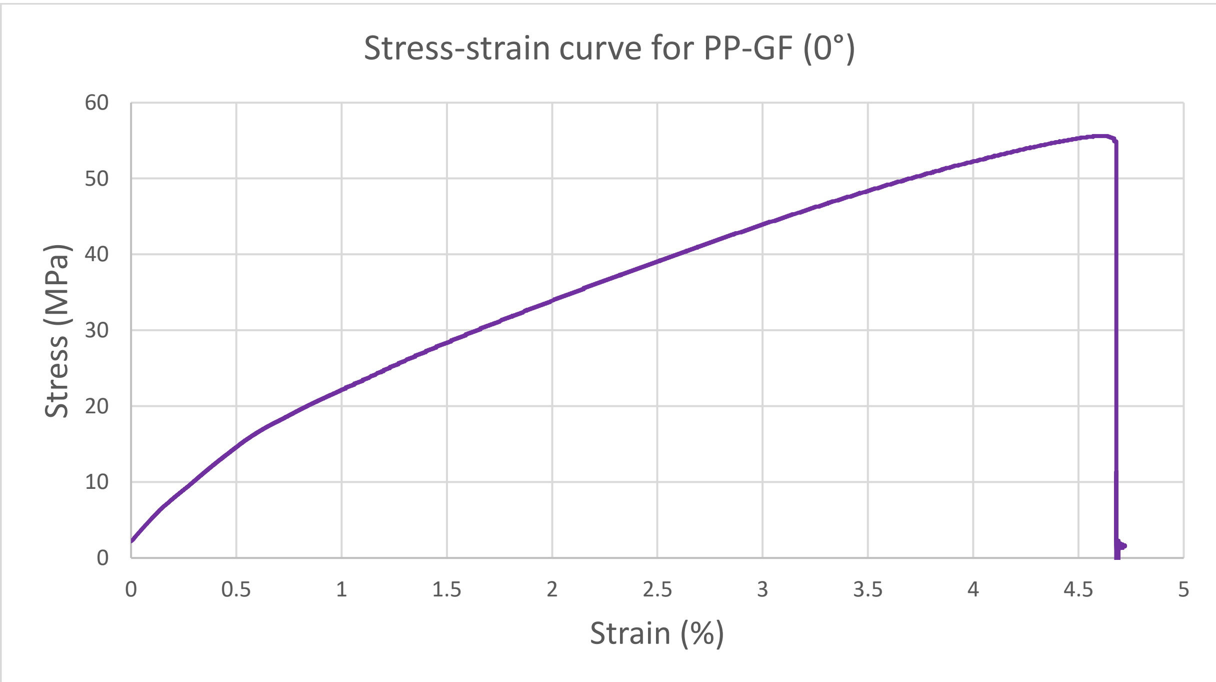

Figure S38. Stress-strain graph for a PP-GF FFF single sample with a print orientation angle equal to 0°.

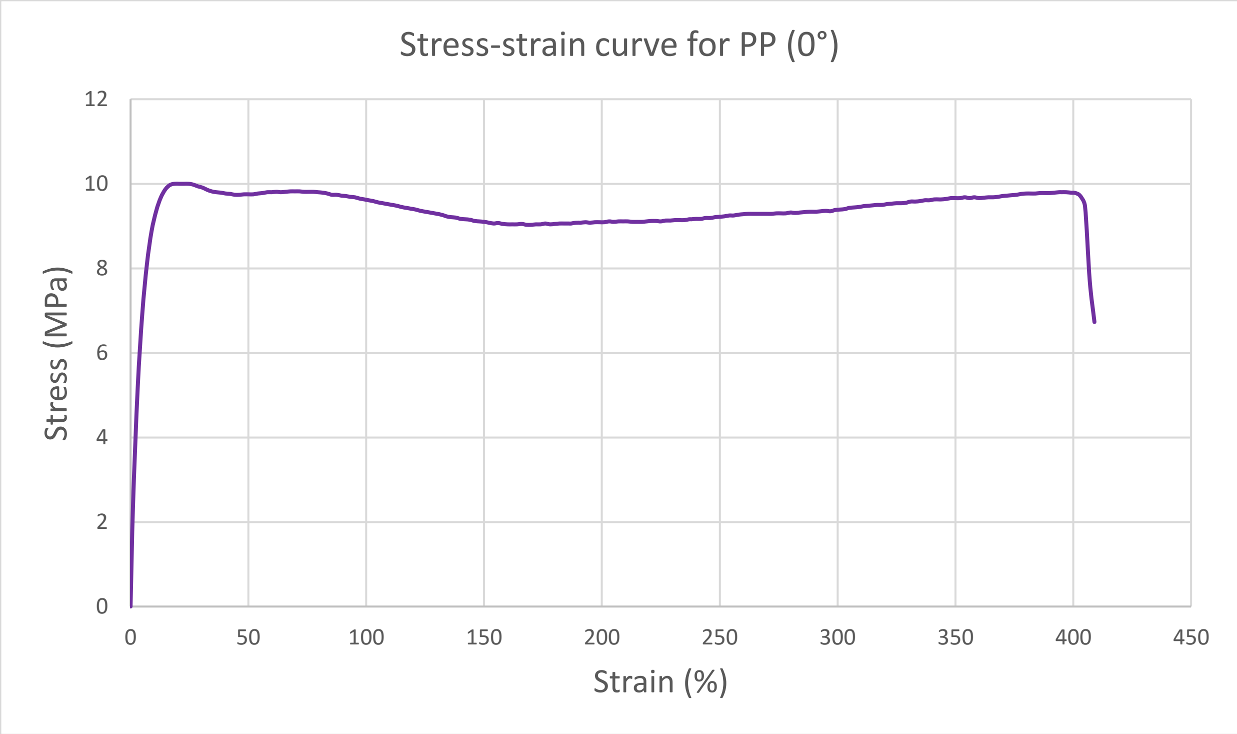

Figure S39. Stress-strain graph for a PP FFF single sample with a print orientation angle equal to 0°.

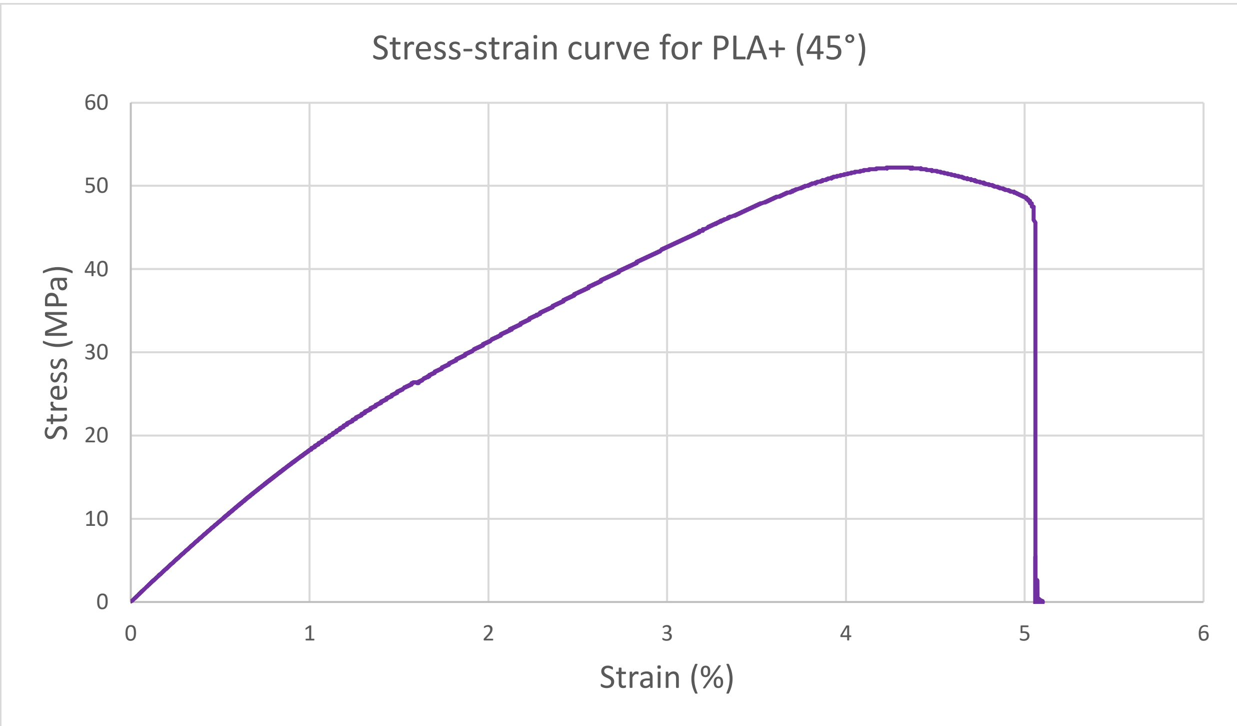

Figure S40. Stress-strain graph for a PLA+ FFF single sample with a print orientation angle equal to 45°.

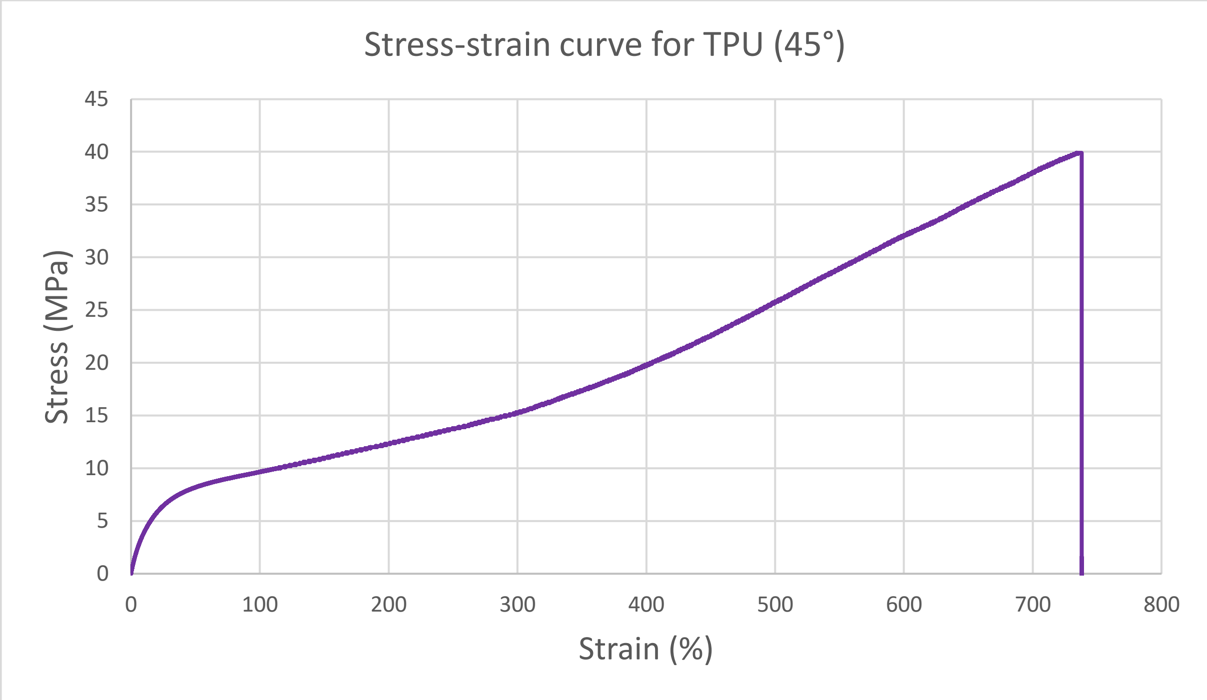

Figure S41. Stress-strain graph for a TPU FFF single sample with a print orientation angle equal to 45°.

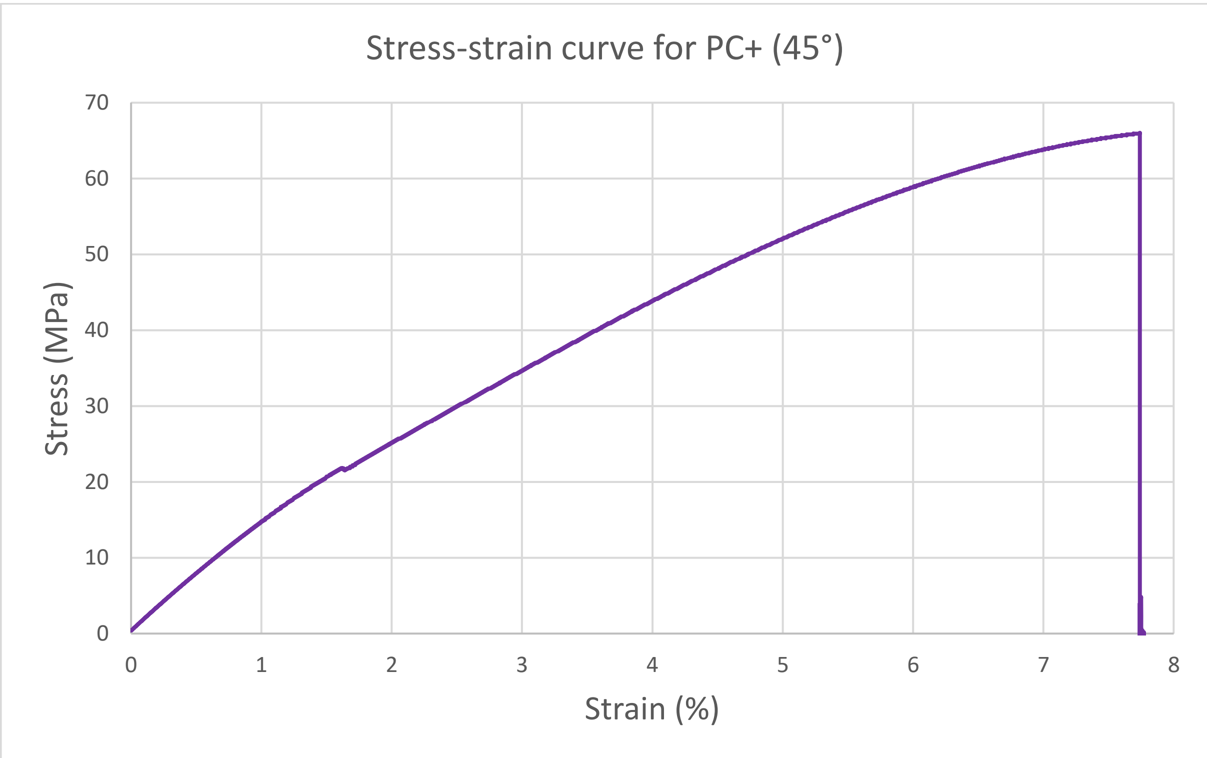

Figure S42. Stress-strain graph for a PC+ FFF single sample with a print orientation angle equal to 45°.

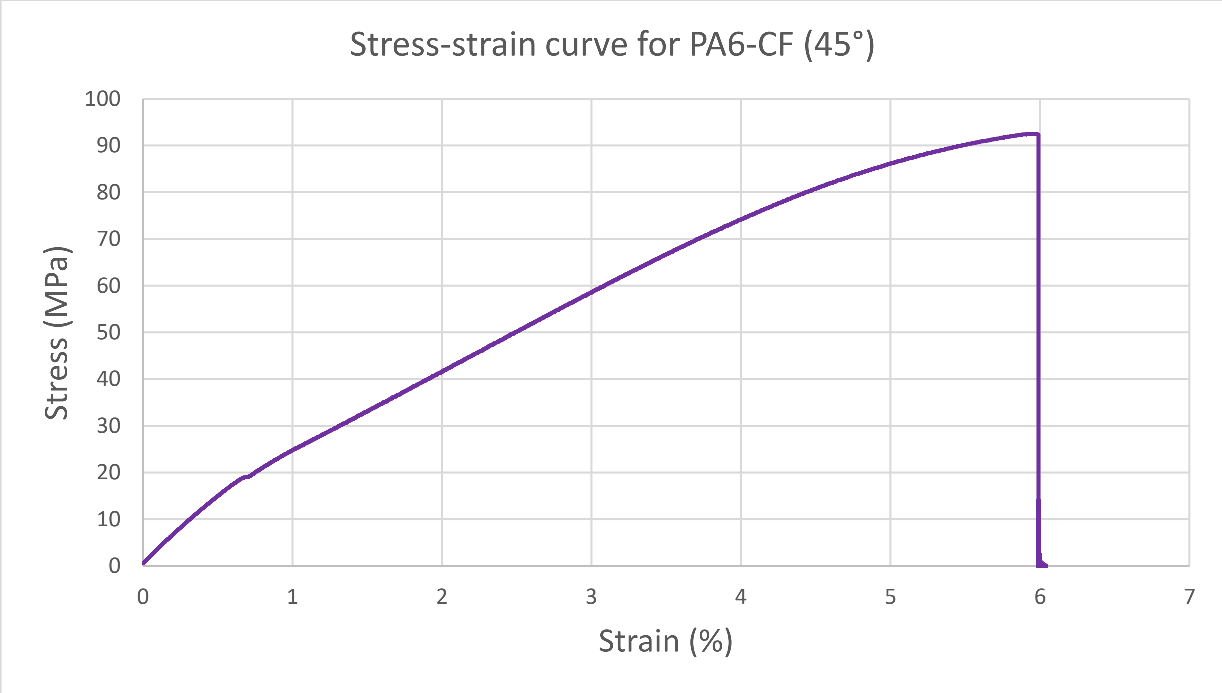

Figure S43. Stress-strain graph for a PA6-CF FFF single sample with a print orientation angle equal to 45°.

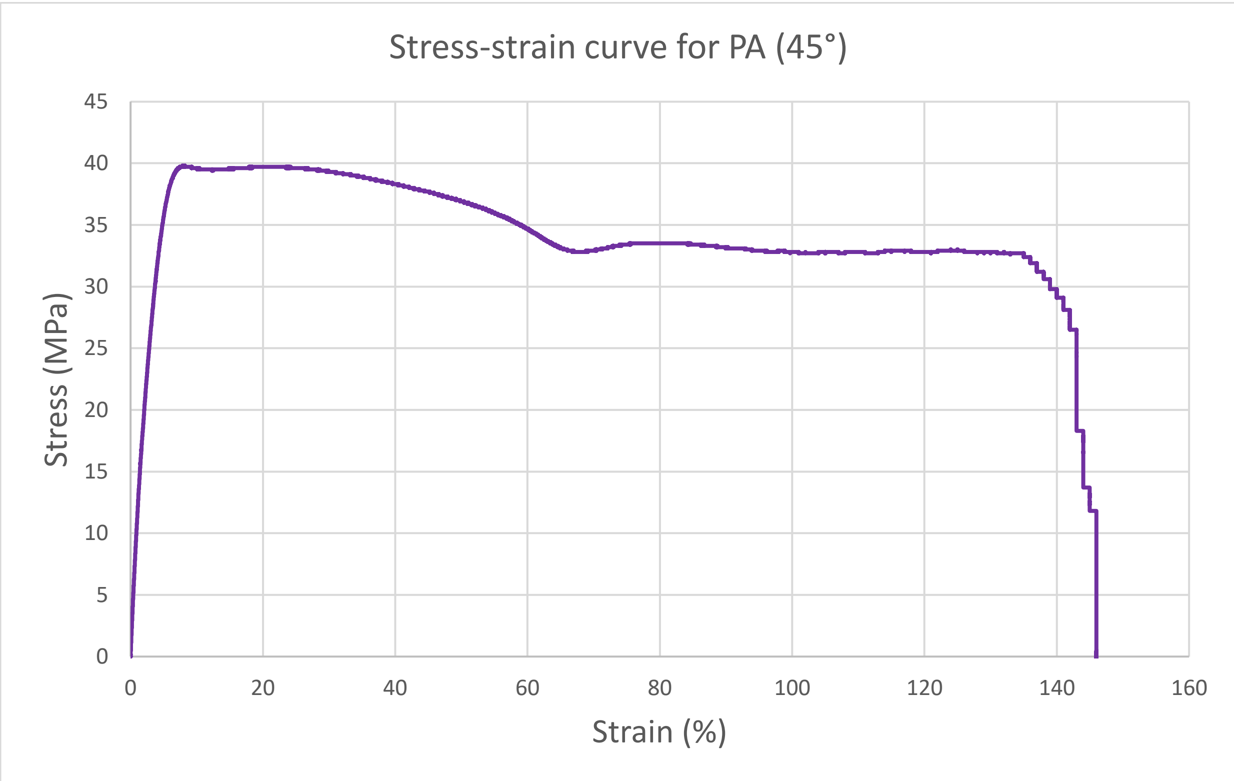

Figure S44. Stress-strain graph for a PA FFF single sample with a print orientation angle equal to 45°.

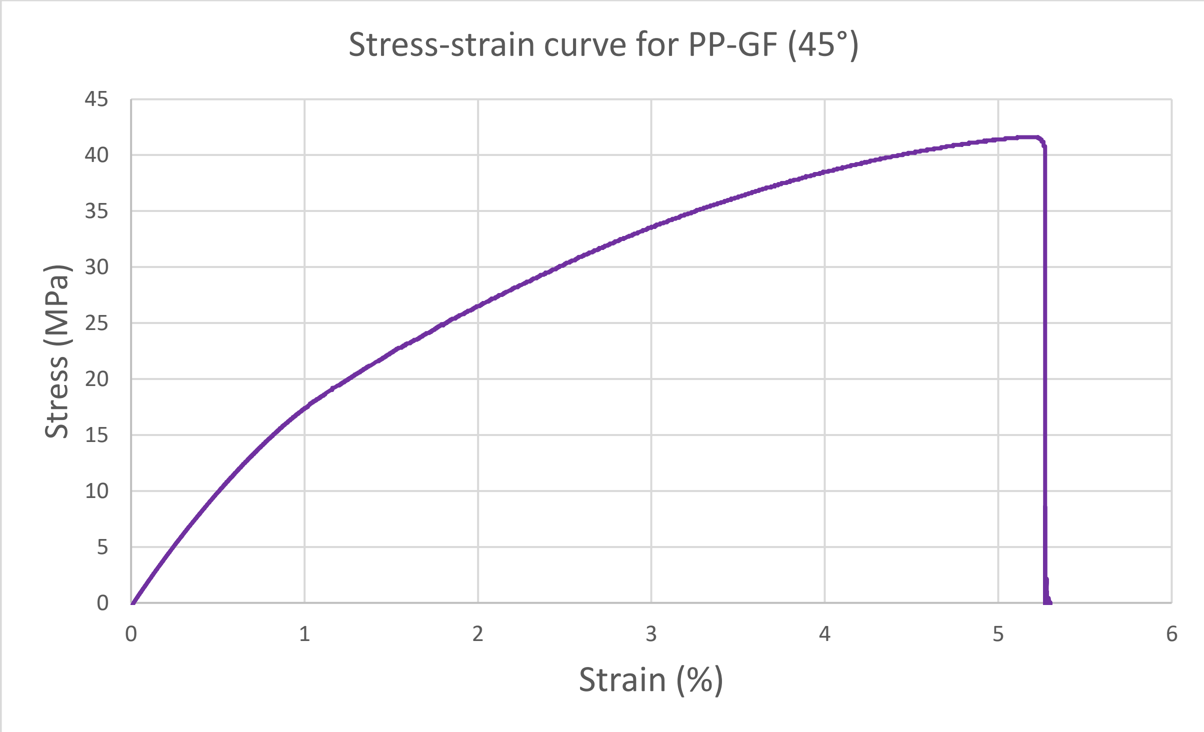

Figure S45. Stress-strain graph for a PP-GF FFF single sample with a print orientation angle equal to 45°.

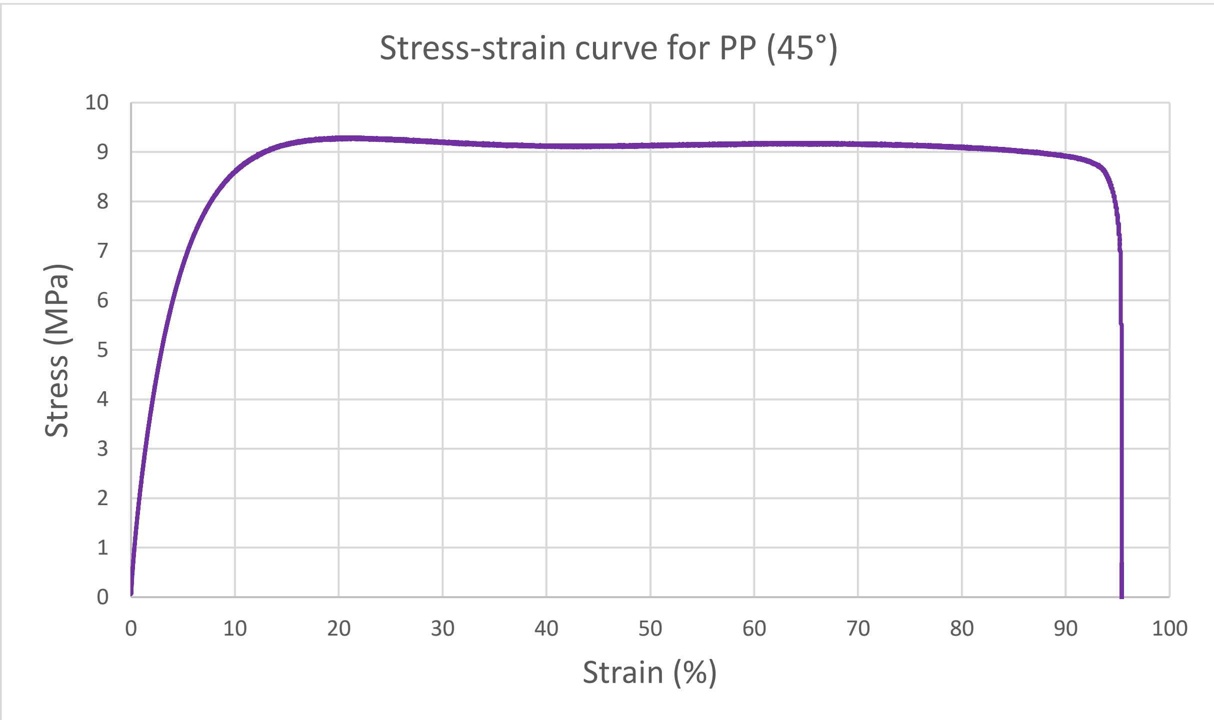

Figure S46. Stress-strain graph for a PP FFF single sample with a print orientation angle equal to 45°.

5. Study of the impermeability of the FFF parts

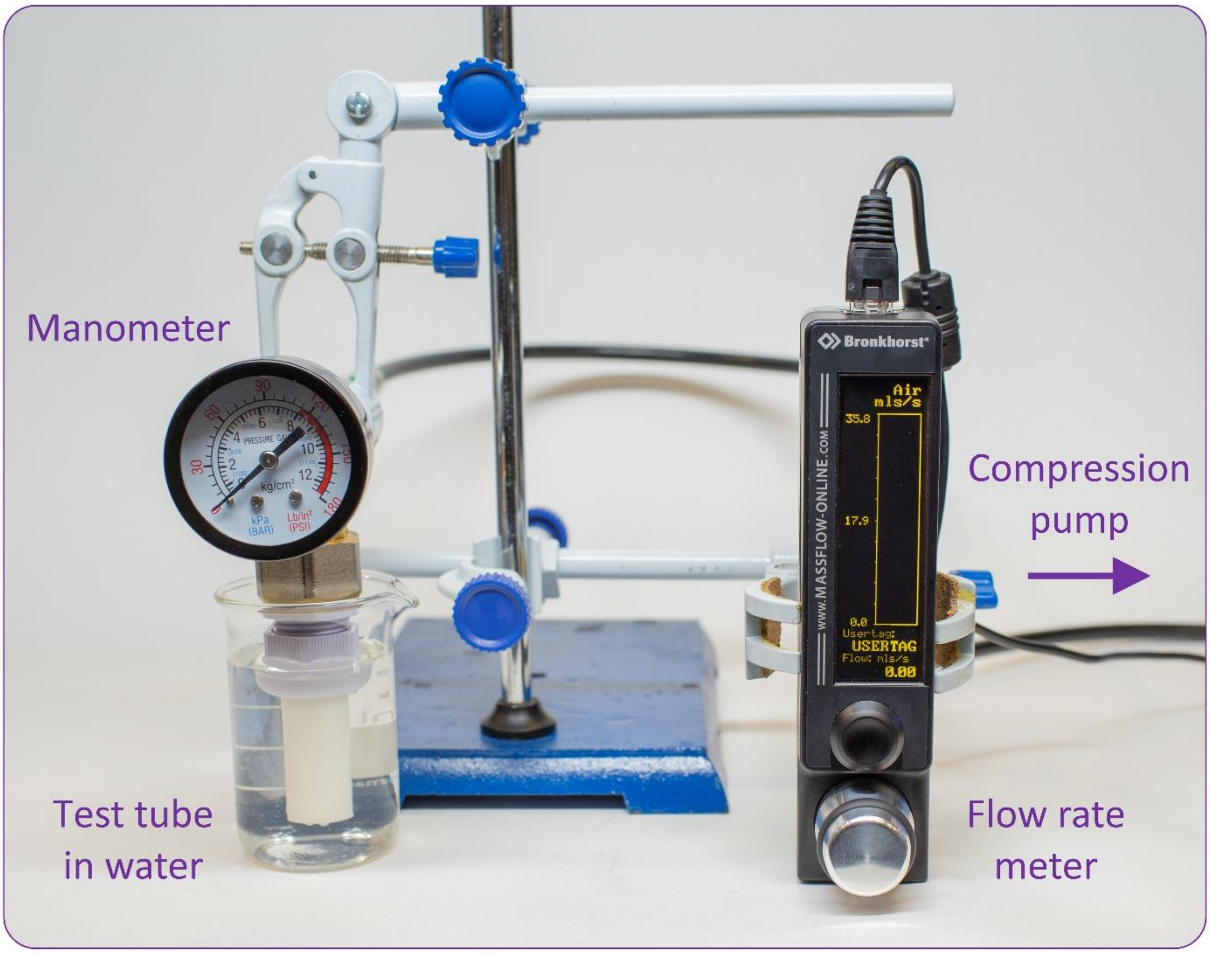

Figure S47. Installation for determining the microporosity of products.

Table S3. Influence of printing parameters on the impermeability and weight of test tubes printed from PLA+.

Extrusion multiplier (k-value)	Extrusion width (w)	Impermeability	Sample weight (g)	Flow rate meter readings (mL/sec)
		PLA+		
0.85	0.5	-	4.75	46.90*
0.85	0.5	-	4.75	46.90
0.85	0.5	-	4.82	46.90
mean value		**-**	**4.77**	**46.90**
0.95	0.5	-	5.31	22.03
0.95	0.5	-	5.31	25.79
0.95	0.5	-	5.35	21.25
mean value		**-**	**5.32**	**23.02**
1.05	0.5	-	5.87	4.85

1.05	0.5	-	5.88	7.51
1.05	0.5	-	5.95	0.59
mean value		**-**	**5.90**	**4.32**
1.1	0.5	-	6.14	1.97
1.1	0.5	-	6.14	3.00
1.1	0.5	-	6.23	0.00
mean value		**-**	**6.17**	**1.66**
0.85	0.6	-	5.70	0.20
0.85	0.6	-	5.63	5.47
0.85	0.6	-	5.64	4.07
mean value		**-**	**5.66**	**3.25**
0.95	0.6	-	6.29	0.00
0.95	0.6	-	6.30	0.00
0.95	0.6	+	6.37	0.00
mean value		**-**	**6.32**	**> 0.00****
1.05	0.6	+	6.95	0.00
1.05	0.6	+	6.94	0.00
1.05	0.6	+	7.05	0.00
mean value		**+**	**6.98**	**0.00**
1.1	0.6	+	7.26	0.00
1.1	0.6	+	7.24	0.00
1.1	0.6	+	7.40	0.00
mean value		**+**	**7.30**	**0.00**
0.85	0.7	-	5.64	1.25
0.85	0.7	-	5.63	0.79
0.85	0.7	-	5.72	0.18
mean value		**-**	**5.66**	**0.00**
0.95	0.7	+	6.31	0.00
0.95	0.7	+	6.32	0.00
0.95	0.7	+	6.40	0.00
mean value		**+**	**6.34**	**0.00**
1.05	0.7	+	6.95	0.00
1.05	0.7	+	6.98	0.00
1.05	0.7	+	7.07	0.00
mean value		**+**	**7.00**	**0.00**
1.1	0.7	+	7.27	0.00
1.1	0.7	+	7.26	0.00
1.1	0.7	+	7.38	0.00
mean value		**+**	**7.30**	**0.00**

*upper limit of sensitivity of the flow meter, ml/s

**outside the lower limit of the flow meter sensitivity

Table S4. Influence of printing parameters on the impermeability and weight of test tubes printed from PA6-CF.

Extrusion multiplier (k-value)	Extrusion width (w)	Impermeability	Sample weight (g)	Flow rate meter readings (mL/sec)
PA6-CF				
0.85	0.5	-	4.71	46.90*
0.85	0.5	-	4.72	46.90
0.85	0.5	-	4.71	46.90
mean value		**-**	**4.71**	**46.90**
0.95	0.5	-	5.24	38.90
0.95	0.5	-	5.23	40.61
0.95	0.5	-	5.22	41.92
mean value		**-**	**5.23**	**40.48**
1.05	0.5	-	5.64	12.42
1.05	0.5	-	5.80	8.64
1.05	0.5	-	5.70	7.98
mean value		**-**	**5.71**	**9.68**
1.1	0.5	-	6.03	2.77
1.1	0.5	-	6.09	1.86
1.1	0.5	-	6.05	2.95
mean value		**-**	**6.06**	**2.53**
0.85	0.6	-	5.54	2.47
0.85	0.6	-	5.54	4.31
0.85	0.6	-	5.60	1.49
mean value		**-**	**5.66**	**5.56**
0.95	0.6	-	6.31	0.00
0.95	0.6	-	6.27	0.00
0.95	0.6	-	6.18	0.00
mean value		**-**	**6.32**	**> 0.00**
1.05	0.6	+	7.00	0.00
1.05	0.6	+	6.99	0.00
1.05	0.6	+	6.87	0.00
mean value		**+**	**6.98**	**0.00**
1.1	0.6	+	7.23	0.00
1.1	0.6	+	7.21	0.00
1.1	0.6	+	7.19	0.00
mean value		**+**	**7.30**	**0.00**
0.85	0.7	-	5.61	0.08
0.85	0.7	-	5.59	0.00
0.85	0.7	-	5.55	0.00
mean value		**-**	**5.58**	**0.03**
0.95	0.7	+	6.24	0.00

0.95	0.7	+	6.27	0.00
0.95	0.7	+	6.26	0.00
mean value		**+**	**6.26**	**0.00**
1.05	0.7	+	6.87	0.00
1.05	0.7	+	6.91	0.00
1.05	0.7	+	6.88	0.00
mean value		**+**	**6.89**	**0.00**
1.1	0.7	+	7.19	0.00
1.1	0.7	+	7.19	0.00
1.1	0.7	+	7.17	0.00
mean value		**+**	**7.18**	**0.00**

Table S5. Influence of printing parameters on the impermeability and weight of test tubes printed from PA.

Extrusion multiplier (k-value)	Extrusion width (w)	Impermeability	Sample weight (g)	Flow rate meter readings (mL/sec)
PA				
0.85	0.6	-	5.01	8.31
0.85	0.6	-	4.96	2.74
0.85	0.6	-	5.00	3.07
mean value		**-**	**4.99**	**4.71**
0.95	0.6	-	5.69	0.00
0.95	0.6	-	5.66	0.00
0.95	0.6	-	5.67	0.00
mean value		**-**	**5.67**	**> 0.00***
1.05	0.6	+	6.14	0.00
1.05	0.6	+	6.11	0.00
1.05	0.6	+	6.10	0.00
mean value		**+**	**6.12**	**0.00**
1.1	0.6	+	6.52	0.00
1.1	0.6	+	6.52	0.00
1.1	0.6	+	6.52	0.00
mean value		**+**	**6.52**	**0.00**

*outside the lower limit of the flow meter sensitivity

Table S6. Influence of printing parameters on the impermeability and weight of test tubes printed from PP-GF.

Extrusion multiplier (k-value)	Extrusion width (w)	Impermeability	Sample weight (g)	Flow rate meter readings (mL/sec)
PP-GF				
0.85	0.6	-	5.22	2.96
0.85	0.6	-	5.20	7.31
0.85	0.6	-	5.21	3.39
mean value		**-**	**5.21**	**4.55**
0.95	0.6	-	5.86	1.43
0.95	0.6	-	5.85	0.00
0.95	0.6	-	5.84	0.09
mean value		**-**	**5.85**	**0.51**
1.05	0.6	+	6.36	0.00
1.05	0.6	-	6.34	0.00
1.05	0.6	+	6.33	0.00
mean value		**-**	**6.34**	**> 0.00***
1.1	0.6	+	6.69	0.00
1.1	0.6	+	6.67	0.00
1.1	0.6	+	6.69	0.00
mean value		**+**	**6.68**	**0.00**

*outside the lower limit of the flow meter sensitivity

Table S7. Influence of printing parameters on the impermeability and weight of test tubes printed from PP.

Extrusion multiplier (k-value)	Extrusion width (w)	Impermeability	Sample weight (g)	Flow rate meter readings (mL/sec)
PP				
0.85	0.6	+	4.02	0.00
0.85	0.6	+	3.97	0.00
0.85	0.6	+	4.04	0.00
mean value		**+**	**4.01**	**0.00**
0.95	0.6	+	4.49	0.00
0.95	0.6	+	4.41	0.00
0.95	0.6	+	4.42	0.00
mean value		**+**	**4.44**	**0.00**
1.05	0.6	+	4.87	0.00
1.05	0.6	+	4.85	0.00
1.05	0.6	+	4.96	0.00
mean value		**+**	**4.89**	**0.00**

Table S8. Influence of printing parameters on the impermeability and weight of test tubes printed from TPU.

Extrusion multiplier (k-value)	Extrusion width (w)	Impermeability	Sample weight (g)	Flow rate meter readings (mL/sec)
TPU				
0.85	0.6	-	5.24	0.13
0.85	0.6	-	5.24	0.41
0.85	0.6	-	5.24	46.90
mean value		**-**	**5.24**	**15.81**
0.95	0.6	-	5.87	15.43
0.95	0.6	+	5.85	0.00
0.95	0.6	+	5.88	0.00
mean value		**-**	**5.87**	**5.14**
1.05	0.6	+	6.48	0.00
1.05	0.6	-	6.48	0.00
1.05	0.6	+	6.47	0.00
mean value		**-**	**6.48**	**0.00**
1.1	0.6	+	6.76	0.00
1.1	0.6	+	6.77	0.00
1.1	0.6	+	6.77	0.00
mean value		**+**	**6.77**	**0.00**

Table S9. Influence of printing parameters on the impermeability and weight of test tubes printed from PC+.

Extrusion multiplier (k-value)	Extrusion width (w)	Impermeability	Sample weight (g)	Flow rate meter readings (mL/sec)
PC+				
0.85	0.6	-	5.71	9.12
0.85	0.6	-	5.70	10.16
0.85	0.6	-	5.70	10.78
mean value		**-**	**5.70**	**10.02**
0.95	0.6	-	6.32	1.53
0.95	0.6	-	6.36	1.18
0.95	0.6	-	6.36	1.10
mean value		**-**	**6.35**	**1.27**
1.05	0.6	-	7.04	0.72
1.05	0.6	-	7.02	1.05
1.05	0.6	-	7.02	0.48
mean value		**-**	**7.03**	**0.75**
1.1	0.6	-	7.38	0.57

1.1	0.6	-	7.41	0.27
1.1	0.6	-	7.43	0.57
mean value		**-**	**7.41**	**0.47**
0.85	0.7	-	5.70	2.63
0.85	0.7	-	5.70	2.38
0.85	0.7	-	5.72	3.19
mean value		**-**	**5.71**	**2.73**
1.2	0.6	-	7.79	0.00
1.2	0.6	-	7.78	0.00
1.2	0.6	-	7.79	0.00
mean value		**-**	**7.79**	**> 0.00***
1.3	0.6	+	8.42	0.00
1.3	0.6	+	8.35	0.00
1.3	0.6	+	8.42	0.00
mean value		**+**	**8.40**	**0.00**

*outside the lower limit of the flow meter sensitivity

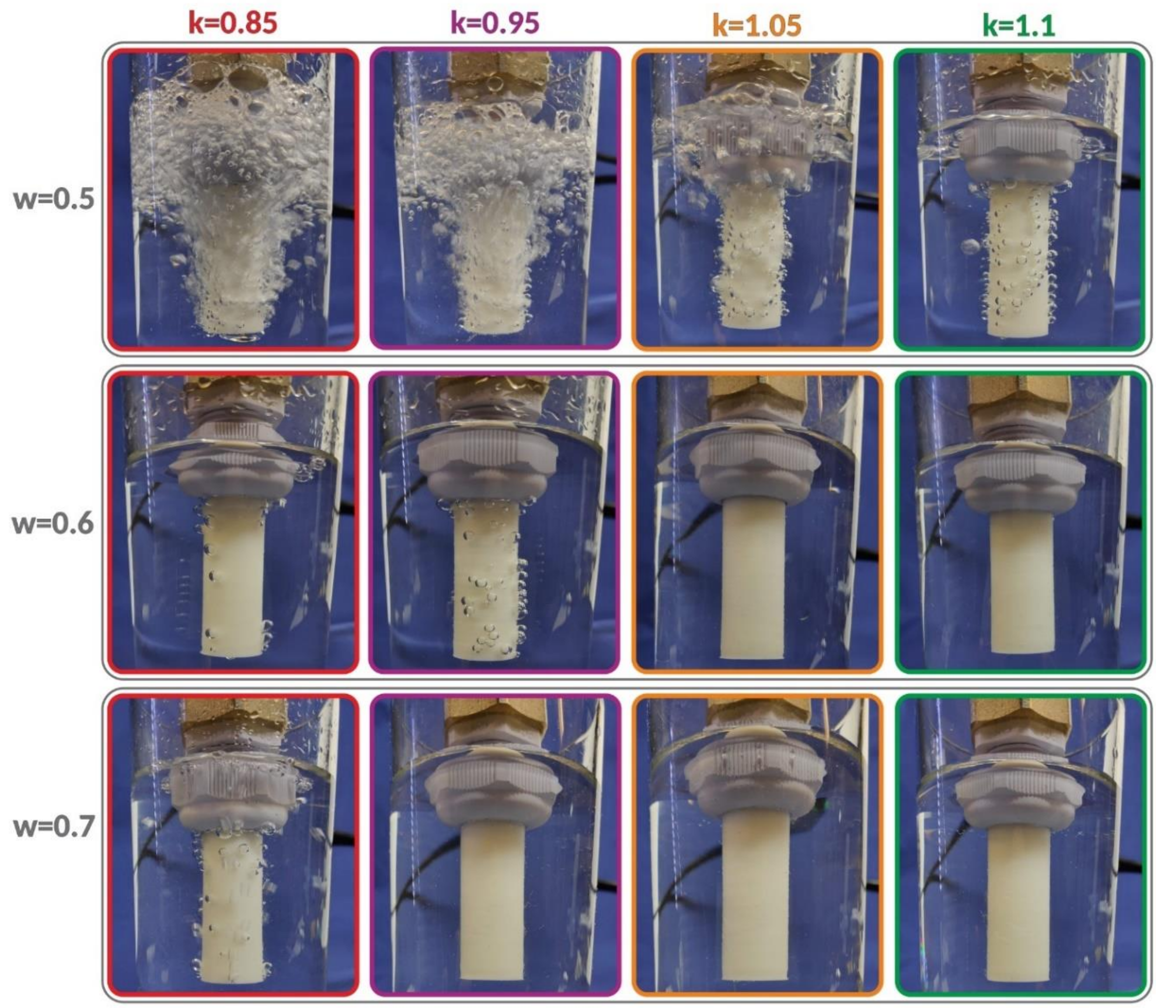

Figure S48. The study of microporosity for PLA+ test tubes.

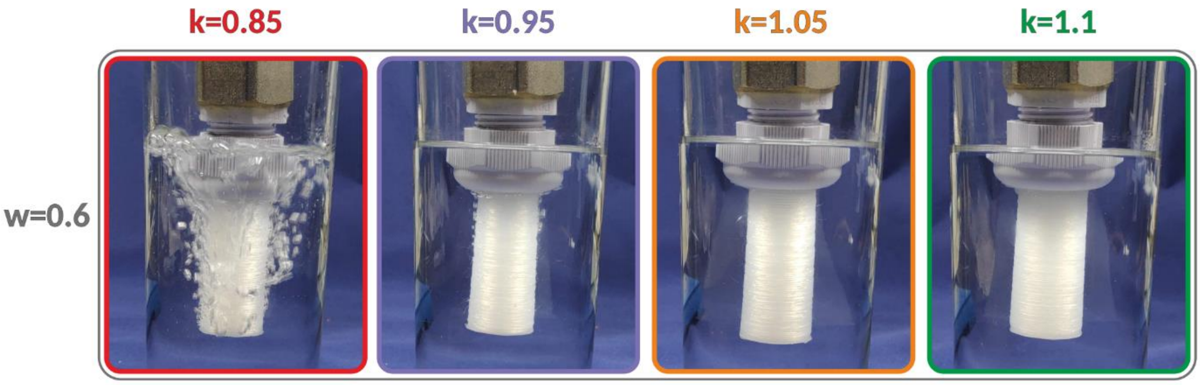

Figure S49. The study of microporosity for PA test tubes.

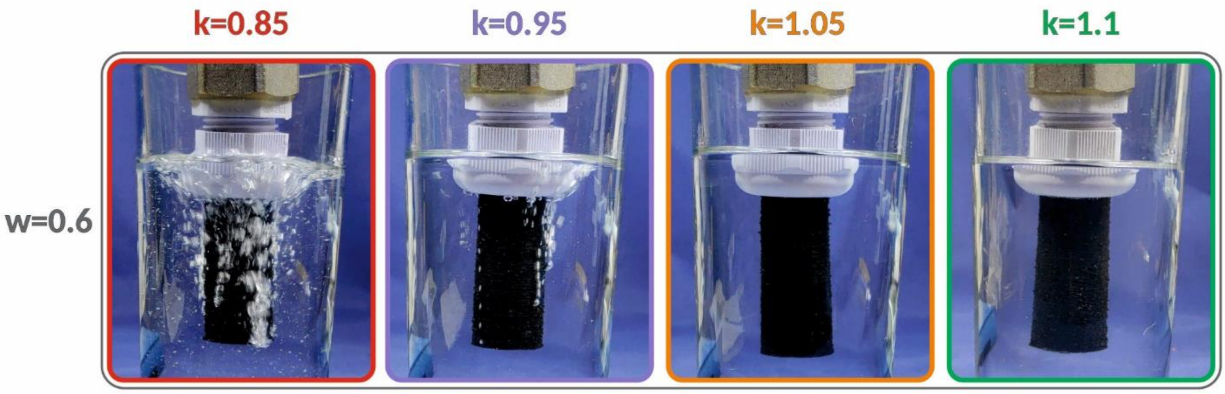

Figure S50. The study of microporosity for PP-GF test tubes.

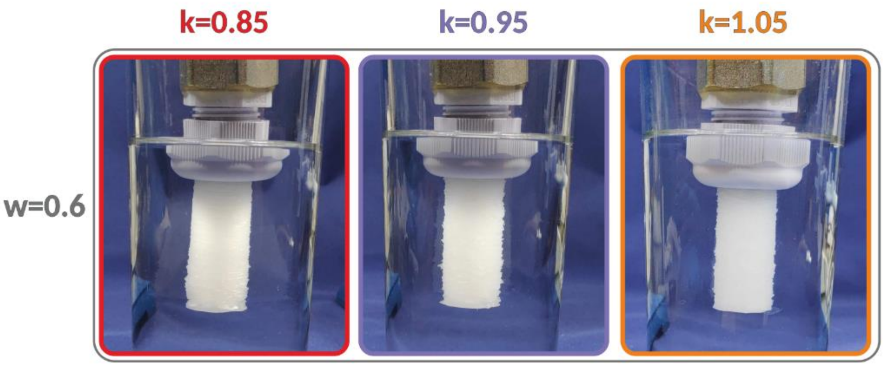

Figure S51. The study of microporosity for PP test tubes.

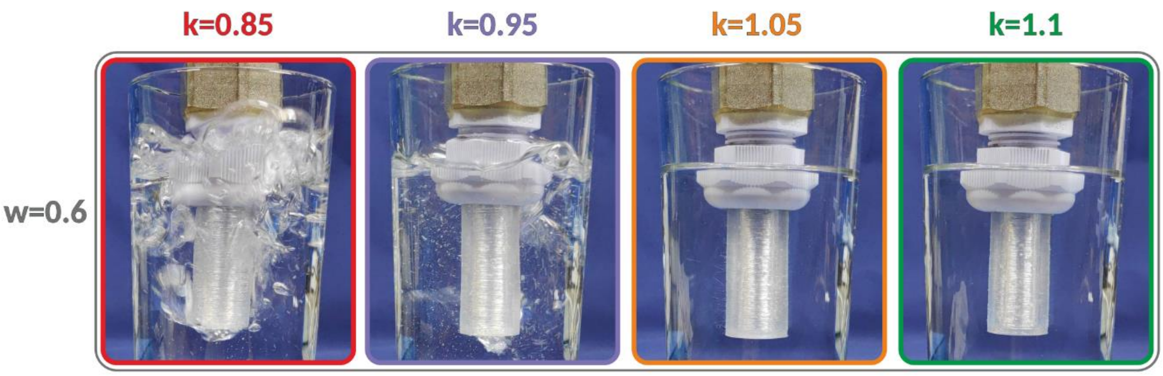

Figure S52. The study of microporosity for TPU test tubes.

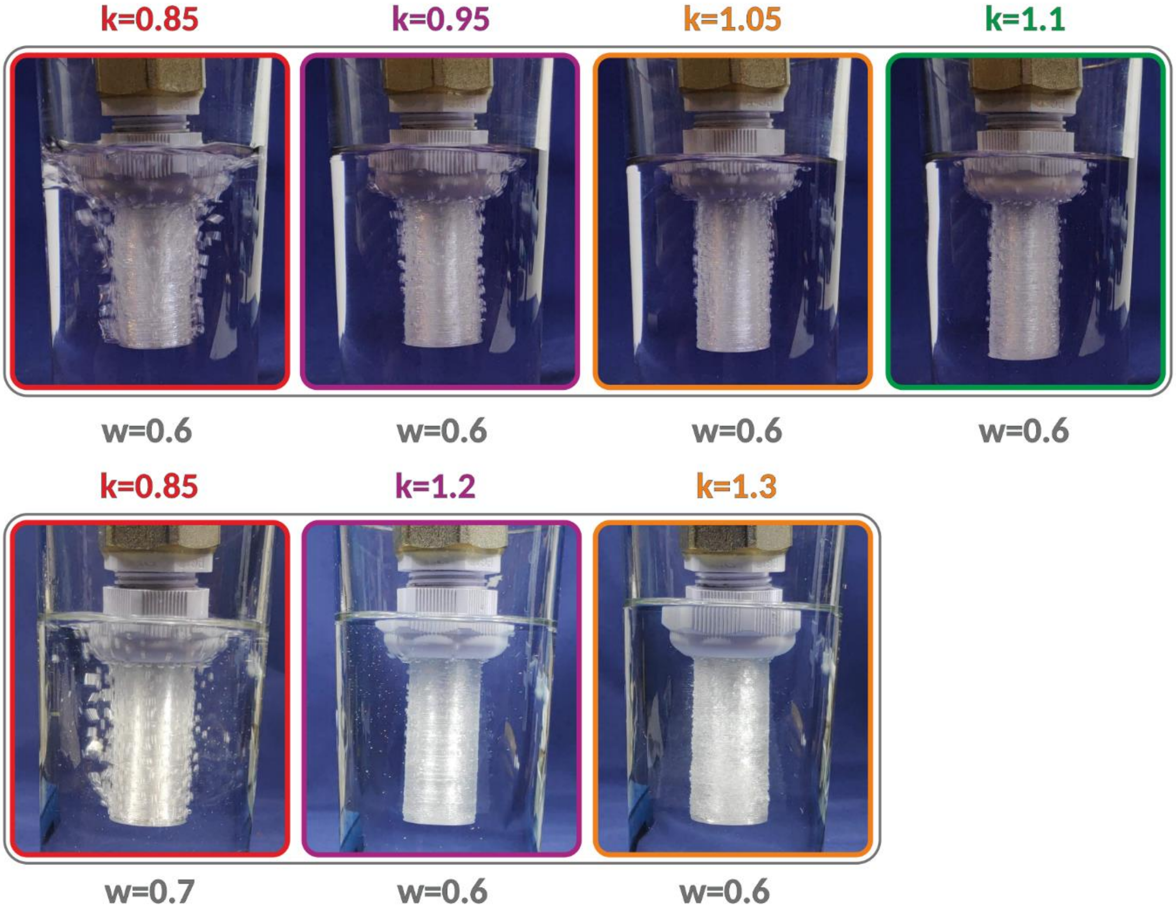

Figure S53. The study of microporosity for PC+ test tubes.

6. The study of shrinkage drawback

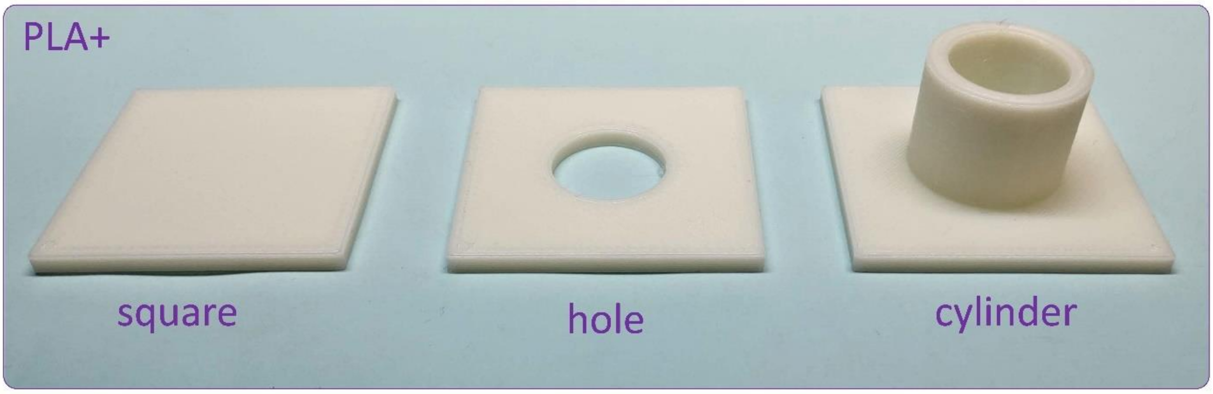

Figure S54. PLA+ parts manufactured by FFF for study of the shrinkage.

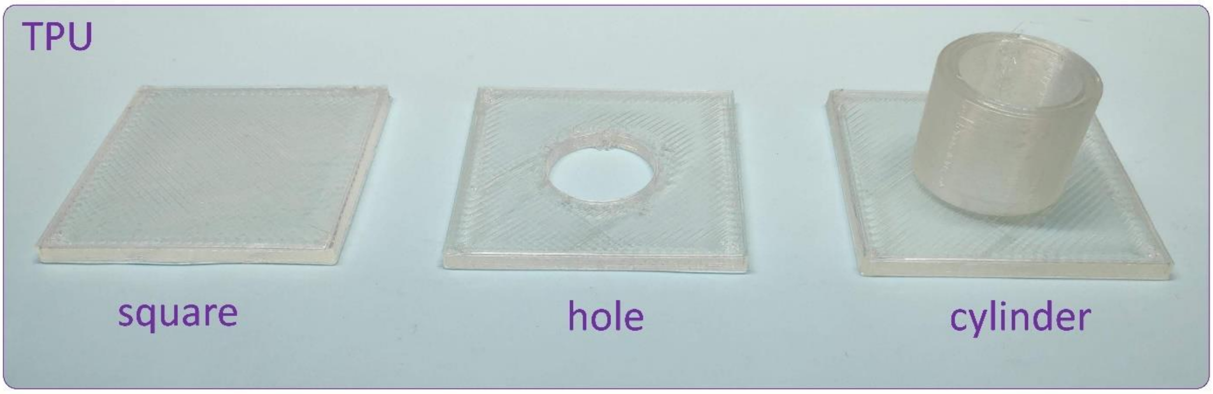

Figure S55. TPU parts manufactured by FFF for study of the shrinkage.

Figure S56. PC+ parts manufactured by FFF for study of the shrinkage.

Figure S57. PA6-CF parts manufactured by FFF for study of the shrinkage.

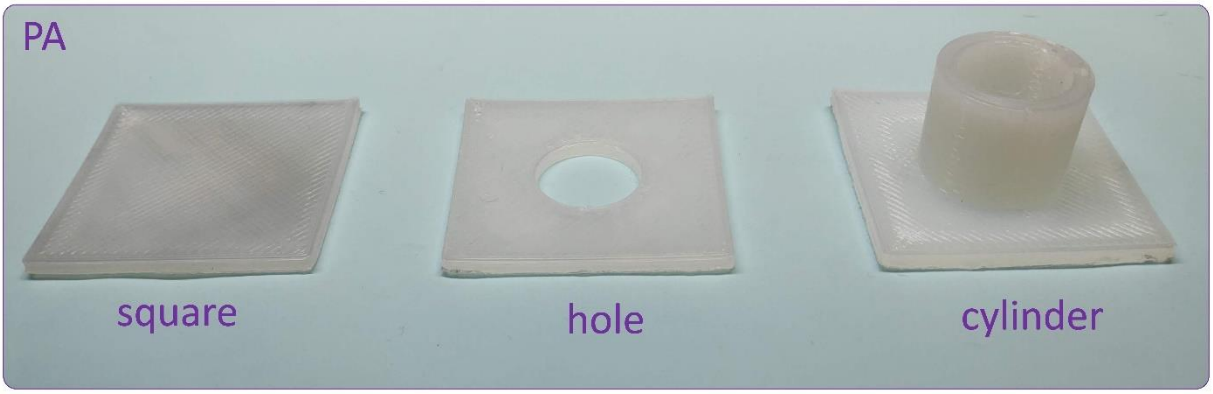

Figure S58. PA parts manufactured by FFF for study of the shrinkage.

Figure S59. PP-GF parts manufactured by FFF for study of the shrinkage.

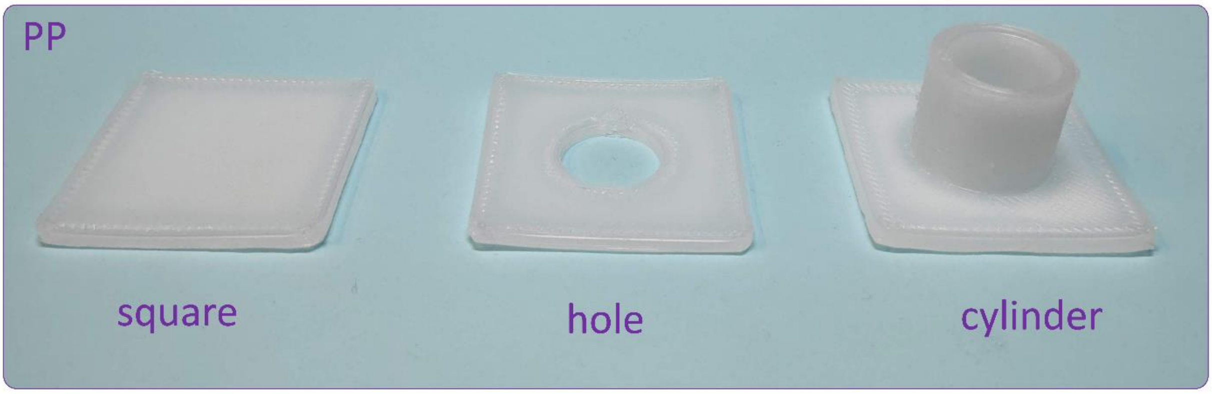

Figure S60. PP parts manufactured by FFF for study of the shrinkage.

Table S10. Shrinkage of parts manufactured by the FFF method.

size	square	displacement from the specified size (%)	hole	displacement from the specified size (%)	cylinder	displacement from the specified size (%)	reference parameters
PLA+							
a_1 [a]	49.94	0.12	50.06	0.12	50.05	0.10	50.00
a_2 [b]	49.94	0.12	50.06	0.12	50.05	0.10	50.00
b [c]	3.23	7.67	3.19	6.33	3.20	6.67	3.00
D_1 [d]	–	–	19.62	1.90	19.18	4.10	20.00
D_2 [e]	–	–	–	–	26.04	0.15	26.00
h [f]	–	–	–	–	22.97	0.13	23.00
TPU							
a_1 [a]	49.64	0.72	49.42	1.16	49.60	0.80	50.00
a_2 [b]	49.57	0.86	49.42	1.16	49.55	0.90	50.00
b [c]	2.80	6.67	2.58	14.00	3.14	4.67	3.00
D_1 [d]	–	–	19.23	3.85	18.86	5.70	20.00
D_2 [e]	–	–	–	–	26.00	0.00	26.00
h [f]	–	–	–	–	22.66	1.48	23.00
PC+							
a_1 [a]	50.40	0.80	50.63	1.26	50.47	0.94	50.00
a_2 [b]	50.61	1.22	50.40	0.80	50.57	1.14	50.00
b [c]	3.03	1.00	3.07	2.33	3.27	9.00	3.00
D_1 [d]	–	–	19.17	4.15	19.01	4.95	20.00
D_2 [e]	–	–	–	–	26.41	1.58	26.00
h [f]	–	–	–	–	22.87	0.57	23.00
PA6-CF							
a_1 [a]	51.39	2.78	51.22	2.44	51.06	2.12	50.00
a_2 [b]	51.24	2.48	51.22	2.44	51.01	2.02	50.00
b [c]	3.14	4.67	3.30	10.00	3.64	21.33	3.00
D_1 [d]	–	–	18.74	6.30	18.48	7.60	20.00
D_2 [e]	–	–	–	–	27.36	5.23	26.00
h [f]	–	–	–	–	22.87	0.57	23.00
PA							
a_1 [a]	49.82	0.36	49.75	0.50	49.84	0.32	50.00
a_2 [b]	49.65	0.70	49.62	0.76	49.83	0.34	50.00
b [c]	2.94	2.00	2.92	2.67	3.23	7.67	3.00
D_1 [d]	–	–	19.05	4.75	18.74	6.30	20.00
D_2 [e]	–	–	–	–	26.14	0.54	26.00
h [f]	–	–	–	–	22.71	1.26	23.00
PP-GF							
a_1 [a]	51.00	2.00	51.17	2.34	51.23	2.46	50.00
a_2 [b]	50.70	1.40	51.19	2.38	51.03	2.06	50.00
b [c]	3.10	3.33	3.10	3.33	3.39	13.00	3.00
D_1 [d]	–	–	19.04	4.80	18.60	7.00	20.00
D_2 [e]	–	–	–	–	26.93	3.58	26.00
h [f]	–	–	–	–	22.83	0.74	23.00
PP							
a_1 [a]	48.25	3.50	48.22	3.56	48.00	4.00	50.00
a_2 [b]	48.29	3.42	48.40	3.20	48.64	2.72	50.00
b [c]	2.83	5.67	2.79	7.00	3.09	3.00	3.00
D_1 [d]	–	–	18.97	5.15	18.74	6.30	20.00
D_2 [e]	–	–	–	–	24.95	4.04	26.00
h [f]	–	–	–	–	23.10	0.43	23.00

[a] width (mm); [b] width (mm); [c] depth (mm); [d] inside diameter (mm); [i] external diameter (mm); [f] cylinder height + b (mm).

7. Transfer hydrogenation in FFF batch reactor

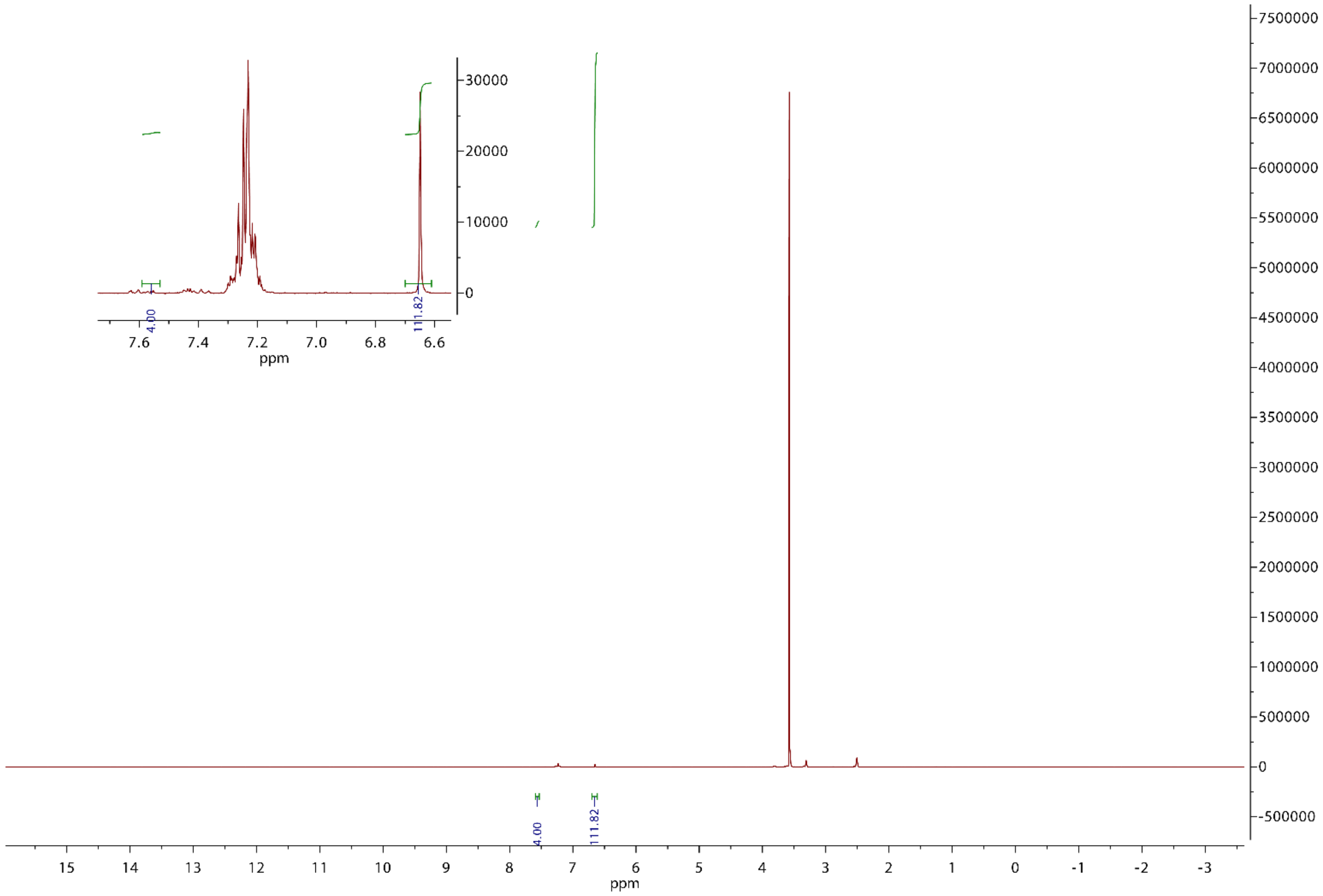

Figure S61. ^{1}H NMR spectrum of the reaction mixture after hydrogenation in FFF batch PA reactor. The first experimental point for averaging the value of the conversion of diphenylacetylene.

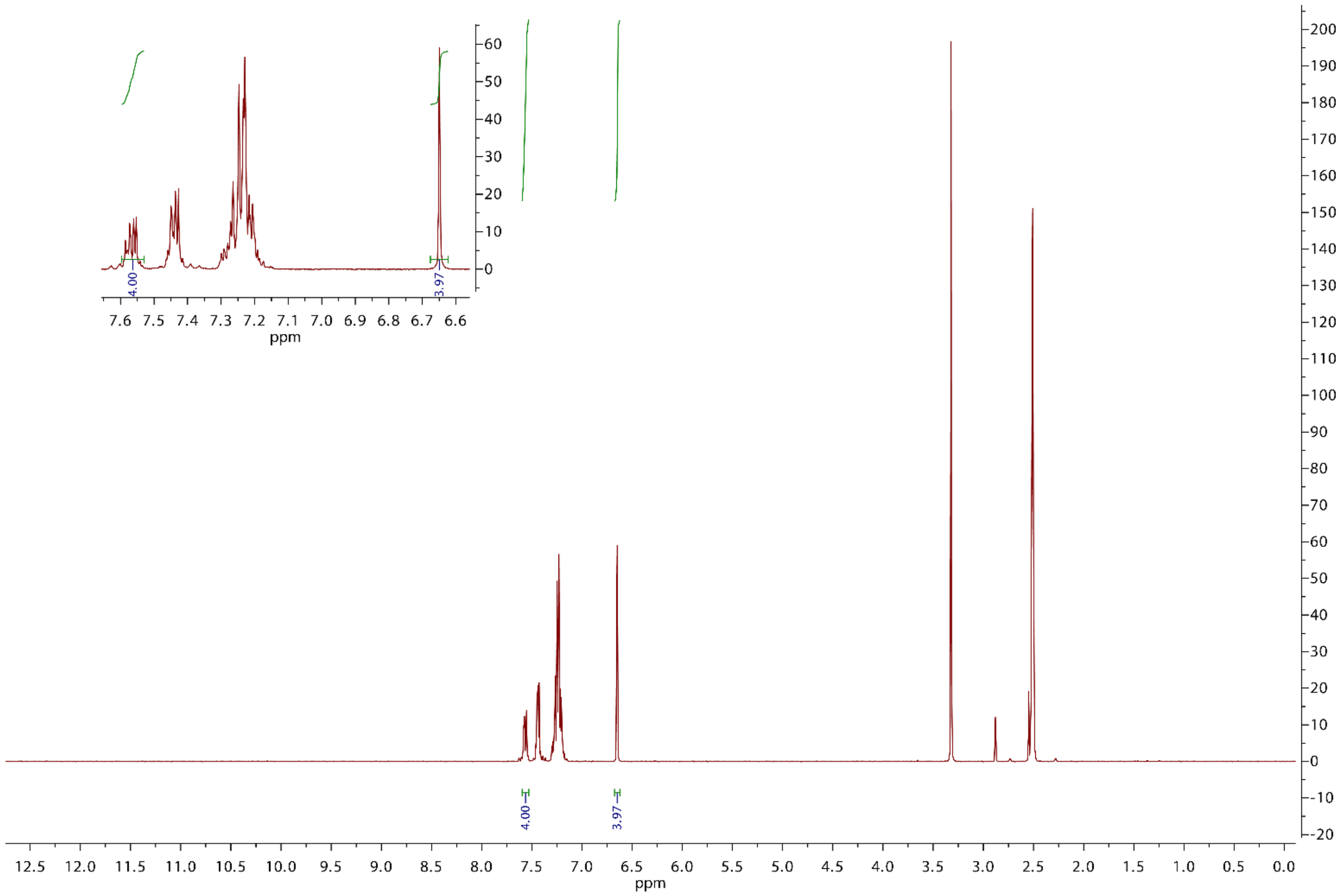

Figure S62. [1]H NMR spectrum of the reaction mixture after hydrogenation in FFF batch PA reactor. The second experimental point for averaging the value of the conversion of diphenylacetylene.

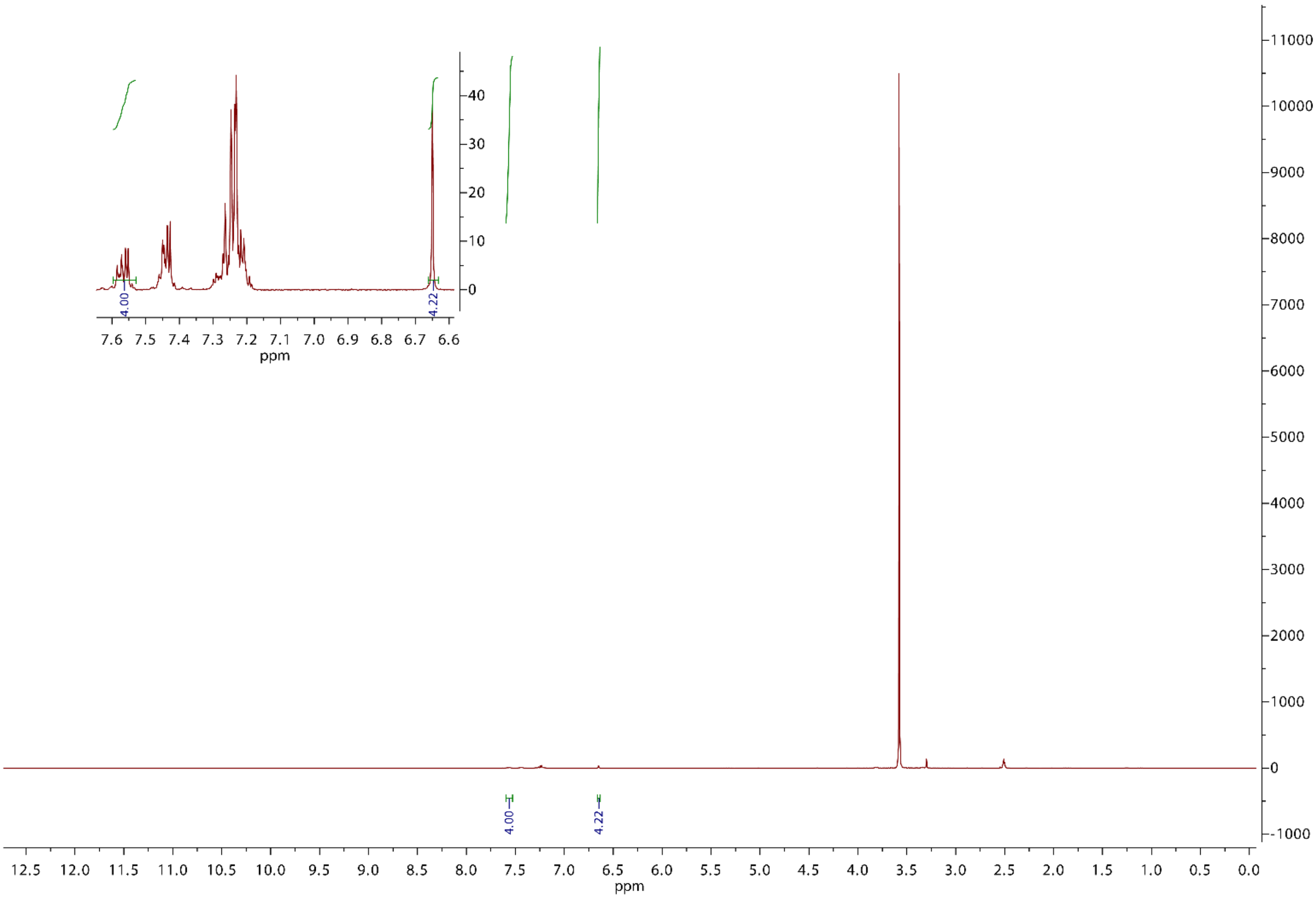

Figure S63. ^{1}H NMR spectrum of the reaction mixture after hydrogenation in FFF batch PA reactor. The third experimental point for averaging the value of the conversion of diphenylacetylene.

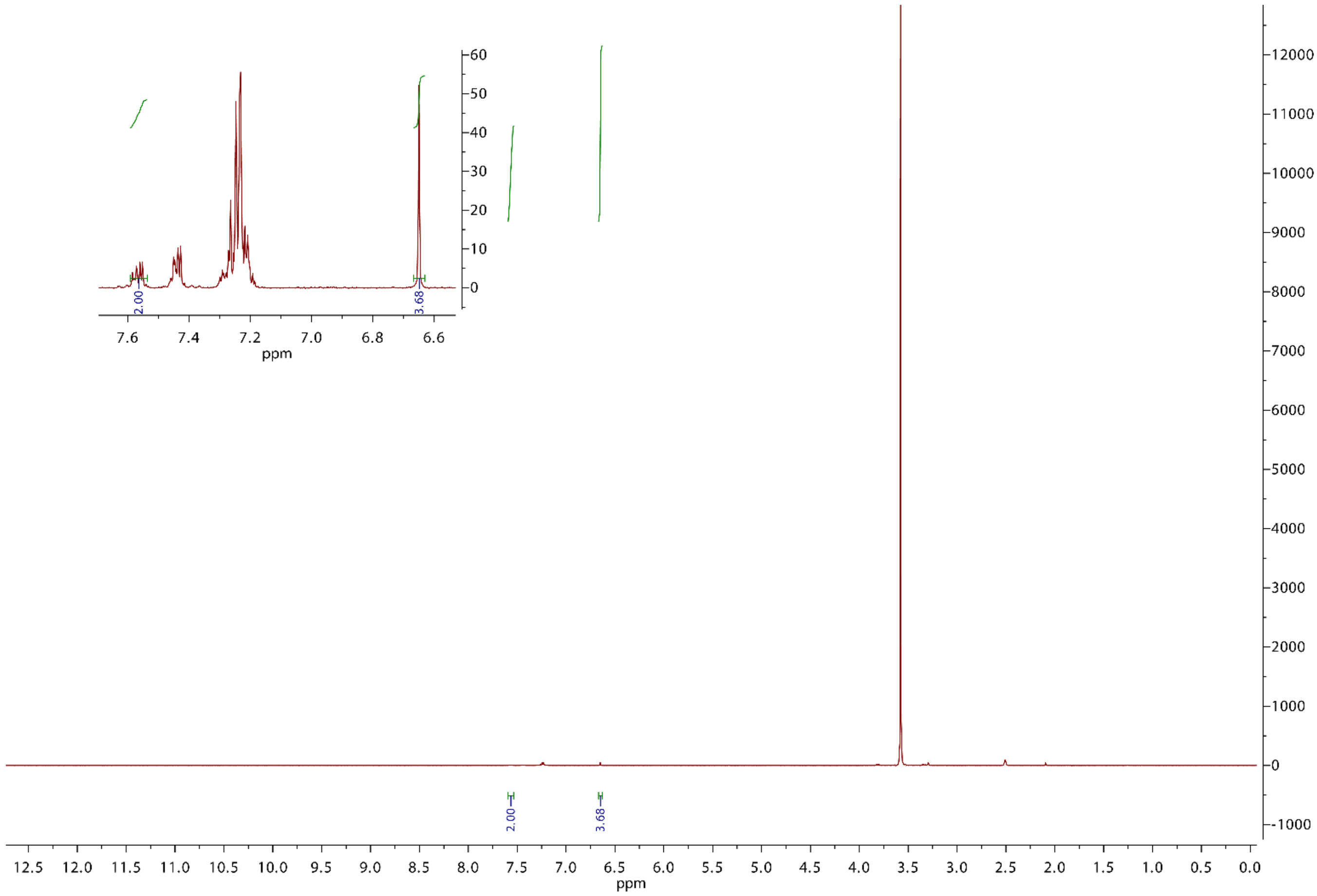

Figure S64. ^{1}H NMR spectrum of the reaction mixture after hydrogenation in FFF batch PA reactor. The fourth experimental point for averaging the value of the conversion of diphenylacetylene.

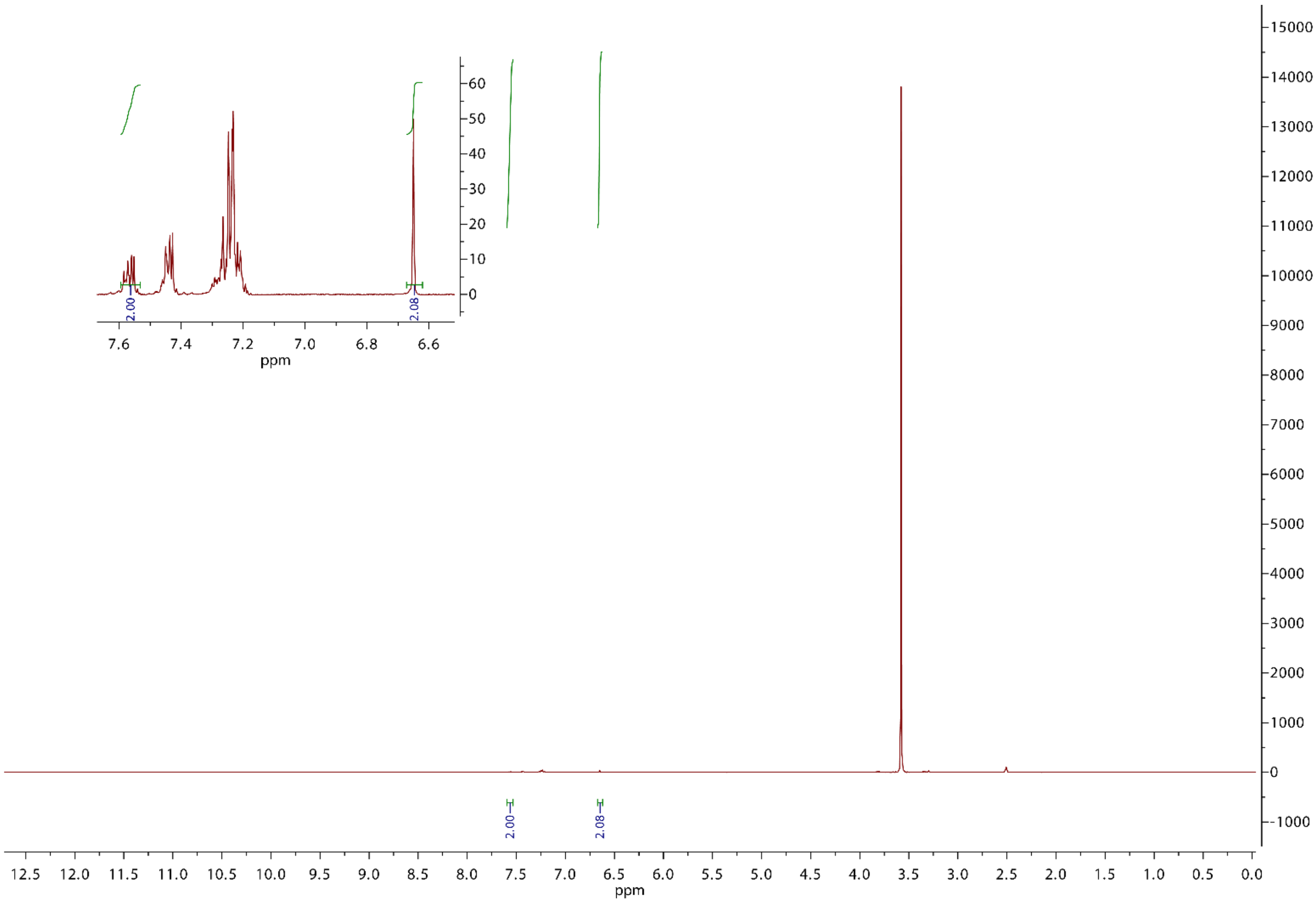

Figure S65. ^1H NMR spectrum of the reaction mixture after hydrogenation in FFF batch PA reactor. The fifth experimental point for averaging the value of the conversion of diphenylacetylene.

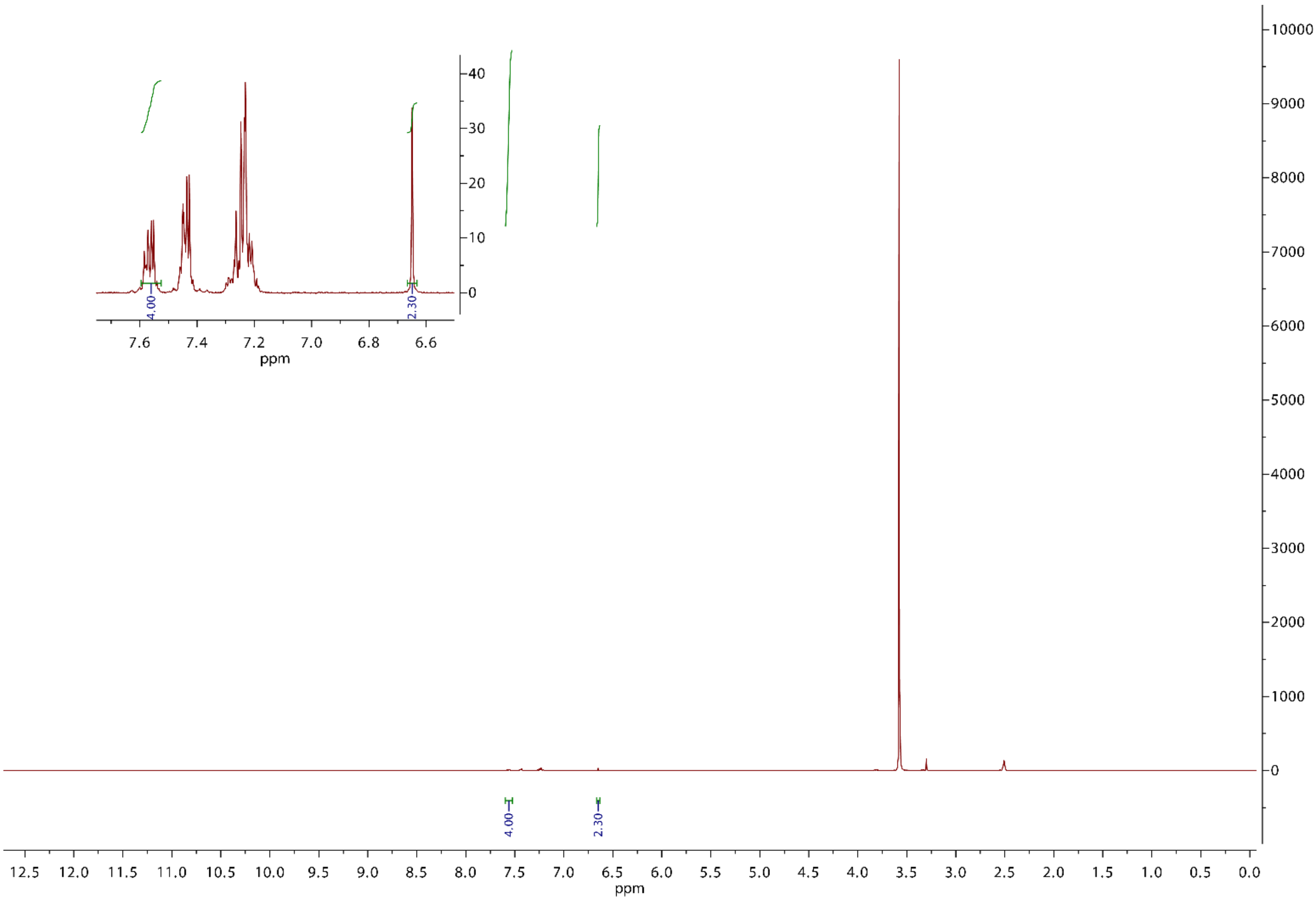

Figure S66. ^{1}H NMR spectrum of the reaction mixture after hydrogenation in FFF batch PA6-CF reactor. The first experimental point for averaging the value of the conversion of diphenylacetylene.

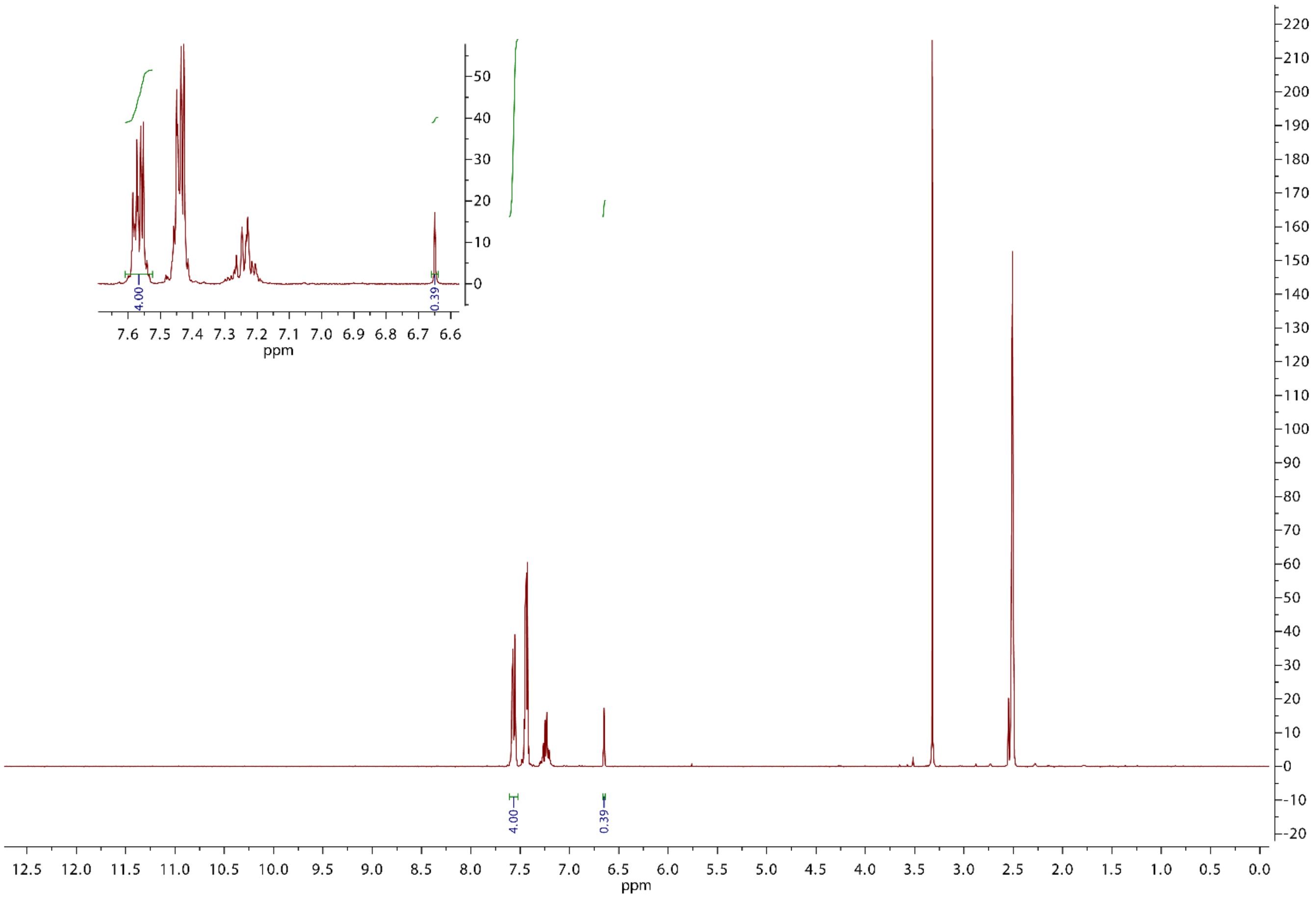

Figure S67. ^{1}H NMR spectrum of the reaction mixture after hydrogenation in FFF batch PA6-CF reactor. The second experimental point for averaging the value of the conversion of diphenylacetylene.

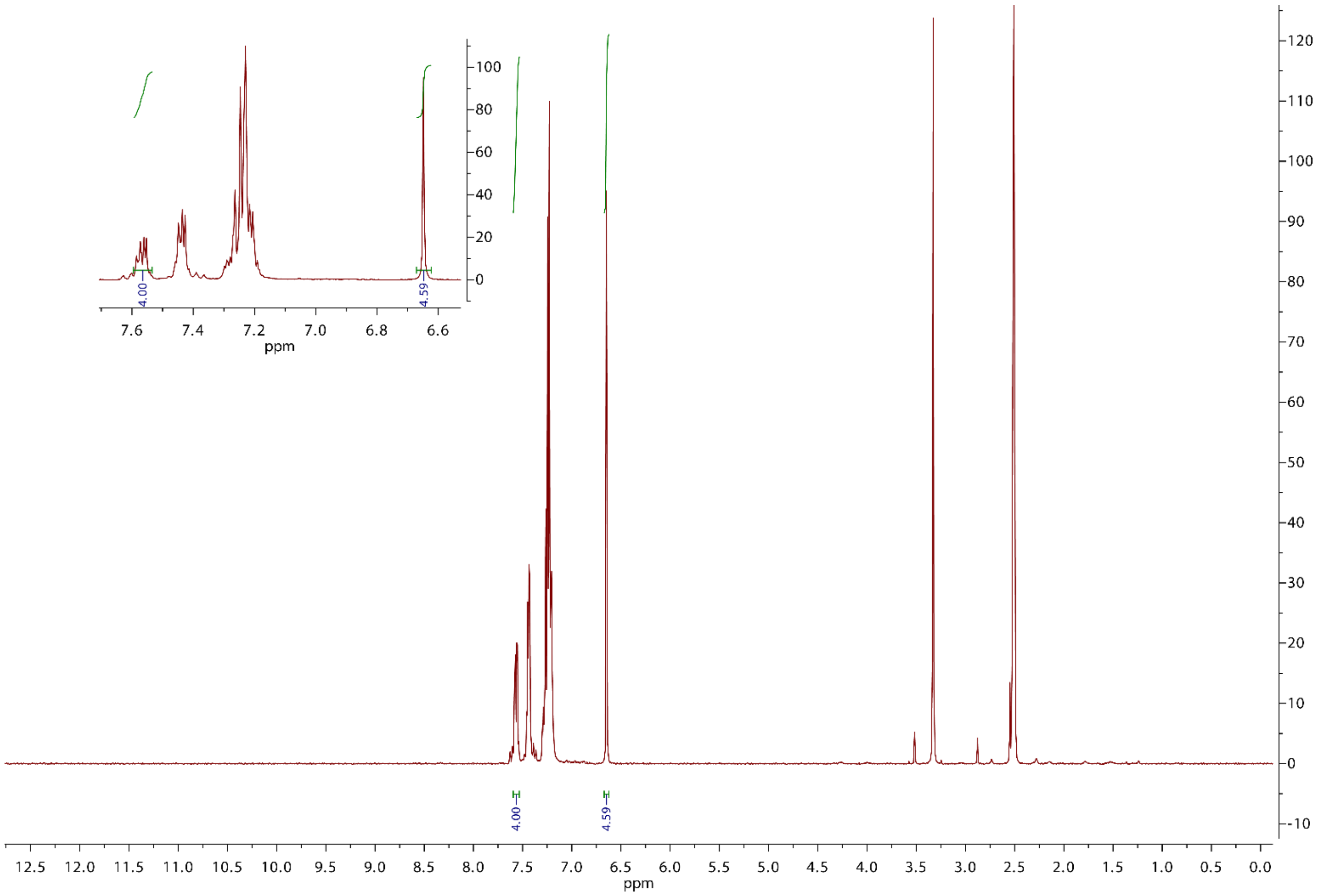

Figure S68. ^1H NMR spectrum of the reaction mixture after hydrogenation in FFF batch PA6-CF reactor. The third experimental point for averaging the value of the conversion of diphenylacetylene.

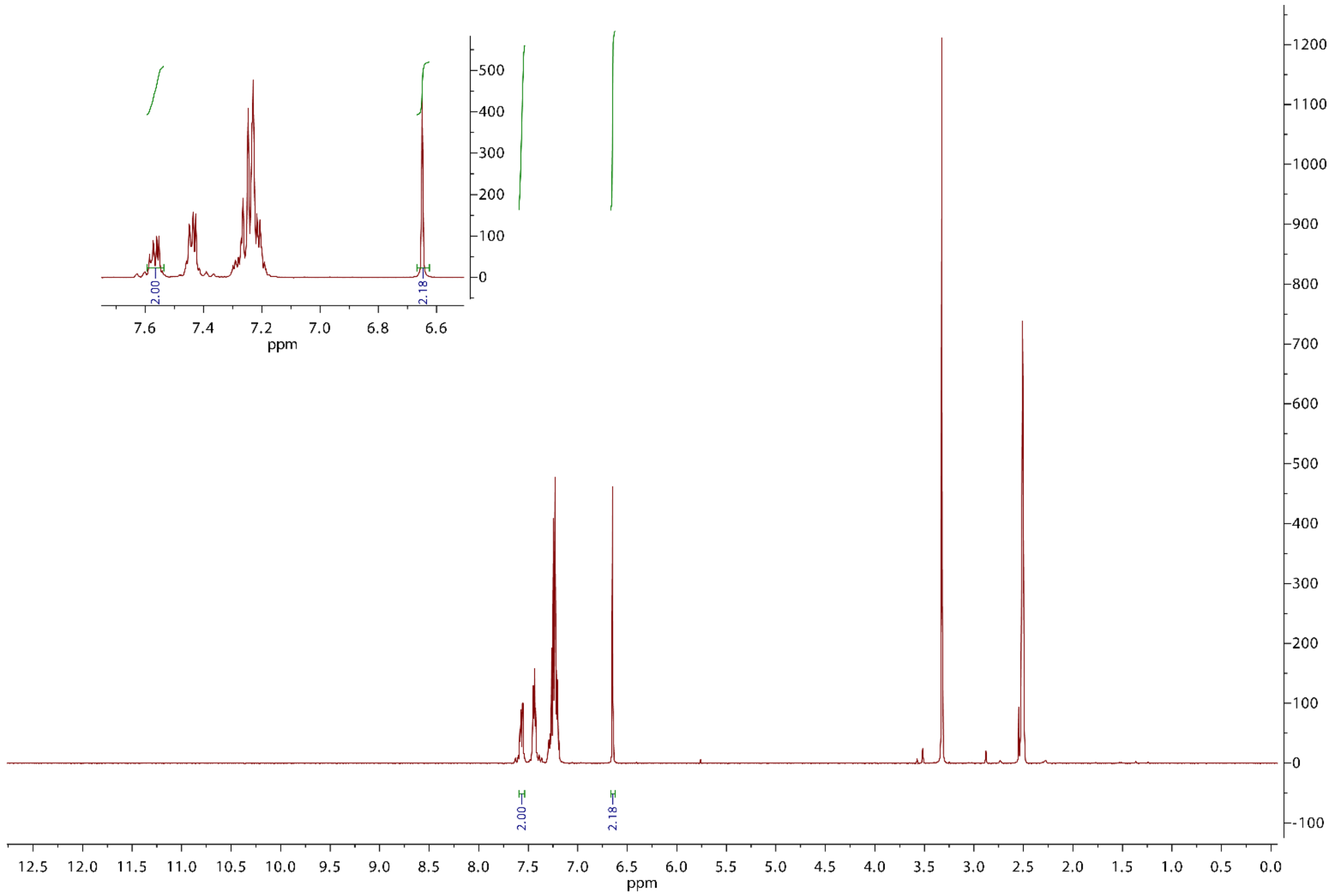

Figure S69. ^{1}H NMR spectrum of the reaction mixture after hydrogenation in FFF batch PA6-CF reactor. The fourth experimental point for averaging the value of the conversion of diphenylacetylene.

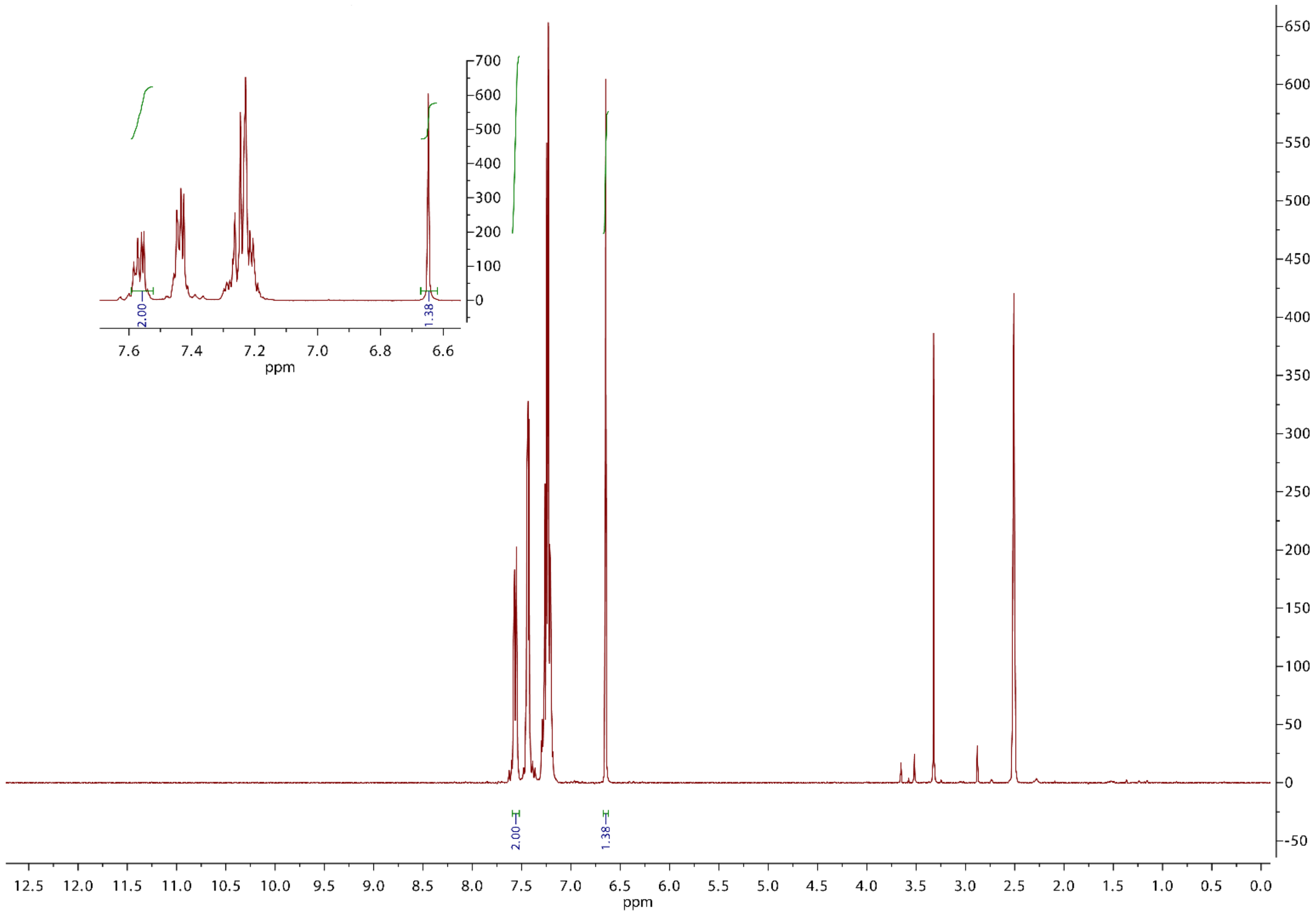

Figure S70. ^{1}H NMR spectrum of the reaction mixture after hydrogenation in FFF batch PA6-CF reactor. The fifth experimental point for averaging the value of the conversion of diphenylacetylene.

8. Transfer hydrogenation in FFF flow reactor

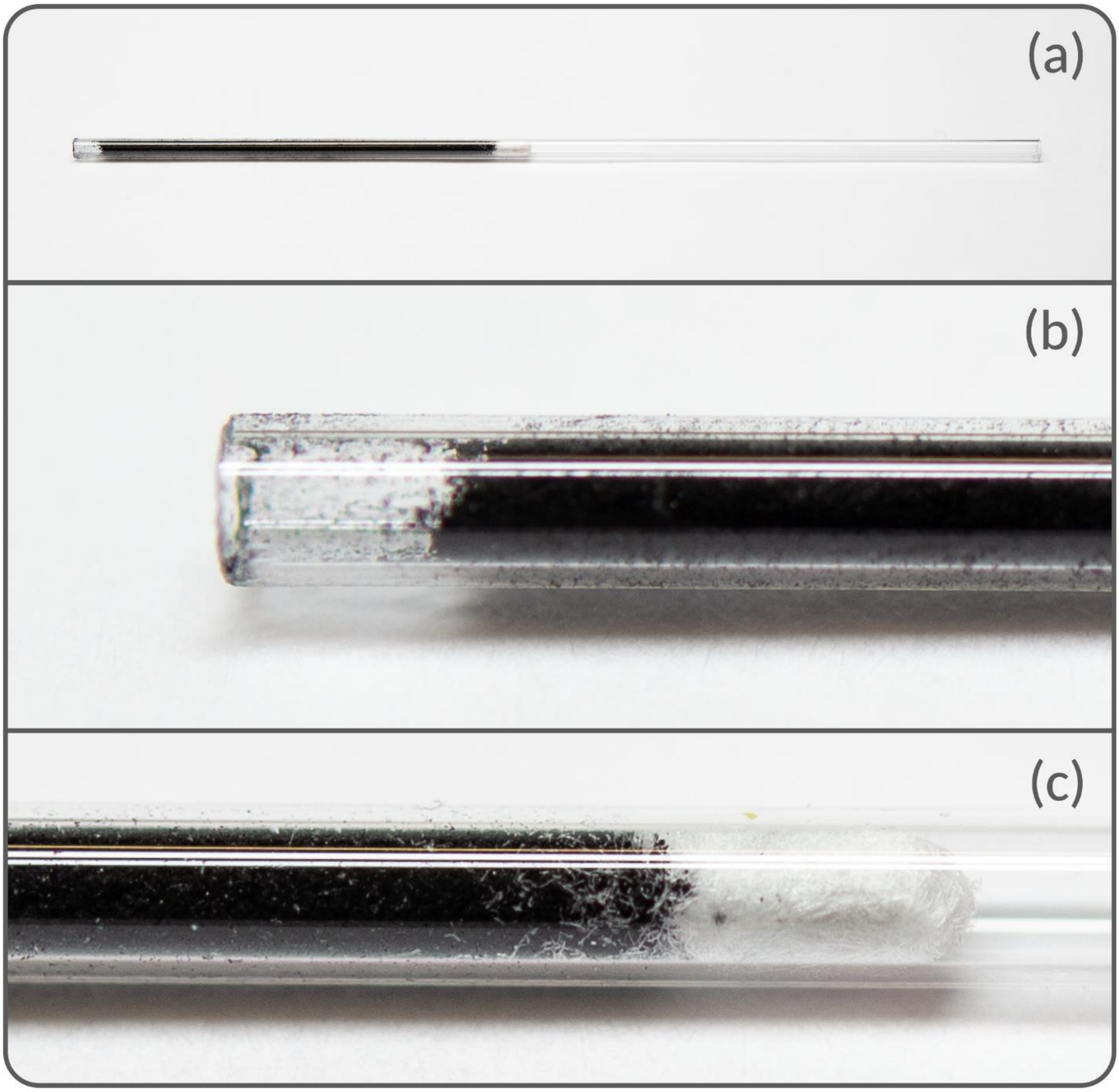

Figure S71. Catalytic tube with filter, filled Pd/C (10%) and K_2CO_3.

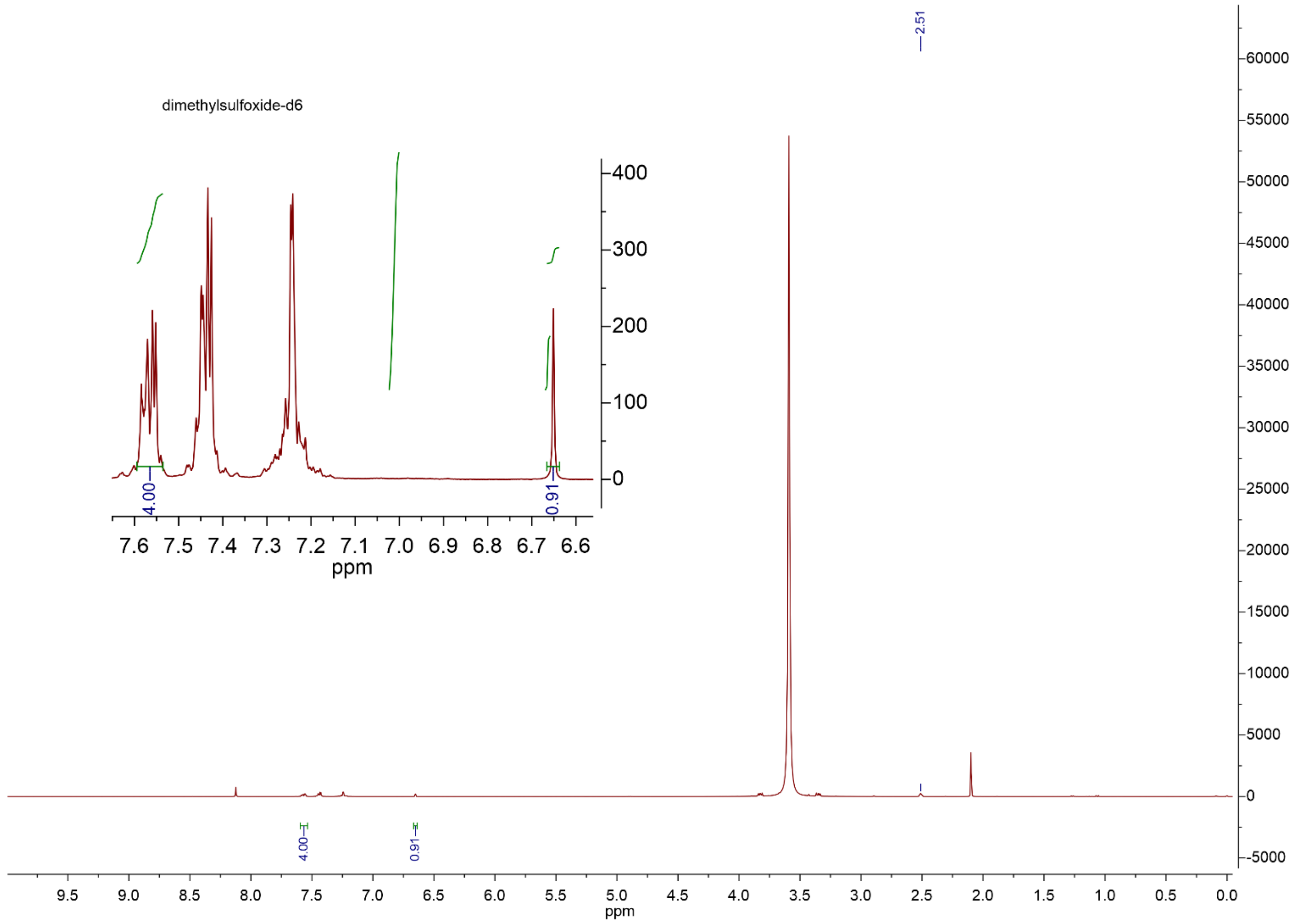

Figure S72. ^{1}H NMR spectrum of the reaction mixture after hydrogenation in the first FFF module of the PA6-CF flow reactor system.

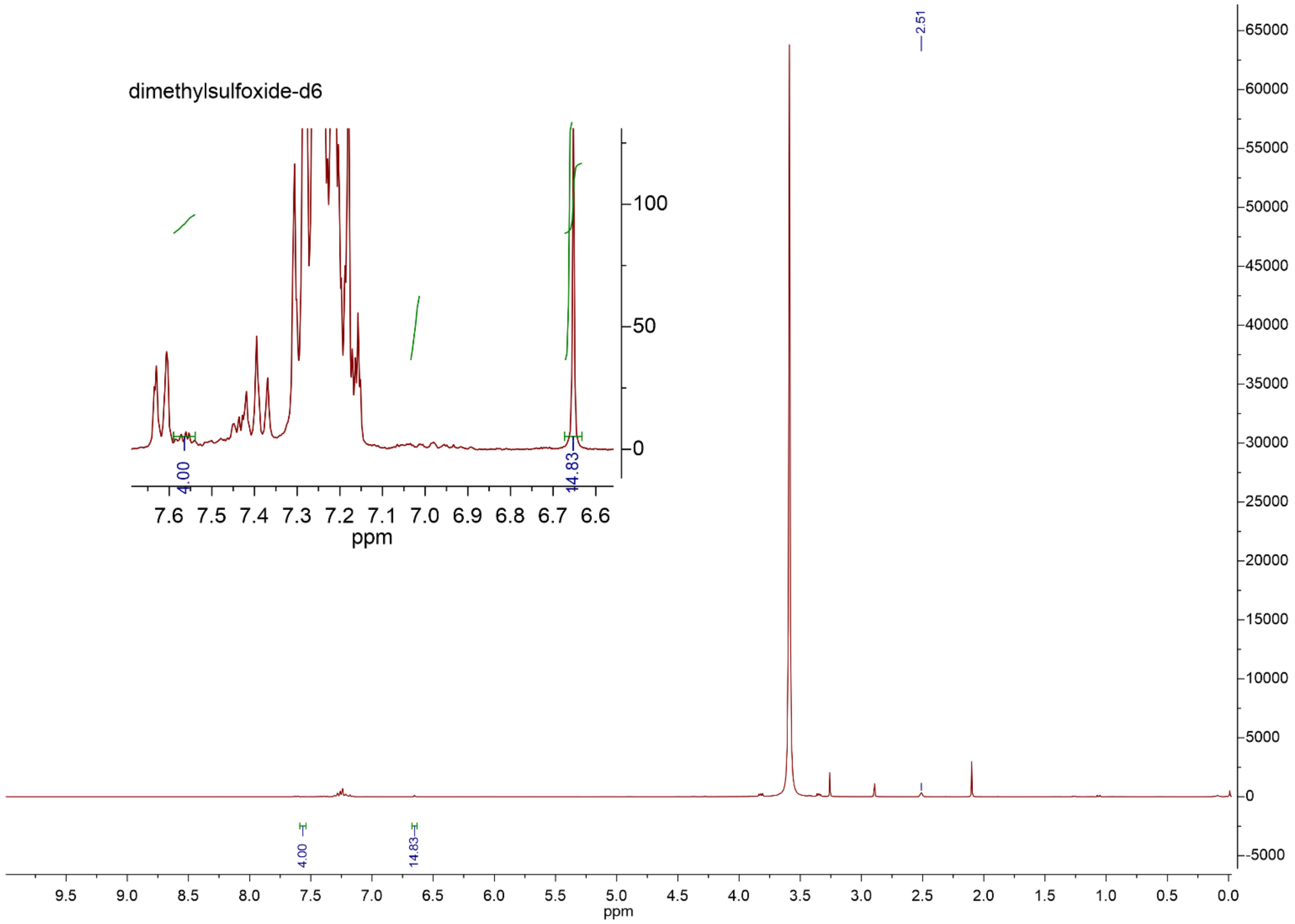

Figure S73. ^{1}H NMR spectrum of the reaction mixture after hydrogenation in the second FFF module of the PA6-CF flow reactor system.